DISSERTATION

# THE CHROMATIN BINDING FACTOR SPN1 CONTRIBUTES TO GENOME INSTABILITY IN SACCHAROMYCES CEREVISIAE

Submitted by

Alison K. Thurston

Department of Biochemistry and Molecular Biology

In partial fulfillment of the requirements

For the Degree of Doctor of Philosophy

Colorado State University

Fort Collins, Colorado

Spring 2018

Doctoral Committee:

Advisor: Laurie Stargell

Susan Bailey
Jennifer DeLuca
Jeffrey Hansen
Karolin Luger

# ABSTRACT


## THE CHROMATIN BINDING FACTOR SPN1 CONTRIBUTES TO GENOME INSTABILITY IN SACCHAROMYCES CEREVISIAE

Maintaining the genetic information is the most important role of a cell. Alteration to the DNA sequence is generally thought of as harmful, as it is linked with many forms of cancer and hereditary diseases. Contrarily, some level of genome instability (mutations, deletions, amplifications) is beneficial to an organism by allowing for adaptation to stress and survival. Thus, the maintenance of a “healthy level” of genome stability/instability is a highly regulated process. In addition to directly processing the DNA, the cell can regulate genome stability through chromatin architecture. The accessibility of DNA for cellular machinery, damaging agents and spontaneous recombination events is limited by level of chromatin compaction. Remodeling of the chromatin for transcription, repair and replication occurs through the actions of ATP remodelers, histone chaperones, and histone modifiers. These complexes work together to create access for DNA processing and to restore the chromatin to its pre-processed state. As such, many of the chromatin architecture factors have been implicated in genome stability. In this study, we have examined the role of the yeast protein Spn1 in maintaining the genome. Spn1 is an essential and conserved transcription elongation factor and chromatin binding factor. As anticipated, we observed that Spn1 contributes to the maintenance of the genome. Unexpectedly, our data revealed that Spn1 contributes to promoting genome instability. Investigation into a unique growth phenotype in which cells expressing a mutant form of Spn1 displayed resistance to the damaging agent, methyl methanesulfonate revealed Spn1 influences pathway selection during DNA damage tolerance. DNA damage tolerance is utilized during replication and G2 to bypass lesions, which could permanently stall replication machinery. This pathway congruently

promotes and prevents genome instability. We theorize that these outcomes are due to the ability of Spn1 to influence chromatin structure throughout the cell cycle.

# ACKNOWLEDGEMENTS

Obtaining a PhD has been a long hard journey, and while the research is independent, I did accomplish it alone. First, I would like to thank my advisor, Dr. Laurie Stargell. I respect her outlook on research, education and our responsibility to the public. Not only has she guided my intellectual approach to research but she stresses the importance of communication to fellow scientists and the general public. In the future, I will approach my writing and public speaking as if she is there guiding me and telling me to keep it simple. Her generosity and encouragement allowed me to pursue opportunities which were important for success in graduate school and for my future career.

To my laboratory members: Dr. Cathy Radebaugh, Dr. Xu Chen, and Dr. Lillian Huang; thank you for sharing your wisdom with me. I have enjoyed working with you every day and hope that in the future I will always be lucky enough to work in such a caring, motivating, talented and inspiring environment.

I would like to thank my graduate committee: Dr. Susan Bailey, Dr. Jennifer DeLuca, Dr. Karolin Luger and Dr. Jeffrey Hansen. I appreciate the time and guidance you have all contributed to my success. Jeff, I would like to thank you specifically for your encouragement and perspective. I truly valued working with you and appreciate the opportunities to teach in your classes. Additionally, I would like thank the Biochemistry and Molecular Biology Department and Colorado State University.

Furthermore, I would like to acknowledge Dr. Juan Lucas Argueso. I am grateful for the time and conversations spent answering my questions, advising me on experimentation, and your insight into my project.

I would like to thank my fellow Stargell Laboratory graduate students: Dr, Sha Li and Dustin Steele. I will miss our conversations and the comradery and I am excited for all of our futures. Furthermore, I cannot image graduate school without Jen Shattuck, Dr. Melissa Ford and Sarah Bollinger. As colleagues, classmates and friends, you all made the journey much more enjoyable.

I am grateful to Dr. Robyn Barbato, the Barbato Laboratory members, the Cold Regions Research and Engineering Laboratory (CRREL) and the DHS-STEM program for the opportunity, welcoming environment and funding for my research internship. Robyn, you are great mentor and I appreciate the freedom granted to pursue research in your laboratory.

To my family, I am thankful for all your support and belief in me. The visits and care packages were needed pick me ups. I know that you will always be there. Perhaps now I will have time for a massage. Finally, I would like to thank Eric. You were there night and day. I am glad and thankful that you decided to take this journey with me.

.

TABLE OF CONTENTS

# CHAPTER 1: REVIEW OF THE LITERATURE

## 1.1 Genome Stability/Instability

Maintaining the genome is the most important function of a cell. Instability within the genome contributes to cancer, aging and genetic diseases (AGUILERA and GARCIA-MUSE 2013; VIJG and SUH 2013). Genome instability encompasses point mutations, deletions, duplications, translocations; and chromosome instability (CIN) (AGUILERA and GARCIA-MUSE 2013; SKONECZNA *et al.* 2015). CIN refers to the instability of a chromosome (whole or partial), which results in unequal distribution to the daughter cells (STIRLING *et al.* 2011). There are many causes of genome instability including replication dysfunction, cell cycle checkpoint dysfunction, DNA repair recognition and processing defects, repetitive sequences, defects in nucleosome assembly and disassembly, unregulated higher order chromatin structure, telomere dysfunction and metabolism byproducts (KOLODNER *et al.* 2002; WELLINGER and ZAKIAN 2012; AGUILERA and GARCIA-MUSE 2013; VIJG and SUH 2013; SKONECZNA *et al.* 2015; CHATTERJEE and WALKER 2017). In response to all these assaults on the DNA sequence, cells have developed sophisticated and overlapping mechanisms to prevent, detect and limit genome instability (Figure 1.1). However, some level of genome instability is tolerated by the cell and is necessary for evolution and natural selection (SKONECZNA *et al.* 2015).

## 1.2 DNA Damage Repair Pathways

The DNA repair pathways are responsible for the detection and correction of DNA strand breaks, a variety of lesions, and DNA crosslinks. There are five major DNA damage repair pathways, base excision repair (BER), mismatch repair (MMR), nucleotide excision repair (NER), homologous recombination (HR) and non-homologous end joining (NHEJ) (CHATTERJEE and WALKER 2017). Mismatches, non-helix distorting lesions such as methylation and oxidation, and abasic sites are primarily repaired through the base excision repair (BER) and mismatch repair

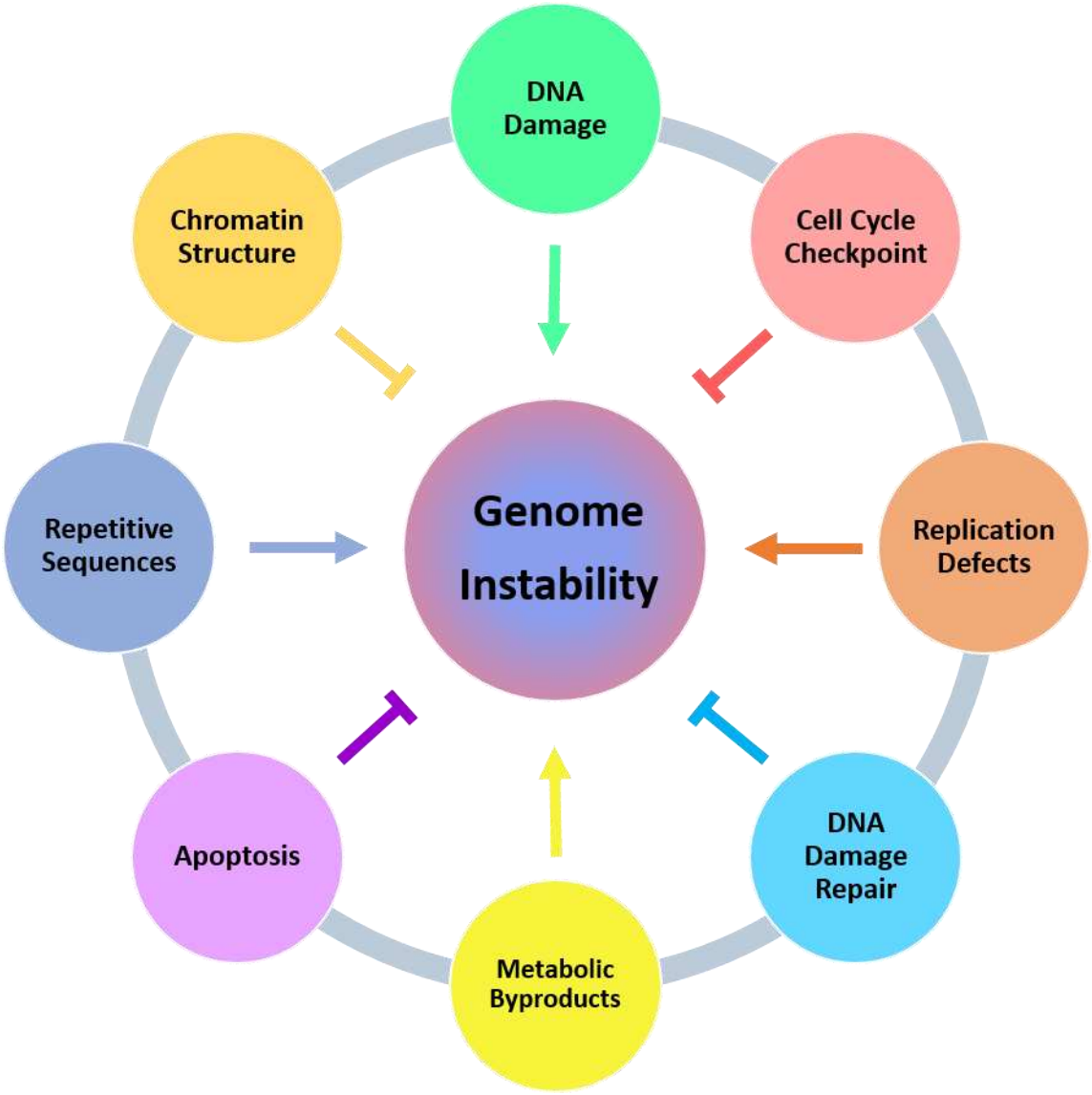


**Figure 1.1. Maintaining the genome is a balancing act.** Image depicts examples of causes (arrows) of genome instability and examples of deterrents (inhibitory sign) of genome instability.

(MMR) pathways (WALLACE 2014; BAUER *et al.* 2015; CHATTERJEE and WALKER 2017). Bulky adducts such as thymine dimers caused by UV, are primarily repaired through nucleotide excision repair (NER). NER is comprised of global genome NER (GG-NER) and transcription coupled NER (TC-NER) (CHATTERJEE and WALKER 2017). Homologous recombination (HR) utilizes homologous sequences as a template to resynthesize areas of damaged DNA. Non-homologous end joining (NHEJ) rejoins the two ends of the broken DNA; this can be done in an error free or error prone manner (CHATTERJEE and WALKER 2017). The pathway that corrects the damaged DNA depends on the type of damage, cell cycle phase, and chromatin context (BRANZEI and FOIANI 2008).

In addition to DNA repair pathways, the DNA damage tolerance (DDT) pathway allows bypass of DNA damage or chromatin distortion that slows or pauses the replication forks. Replication fork collapse or repair involving cleavage of the phosphate backbone can result in double strand breaks (DSBs) (HUSTEDT *et al.* 2013). Thus the cells utilize lower fidelity polymerases or template switch, a form of HR, to bypass the damage (BRANZEI and SZAKAL 2016). These bypass mechanisms can occur during S phase or be postponed to G2 (BRANZEI and SZAKAL 2016).

### 1.3 Assessment of Genome Instability

There have been many assays designed to evaluate the different types of genome instability in yeast. These assays detect forward spontaneous mutation rate, damage induced mutation rate, gross chromosomal rearrangements (GCR), loss of heterozygosity (LOH), copy number variations (CVN), and chromosome transmission fidelity (CTF) to name a few (Table 1.1) (YUEN *et al.* 2007; STIRLING *et al.* 2011; KUMARAN *et al.* 2013). Genome wide studies using many of these assays have been performed using the deletion collection, decreased abundance of mRNA perturbation (DAmP) collection and conditional alleles (HUANG *et al.* 2003; YUEN *et al.* 2007; STIRLING *et al.* 2011). Whole genome screens aid in identifying pathways and novel genes

Table 1.1 Methods of measuring genomic instability in vivo

| **Assay** | **Explanation** | **References** |
|---|---|---|
| Mutation Rate by Fluctuation Analysis | Evaluates spontaneous forward mutation rates and damage induced mutation rates. | *(LURIA and DELBRUCK 1943; FOSTER 2006)* |
| Loss of Heterozygosity | Evaluates recombination events by the inactivation of a functional allele at a heterozygous locus. | (ACUNA *et al.* 1994; ANDERSEN *et al.* 2008) |
| Gross Chromosomal Rearrangements | Evaluates genome instability that is not caused by single point mutations or frame shifts. This would include translocations, fusions, duplications, and deletions. | (CHEN and KOLODNER 1999) |
| Copy number Variation | Evaluates duplications or deletions of genes or regions within the genome. | (ZHANG *et al.* 2013) |
| Rad52 foci formation | Detection of double strand breaks in cells | (CONDE and SAN-SEGUNDO 2008) |
| Chromosome Transmission Fidelity | Evaluates chromosome segregation with the use of an artificial chromosome | (YUEN *et al.* 2007; STIRLING *et al.* 2011) |
| HO Endonuclease | Monitor the repair of a site directed double strand break through many recombination pathways. | (JENSEN *et al.* 1983; SUGAWARA and HABER 2012) |
| Bimater | Examine mitotic recombination by measuring mating competency in heteroallelic (*MATa/MATα*) diploids. | (SPENCER *et al.* 1990; YUEN *et al.* 2007) |
| A-like Faker | Assesses chromosome loss, gene conversions, deletions and gross chromosomal rearrangements through measuring mating events due to loss of *MATα* locus. | (YUEN *et al.* 2007; NOVOA *et al.* 2018) |

responsible for maintaining genetic stability. Gene products involved in a large array of biological processes have been identified by these screens, including DNA repair and replication, DNA processing and chromatin maintenance, lipid synthesis, proteasome, cell wall integrity and others (HUANG *et al.* 2003; YUEN *et al.* 2007; STIRLING *et al.* 2011).

Interestingly, 28% of essential genes examined tested positive for strong CIN phenotypes opposed to only 7% of non-essential genes (STIRLING *et al.* 2011). Genes in which mutation or deletion causes increased genome instability are referred to as mutator genes. This nomenclature is counterintuitive, as the designation is a result of mutation or deletion of the gene. In other words, the wildtype function of a mutator gene's derivative directly or indirectly maintains decreased levels of genome instability. Many of the classical DNA damage repair genes fall within this category, as their function is to maintain the genome sequence. In addition, many genes identified in these screens have human homologues. Research focused on mutator genes is invaluable but does not give us a complete picture of genome maintenance.

Sequencing of entire genomes using mutation accumulation (MA) yeast strains are utilized to examine the types of spontaneous genome instability that arise and the frequency in which they occur. 145 MA strains were sequenced after passaging for a total of 311,000 generations. 924 spontaneous mutations were measured including 867 single-nucleotide changes and 3 double mutations, 8 insertions under 50 base pairs and 18 deletions under 50 base pairs, 31 whole-chromosome copy-number changes and 3 large copy-number changes >30 kilo bases (ZHU *et al.* 2014). The variety of spontaneous mutations detected suggests that there are many pathways and many gene products, which allow for tolerable levels of genome instability.

A classic example of permissive genome instability is the utilization of the translesion synthesis polymerase, Polζ. When replication machinery encounters a lesion that cannot be navigated, one option of bypass is polymerase switching. The switching of the replicative DNA polymerases for a lower fidelity TLS polymerase may result in the incorporation of an incorrect nucleotide. The

bypass mechanism may cause increases in genome instability but avoids replication fork collapse, which can be lethal. Future studies should include gene products whose wildtype function results in increased genome instability.

### 1.4 Chromatin and Genome Instability

The basic structure of chromatin is formed by the association of DNA with histone proteins; this organization is conserved from yeast to humans. The core nucleosome is comprised of 146 base pairs of double strand DNA wrapped around the canonical histones, H2A, H2B, H3, and H4, in the form of a $(H3\text{-}H4)_2$ tetramer and two H2A-H2B dimers (LUGER *et al.* 1997). Chromatin can be further compacted through post-translational modifications (PTMs) or accessory proteins. Chromatin structure is not static, DNA must be accessible for DNA replication, transcription, and DNA repair. Alteration of the local and global chromatin architecture is performed by a wide range of chromatin remodelers, histone chaperones, and histone modifiers (TSUKUDA *et al.* 2005; GOSPODINOV and HERCEG 2013). The overarching model for accessing the DNA for DNA repair in a chromatin environment is "access-repair-restore" (ODELL *et al.* 2013a; POLO and ALMOUZNI 2015) (Figure 1.2). This term describes the process of removing histones to accommodate repair complexes, followed by the restoration of the native chromatin structure.

Chromatin compaction can provide protection against genome instability. A more open chromatin state increases the probability that the DNA will be damaged, however the damaged DNA is more accessible for repair pathways. In contrast, compacted DNA is more refractory to damage but inhibits access for the repair machinery (NAIR *et al.* 2017). Nucleosome assembly through the actions of the CAF1 complex on newly replicated DNA aids in replication fork stability. Defects in nucleosome assembly after replication can result in DSB, ssDNA gaps and hyper recombination (PRADO and CLEMENTE-RUIZ 2012; AGUILERA and GARCIA-MUSE 2013). Post translational modifications aid in signaling for lesion specific DNA damage response as well as cell cycle stalling for damage repair (HUMPAL *et al.* 2009). Local chromatin architecture can influence

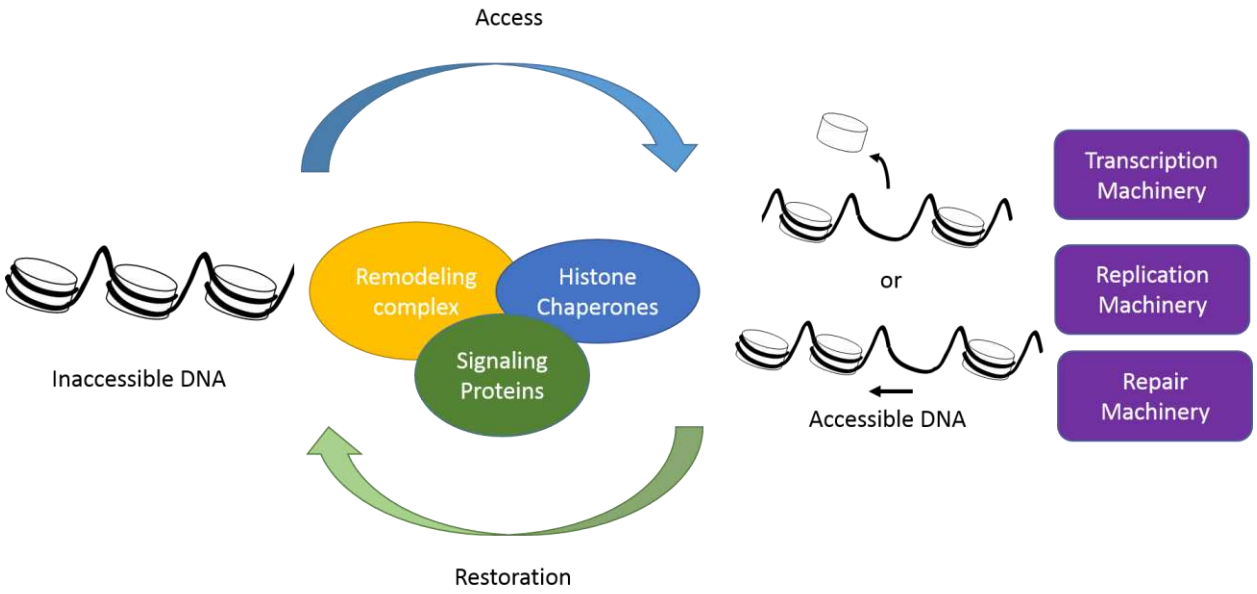


**Figure 1.2. Access, Repair, Restore**. Remodeling factors, histone chaperones, and signaling proteins work together to provide DNA access to the machinery involved in transcription, replication, and repair. After DNA processing the chromatin context must be restored.

pathway selection during DNA damage bypass and at DSBs (VAN ATTIKUM *et al.* 2007; GONZALEZ-HUICI *et al.* 2014). Heterochromatin at highly repetitive sequences prevents aberrant recombination (NAIR *et al.* 2017). As such, many chromatin factors have been identified in maintaining genome stability (PRADO and CLEMENTE-RUIZ 2012; AGUILERA and GARCIA-MUSE 2013).

### 1.5 *SPN1*

Suppresses post recruitment gene number 1 (Spn1) is a transcription elongation and chromatin binding factor (LI *et al.* 2017). The intrinsically disordered tails of Spn1 are responsible for histone, DNA and nucleosomes binding (LI *et al.* 2017), while the ordered core domain binds RNAPII and Spt6 (FISCHBECK *et al.* 2002; MCDONALD *et al.* 2010) (Figure 1.3). Historically, the function of Spn1 has been connected with Spt6, another histone chaperone, during transcription elongation. One model suggests that the Spn1-Spt6 complex surveys chromatin for proper nucleosome assembly (MCCULLOUGH *et al.* 2015). Experimental data has revealed that these two proteins can function independent of each other (ZHANG *et al.* 2008; ENGEL *et al.* 2015). Spn1 has mild nucleosome assembly functions (LI *et al.* 2017), maintains repressive chromatin (GERARD *et al.* 2015) and loss of the histone, DNA and nucleosome binding results in increased nucleosome occupancy at the activated *CYC1* locus (LI *et al.* 2017). *SPN1* genetically interacts with other histone chaperones including the FACT complex, CAF1 complex, *NAP1*, *VPS75* and *RTT106* (LI *et al.* 2017). Many of these chromatin factors may play a role in genome stability (Table 1.2).

In this study, we examined the role of the yeast protein Spn1 in maintaining the genome. Unexpectedly, our data revealed that Spn1 contributes to promoting genome instability. Moreover, we have uncovered a cell cycle progression dependence on Spn1. We found that depletion of Spn1 results in delay through the G2/M phase of the cell cycle. We theorize that these outcomes are due to the ability of Spn1 to influence chromatin structure during the cell cycle.

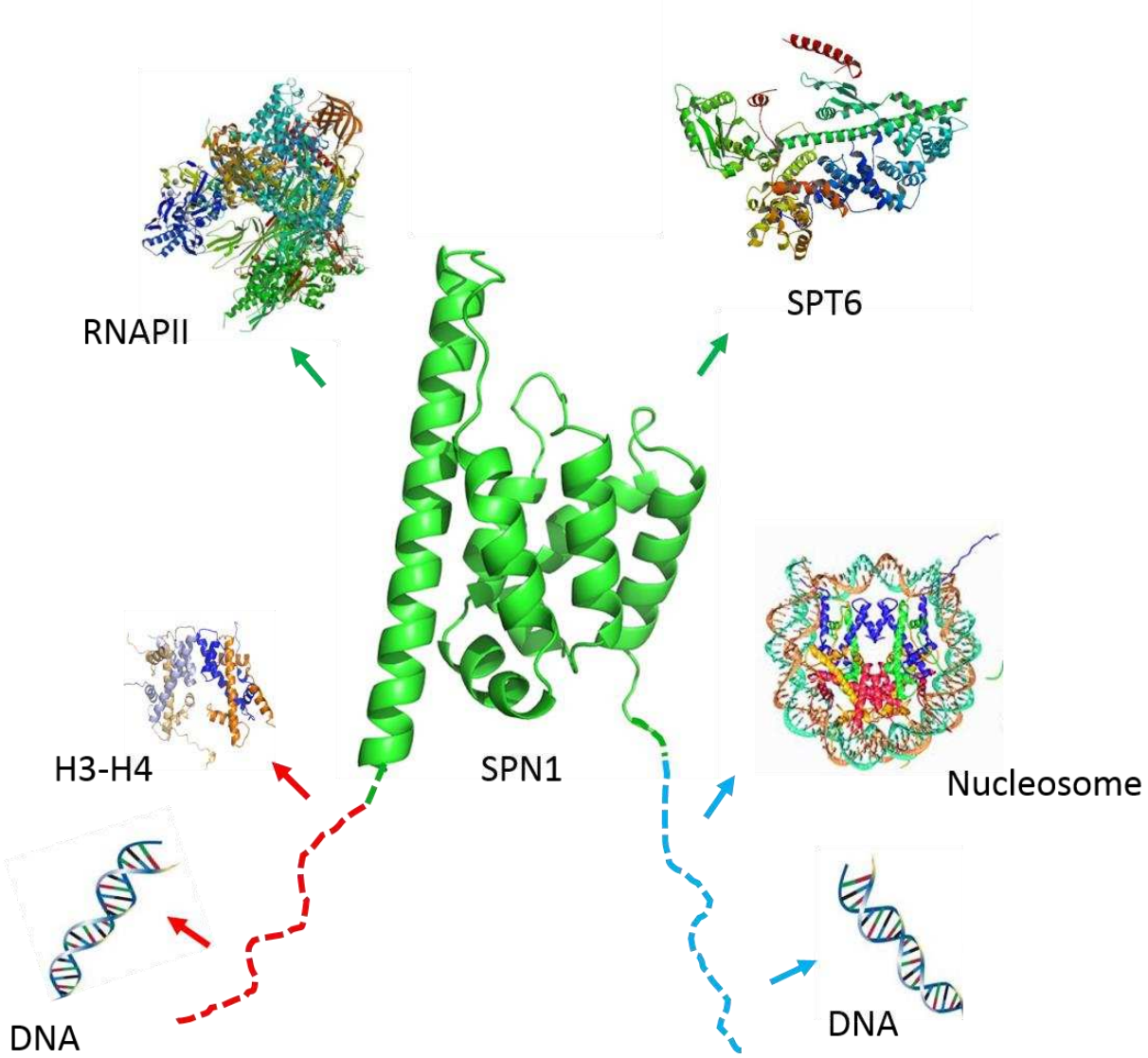


**Figure 1.3. Schematic representation of Spn1 binding partners.** Spn1 contains an ordered core domain (green) and two highly disordered tails (blue and red). Diagram above indicates Spn1 regions important for binding of chromatin factors (blue and red arrows), and other known protein-protein interactions (green arrows). Structures are not to scale; PDB#: 3NFQ (Spn1); PDB# 3PSF (Spt6), PDB# 1I50 (POLII); PDB# 1AOI (histone and nucleosome core particle). Original image made by Sha Li.

Table 1.2 Genome instability resulting from defective chromatin binding factors

| **Chromatin Factor** | **Types of genome instability reported by *Stirling et al. 2011*** |
|---|---|
| Asf1 | BiM, ALF, LOH |
| CAF | LOH, BiM |
| Rtt106 | CTF |
| FACT | GCR, CTF |
| Spn1 | CTF |
| CTF: chromosome transmission fidelity, LOH: loss of heterozygosity, BiM: bimater, GCF: gross chromosomal rearrangements, ALF: A-like faker | |

# CHAPTER 2. MATERIALS AND METHODS

## 2.1 Yeast Strains and Culturing

### *2.1.1 Culturing*

All strains were grown and experiments were performed in yeast peptone dextrose (2%) liquid cultures at 30°C unless otherwise indicated.

### *2.1.2 Spn1 mutants in deletion strains*

Description of strains are listed in Table 2.1. Description of plasmids are listed in Table 2.2. Description of primers are listed in Table 2.3.

The wild type strain BY4741, (*MAT***a** *his3Δ1 ura3Δ0 leu2Δ0 met15Δ0*) (catalog number YSC1048) and deletion strains were purchased from Thermo Scientific Open. To create strains with *spn1* mutants, deletion collection strains are transformed with a covering plasmid (pUS1) derived from pRS316 (*URA*) containing *SPN1* flanked by the *TOA1* promoter and terminator sequences. Endogenous *SPN1* is replaced by a *LEU2* fragment flanked by *SPN1* promoter (486 bp upstream and 485 bp downstream) sequences by homologous recombination. Deletion of S*PN1* is confirmed by PCR. Plasmids containing mutant alleles of *SPN1* are introduced into the deletion strains by plasmid shuffling (ZHANG *et al.* 2008; LI *et al.* 2017).

### *2.1.3 Phosphorylation mutants*

The pCR311, plasmid was used as a template for the pAT101 and pAT102 plasmids. pAT101 and pAT102 were transformed into L0 strain and shuffled as described above. The pAT101 plasmid was used as a template for pAT103. pAT102 was used as a template to make pAT104 and pAT105. Primers are listed in Table 2.2. To verify mutation, strains were sequenced using STA238 primer and M13 reverse primer. Plasmids pAT103, pAT104, and pAT105 were transformed into the L0, AT141 (*mms2Δ)* and CR82 (*sgs1Δ*) strains and shuffled as described above.

### *2.1.4 Loss of heterozygosity*

To create diploid strains for the loss of heterozygosity assay strain *LOH_1* and *LOH_2* were mated. Diploids were selected on SC-Met-Lys plates resulting in *LOH_3*. To make *LOH_2* the covering plasmid pUS1 was transformed into BY4742 and endogenous *SPN1* is replaced by a *LEU2* fragment flanked by the *SPN1* promoter. Strain *LOH_1* was created by replacing *CAN1* with a *natMX4* fragment including the promoter and terminator and 40 bp of the *CAN1* promoter and terminator. *natMX4* linear DNA was created using protocols, primers and plasmids constructed by the Argueso Laboratory (Table 2.2 and 2.3). Insertion was verified by PCR. Following colony purification of *LOH_3*; pCR311, pCR312 and pAA344 were introduced and shuffled to create the final diploid strains, *LOH_SPN1*, *LOH_spn1*$^{K192N}$ and *LOH_spn1*$^{141-305}$ (Table 2.1).

## 2.2 Phenotypic Assays

To assess the *spn1* growth phenotypes and genetic interactions between *SPN1* and deletion background strains, yeast strains were cultured overnight in YPD. Cultures were diluted and grown to log phase. Cells were collected, washed with sterile water and diluted. Ten-fold dilutions were platted onto the indicated media. Plates were grown at 30°C except for temperature sensitivity growth, which was assessed at 39°C. Images of plates were taken daily. Methyl methanesulfonate (MMS), menadione, camptothecin (CPT) and hydrogen peroxide ($H_20_2$) plates were made fresh before each experiment. UV exposure was performed with a UVP UVLMS-38 light source at a wavelength of 254 nm courtesy of the Santangelo Laboratory at CSU.

## 2.3 Fluctuation Analysis

Indicated strains were patched and grown for 24 hours on YPD. Strains were streaked onto YPD plates and grown for 48 hours. Replicates of each strain were inoculated and allowed to grow for 24 hours in 5 mL of YPD. Cells were washed and appropriate dilutions of cells were plated on YPD and SC-Arg + 60 µg/L canavanine plates. Colonies were counted after two and three day growth, respectively. To calculate the mutation rate of each strain we utilized the FALCOR:

fluctuation analysis calculator program (HALL *et al.* 2009) and the Lea-Coulson method of the median (LEA and COULSON 1949). Statistical significance was determined using the Mann-Whitney non-parametric t-test on the graph pad platform. For damage induced mutation rates the same protocol was followed except strains were streaked onto plates containing YPD+ 0.001% MMS after patching and inoculated into YPD +0.005% MMS cultures. Strains containing the *mms2Δ* background were inoculated in YPD + 0.001% MMS cultures due to strain sensitivity to higher MMS concentrations. Plates and liquid media containing MMS were made fresh.

### 2.4 Loss of Heterozygosity Assay

To examine the loss of heterozygosity a diploid strain containing only one functional copy of *CAN1* was created as described above. Strains were patched and allowed to grow for 24 hours on YPD. Strains were streaked onto YPD plates for single colonies and allowed to grow for 48 hours. Replicates of each strain were inoculated and allowed to grow for 24 hours in 5 mL of YPD. Appropriate dilutions of cells were platted on YPD and SC-Arg + 60 µg/L canavanine plates. Colonies were counted after two and three days respectively. To calculate the LOH rate of each strain we utilized the FALCOR: fluctuation analysis calculator program (HALL *et al.* 2009). We analyzed 27 replicates of each strain using the Lea-Coulson method of the median (LEA and COULSON 1949). Statistical significance was determined using the Mann-Whitney non-parametric t-test on the graph pad platform.

### 2.5 Budding Index

Overnight cultures were diluted and cells were grown to log phase. YPD cultures were split and 0.03% MMS was added to half for 30 minutes. Cells were washed and fixed with formalin, following the GFP fixation protocol from the Koshland Laboratory at UC Berkeley available on their website. At least, 300 cells were counted for each strain. Identification of cell cycle was determined by bud size.

### 2.6 Immunoblotting Analysis

Cells were harvested at log phase and suspended in 0.1 M NaOH for 5 minutes. NaOH was removed and cell pellet was resuspended in lysis buffer (120 mM Tris-HCl [pH 6.8], 12% glycerol, 3.4% SDS, 200 mM dithiothreitol [DTT], 0.004% bromophenol blue), and incubated at 95°C for 5 minutes. To determine levels of Spn1 in Spn1_DAmP strains, NaOH incubation was not carried out. Insoluble cell debris was removed by centrifugation, and total protein was separated on SDS-PAGE gel. The following antibodies were utilized: anti-TBP (1:5,000), anti-H2AS129 phosphorylation (abcam #ab15083, 1:500), anti-rabbit (Li-COR #925-32211, 1:15000), and anti-Spn1 (1:10000). Protein bands were imaged using the Li-COR Odyssey CLx and band quantification was performed using Image Studio.

### 2.7 Micrococcal Nuclease Digestion

The preparation of spheroplast, micrococcal nuclease (MNase) digestion, purification of genomic DNA, and detection of products by indirect end-labeling were carried out as described in (Li *et al.* 2017). Cells were grown in YPD. Cells were washed and resuspended in sorbitol buffer (50mM Tris-Cl pH 7.5, 1M sorbitol, 10mM MgCl2, 2mM DTT, 1 mM PMSF). Cells were treated with zymolase (3.4 mg/ml glucose) at 30°C for spheroplast formation. Cells were resuspended in MNase digestion buffer (0.175 g/ml) (10 mM Tris-Cl pH 7.5, 1 mM CaCl2, 50 mM NaCl, 5mM MgCl 0.5mM Spermidine, 0.75% NP-40, 1mM DTT). Cells were aliquoted and MNase digestion was carried (0-266 mU/µl) out for 30 minutes at 37°C. Digestion was quenched by addition of 100 µl stop solution (140mM EDTA, 3.5% SDS, 0.45 mg/ml Proteinase K) and incubated overnight at 37°C. Samples were treated with RNase A and harvested using standard phenol extraction method followed by ethanol precipitation. The extent of MNase digestion was analyzed by DNA separation on a 1.5% agarose gel and visualized through ethidium bromide staining.

### 2.8 Indirect End Labeling

Detection of *CYC1* digestion products was carried out as described in (CAVALLI and THOMA 1993). A DNA fragment complimentary to downstream of *GAL1* was labeled with 32P using a Random Primer DNA Labeling Kit (TaKaRa Bio Incorporated #6045). DNA samples were digested using EcoRV. The digested samples were run on a 1.5% agarose-TBE gel and run at 5.5V/cm. The DNA was transferred to a Nylon membrane (Gene Screen) using capillary transfer. The DNA was fixed to the membrane using ultra-violet light exposure for 5 minutes while the membrane was still wet. Hybridization proceeded overnight at 65°C. Unincorporated probe was washed away. The membrane was exposed a to phosphorimager screen overnight. Images were acquired using Typhon FLA 9000 (GE Healthcare) and quantified using image quant.

### 2.9 Spn1 Molecules per Cell

Cells were grown overnight in YPD. Cultures were diluted and grown to a ~0.5 OD. Cell count was determined by hemocytometer and aliquots were taken such that the same sample volume for each biological replicate could be run on a gel and the signal of Spn1 would remain within the standard curve. Cell lysate samples were prepared as described above without the NaOH incubation. Each SDS-PAGE gel contained a standard curve (0-10 ng of purified Spn1) and biological samples. Samples were run on 10% SDS-polyacrylamide gel. Polyclonal Spn1 antibody (1:15000) was used to detect Spn1 protein followed by anti-rabbit secondary antibody (1:10,000; Licor P/N 925-32211). Abundance was calculating using the corresponding standard curve and cell count as determined by hemocytometer (GHAEMMAGHAMI *et al.* 2003; MCCULLOUGH *et al.* 2015). The final reported molecules per cell value accounted for a His tagged present on recombinant Spn1. Recombinant Spn1 was provided by Sha Li (LI *et al.* 2017).

### 2.10 Flow Cytometry

DNA staining for flow cytometry was carried out using the protocol described in (ALLEN *et al.* 2006), with a few modifications. Briefly, ~$1x10^7$ log growth cells were collected and fixed overnight

at 4°C in 2 mL 70% ethanol. Cells were washed 2x with Tris buffer (50 mM Tris buffer pH 7.5). RNA was digested by incubating cells in 1 g/mL RNAse A in 1 mL tris buffer overnight in a 37°C water bath. This step is extremely important to degrade all the RNA. The next morning samples were spiked with ~300 mg/mL of RNAse A and left for 1-2 hours to ensure RNA degradation. Samples were spun down and resuspended in 1.5 mL of fresh pepsin solution (5 mg/mL in water with 55 μL of 1M HCl per mL solution) and incubated for 10-15 minutes. Samples were spun down and washed 2x with TE buffer (10 mM Tris and 1 mM EDTA, pH 7.5). Samples were resuspended in SYBR green staining solution (1:10000 SYBR Green in Tris buffer). Samples were stained overnight at 4°C. A non-stained sample was incubated in Tris buffer overnight. Samples were washed 2x in Tris buffer and diluted for sampling. Flow cytometry was carried out with help of Chris Allen. 30,000 cells were counted for cell cycle analysis per sample using a CyAn ADP flow cytometer at 488 nm excitation and collecting fluorescent emission with filters at 530/40 nm for FL-1 parameter. Data was collected using Summit software. Analysis was performed using FlowJo and ModFit software.

### 2.11 Chronological Aging Assay

This experiment was carried out by Adam Almeida. Strains were inoculated in synthetic dropout (SD) media and grown overnight. Cultures were diluted to an OD of 0.1 and grown in SD media for 3 days (72 hours) to ensure cultures have reached stationary phase (**T0**). To determine viability, dilutions of each biological replicate were plated daily onto YPD plates. Dilutions and plating were carried out in triplicate and averaged for each biological replicate. 4-5 biological replicates for each strain was averaged to determine the % viability. The % viability is the ratio of viable colonies at a specific time (**Tn**) over the number of viable colonies at **T0** (stationary phase).

Table 2.1 Strains

| Identifier | Common Name | Description | Source |
|---|---|---|---|
| BY4741 | BY4741 | MATa his3Δ1 leu2Δ0 met15Δ0 ura3Δ0 | Thermo Scientific |
| BY4742 | BY4742 | MATα his3Δ1 leu2Δ0 lys2Δ0 ura3Δ0 | Thermo Scientific |
| LZ0 | LZ0 | BY4741 + *spn1*::LUE2, pRS316-*SPN1* (*URA3*) | Zhang et al |
| LZ1 | *SPN1* | LZ0 + pCR311, lacking pRS316-SPN1 (URA3) | Li et al |
| LZ2 | *spn1*$^{K192N}$ | LZ0 + pCR312, lacking pRS316-SPN1 (URA3) | Li et al |
| LZ3 | *spn1*$^{141-305}$ | LZ0 + pCR344, lacking pRS316-SPN1 (URA3) | Li et al |
| AT102 | *apn1Δ SPN1* | *apn1*::KANMX + *spn1*::LUE2, pCR311 | This study |
| AT103 | *apn1Δ spn1*$^{K192N}$ | *apn1*::KANMX + *spn1*::LUE2, pCR312 | This study |
| AT104 | *apn1Δ spn1*$^{141-305}$ | *apn1*::KANMX + *spn1*::LUE2, pCR344 | This study |
| AT106 | *apn2Δ SPN1* | *apn2*::KANMX + *spn1*::LUE2, pCR311 | This study |
| AT107 | *apn2Δ spn1*$^{K192N}$ | *apn2*::KANMX + *spn1*::LUE2, pCR312 | This study |
| AT108 | *apn2Δ spn1*$^{141-305}$ | *apn2*::KANMX + *spn1*::LUE2, pCR344 | This study |
| AT114 | *clb1Δ SPN1* | *clb1*::KANMX + *spn1*::LUE2, pCR311 | This study |
| AT115 | *clb1Δ spn1*$^{K192N}$ | *clb1*::KANMX + *spn1*::LUE2, pCR312 | This study |
| AT116 | *clb1Δ spn1*$^{141-305}$ | *clb1*::KANMX + *spn1*::LUE2, pCR344 | This study |
| AT118 | *cln3Δ SPN1* | *cln3*::KANMX + *spn1*::LUE2, pCR311 | This study |
| AT119 | *cln3Δ spn1*$^{K192N}$ | *cln3*::KANMX + *spn1*::LUE2, pCR312 | This study |
| AT120 | *cln3Δ spn1*$^{141-305}$ | *cln3*::KANMX + *spn1*::LUE2, pCR344 | This study |
| AT122 | *dot1Δ SPN1* | *dot1*::KANMX + *spn1*::LUE2, pCR311 | This study |
| AT123 | *dot1Δ spn1*$^{K192N}$ | *dot1*::KANMX + *spn1*::LUE2, pCR312 | This study |
| AT124 | *dot1Δ spn1*$^{141-305}$ | *dot1*::KANMX + *spn1*::LUE2, pCR344 | This study |
| AT126 | *exo1Δ SPN1* | *exo1*::KANMX + *spn1*::LUE2, pCR311 | This study |
| AT127 | *exo1Δ spn1*$^{K192N}$ | *exo1*::KANMX + *spn1*::LUE2, pCR312 | This study |
| AT128 | *exo1Δ spn1*$^{141-305}$ | *exo1*::KANMX + *spn1*::LUE2, pCR344 | This study |
| AT130 | *hfm1Δ SPN1* | *hfm1*::KANMX + *spn1*::LUE2, pCR311 | This study |
| AT131 | *hfm1Δ spn1*$^{K192N}$ | *hfm1*::KANMX + *spn1*::LUE2, pCR312 | This study |
| AT132 | *hfm1Δ spn1*$^{141-305}$ | *hfm1*:KANMX + *spn1*::LUE2, pCR344 | This study |
| AT134 | *iws1Δ SPN1* | *isw1*::KANMX + *spn1*::LUE2, pCR311 | This study |
| AT135 | *iws1Δ spn1*$^{K192N}$ | *isw1*::KANMX + *spn1*::LUE2, pCR312 | This study |
| AT136 | *iws1Δspn1*$^{141-305}$ | *isw1*:KANMX + *spn1*::LUE2, pCR344 | This study |
| AT138 | *mag1ΔSPN1* | *mag1*:KANMX + *spn1*::LUE2, pCR311 | This study |
| AT139 | *mag1Δspn1*$^{K192N}$ | *mag1*:KANMX + *spn1*::LUE2, pCR312 | This study |
| AT140 | *mag1Δspn1*$^{141-305}$ | *mag1*KANMX + *spn1*::LUE2, pCR344 | This study |
| AT141 | AT141 | *mms2Δ* + *spn1*::LUE2, pRS316-*SPN1* (*URA3*) | This study |
| AT142 | *mms2Δ SPN1* | *mms2*::KANMX + *spn1*::LUE2, pCR311 | This study |
| AT143 | *mms2Δ spn1*$^{K192N}$ | *mms2::*KANMX + *spn1*::LUE2, pCR312 | This study |

| | | | |
|---|---|---|---|
| AT144 | *mms2Δ spn1*$^{141-305}$ | *mms2::*KANMX + *spn1*::LUE2, pCR344 | This study |
| AT146 | *msn2ΔSPN1* | *msn2*::KANMX + *spn1*::LUE2, pCR311 | This study |
| AT147 | *msn2Δspn1*$^{K192N}$ | *msn2::*KANMX + *spn1*::LUE2, pCR312 | This study |
| AT148 | *msn2Δspn1*$^{141-305}$ | *msn2::*KANMX + *spn1*::LUE2, pCR344 | This study |
| AT150 | *msn4ΔSPN1* | *msn4:*:KANMX + *spn1*::LUE2, pCR311 | This study |
| AT151 | *msn4Δspn1*$^{K192N}$ | *msn4::*KANMX + *spn1*::LUE2, pCR312 | This study |
| AT152 | *msn4Δspn1*$^{141-305}$ | *msn4::*KANMX + *spn1*::LUE2, pCR344 | This study |
| AT154 | *ntg1ΔSPN1* | *ntg1:*:KANMX + *spn1*::LUE2, pCR311 | This study |
| AT155 | *ntg1Δspn1*$^{K192N}$ | *ntg1::*KANMX + *spn1*::LUE2, pCR312 | This study |
| AT156 | *ntg1Δspn1*$^{141-305}$ | *ntg1::*KANMX + *spn1*::LUE2, pCR344 | This study |
| AT162 | *rad14ΔSPN1* | *rad14:*:KANMX + *spn1*::LUE2, pCR311 | This study |
| AT163 | *rad14Δspn1*$^{K192N}$ | *rad14::*KANMX + *spn1*::LUE2, pCR312 | This study |
| AT164 | *rad14Δspn1*$^{141-305}$ | *rad14::*KANMX + *spn1*::LUE2, pCR344 | This study |
| AT166 | *rad18ΔSPN1* | *rad18:*:KANMX + *spn1*::LUE2, pCR311 | This study |
| AT167 | *rad18Δspn1*$^{K192N}$ | *rad18::*KANMX + *spn1*::LUE2, pCR312 | This study |
| AT168 | *rad18Δspn1*$^{141-305}$ | *rad18::*KANMX + *spn1*::LUE2, pCR344 | This study |
| AT170 | *rad23ΔSPN1* | *rad23:*:KANMX + *spn1*::LUE2, pCR311 | This study |
| AT171 | *rad23Δspn1*$^{K192N}$ | *rad23::*KANMX + *spn1*::LUE2, pCR312 | This study |
| AT172 | *rad23Δspn1*$^{141-305}$ | *rad23::*KANMX + *spn1*::LUE2, pCR344 | This study |
| AT174 | *rad26ΔSPN1* | *rad26:*:KANMX + *spn1*::LUE2, pCR311 | This study |
| AT175 | *rad26Δspn1*$^{K192N}$ | *rad26::*KANMX + *spn1*::LUE2, pCR312 | This study |
| AT176 | *rad26Δspn1*$^{141-305}$ | *rad26::*KANMX + *spn1*::LUE2, pCR344 | This study |
| AT178 | *rad30ΔSPN1* | *rad30:*:KANMX + *spn1*::LUE2, pCR311 | This study |
| AT179 | *rad30Δspn1*$^{K192N}$ | *rad30::*KANMX + *spn1*::LUE2, pCR312 | This study |
| AT180 | *rad30Δspn1*$^{141-305}$ | *rad30::*KANMX + *spn1*::LUE2, pCR344 | This study |
| AT182 | *rad5Δ SPN1* | *rad5:*:KANMX + *spn1*::LUE2, pCR311 | This study |
| AT183 | *rad5Δ spn1*$^{K192N}$ | *rad5::*KANMX + *spn1*::LUE2, pCR312 | This study |
| AT184 | *rad5Δ spn1*$^{141-305}$ | *rad5::*KANMX + *spn1*::LUE2, pCR344 | This study |
| AT186 | *rad51Δ SPN1* | *rad51:*:KANMX + *spn1*::LUE2, pCR311 | This study |
| AT187 | *rad51Δ spn1*$^{K192N}$ | *rad51:*KANMX + *spn1*::LUE2, pCR312 | This study |
| AT188 | *rad51Δ spn1*$^{141-305}$ | *rad51:*KANMX + *spn1*::LUE2, pCR344 | This study |
| AT194 | *rad55Δ SPN1* | *rad55:*:KANMX + *spn1*::LUE2, pCR311 | This study |
| AT195 | *rad55Δ spn1*$^{K192N}$ | *rad55:*KANMX + *spn1*::LUE2, pCR312 | This study |
| AT196 | *rad55Δ spn1*$^{141-305}$ | *rad55:*KANMX + *spn1*::LUE2, pCR344 | This study |
| AT198 | *rad57Δ SPN1* | *rad57:*:KANMX + *spn1*::LUE2, pCR311 | This study |
| AT199 | *rad57Δ spn1*$^{K192N}$ | *rad57:*KANMX + *spn1*::LUE2, pCR312 | This study |
| AT200 | *rad57Δ spn1*$^{141-305}$ | *rad57:*KANMX + *spn1*::LUE2, pCR344 | This study |
| AT202 | *rev1ΔSPN1* | *rev1:*:KANMX + *spn1*::LUE2, pCR311 | This study |

| | | | |
|---|---|---|---|
| AT203 | *rev1Δspn1*$^{K192N}$ | *rev1::*KANMX + *spn1*::LUE2, pCR312 | This study |
| AT204 | *rev1Δspn1*$^{141-305}$ | *rev1::*KANMX + *spn1*::LUE2, pCR344 | This study |
| AT206 | *rev3ΔSPN1* | *rev3::*KANMX + *spn1*::LUE2, pCR311 | This study |
| AT207 | *rev3Δspn1*$^{K192N}$ | *rev3::*KANMX + *spn1*::LUE2, pCR312 | This study |
| AT208 | *rev3Δspn1*$^{141-305}$ | *rev3::*KANMX + *spn1*::LUE2, pCR344 | This study |
| AT210 | *rev7ΔSPN1* | *rev7::*KANMX + *spn1*::LUE2, pCR311 | This study |
| AT211 | *rev7Δspn1*$^{K192N}$ | *rev7::*KANMX + *spn1*::LUE2, pCR312 | This study |
| AT212 | *rev7Δspn1*$^{141-305}$ | *rev7::*KANMX + *spn1*::LUE2, pCR344 | This study |
| AT214 | *rmi1ΔSPN1* | *rmi1::*KANMX + *spn1*::LUE2, pCR311 | This study |
| AT215 | *rmi1Δspn1*$^{K192N}$ | *rmi1::*KANMX + *spn1*::LUE2, pCR312 | This study |
| AT216 | *rmi1Δspn1*$^{141-305}$ | *rmi1::*KANMX + *spn1*::LUE2, pCR344 | This study |
| AT218 | *sae2ΔSPN1* | *sae2::*KANMX + *spn1*::LUE2, pCR311 | This study |
| AT219 | *sae2Δspn1*$^{K192N}$ | *sae2::*KANMX + *spn1*::LUE2, pCR312 | This study |
| AT220 | *sae2Δspn1*$^{141-305}$ | *sae2::*KANMX + *spn1*::LUE2, pCR344 | This study |
| AT222 | *siz1ΔSPN1* | *siz1::*KANMX + *spn1*::LUE2, pCR311 | This study |
| AT223 | *siz1Δspn1*$^{K192N}$ | *siz1::*KANMX + *spn1*::LUE2, pCR312 | This study |
| AT224 | *siz1Δspn1*$^{141-305}$ | *siz1::*KANMX + *spn1*::LUE2, pCR344 | This study |
| AT226 | *srs2ΔSPN1* | *srs2::*KANMX + *spn1*::LUE2, pCR311 | This study |
| AT227 | *srs2Δspn1*$^{K192N}$ | *srs2::*KANMX + *spn1*::LUE2, pCR312 | This study |
| AT228 | *srs2Δspn1*$^{141-305}$ | *srs2::*KANMX + *spn1*::LUE2, pCR344 | This study |
| AT230 | *tel1ΔSPN1* | *tel1::*KANMX + *spn1*::LUE2, pCR311 | This study |
| AT231 | *tel1Δspn1*$^{K192N}$ | *tel1::*KANMX + *spn1*::LUE2, pCR312 | This study |
| AT232 | *tel1Δspn1*$^{141-305}$ | *tel1::*KANMX + *spn1*::LUE2, pCR344 | This study |
| AT234 | *top3ΔSPN1* | *top3::*KANMX + *spn1*::LUE2, pCR311 | This study |
| AT235 | *top3Δspn1*$^{K192N}$ | *top3::*KANMX + *spn1*::LUE2, pCR312 | This study |
| AT236 | *top3Δspn1*$^{141-305}$ | *top3::*KANMX + *spn1*::LUE2, pCR344 | This study |
| AT238 | *ubc13ΔSPN1* | *ubc13::*KANMX + *spn1*::LUE2, pCR311 | This study |
| AT239 | *ubc13Δspn1*$^{K192N}$ | *ubc13::*KANMX + *spn1*::LUE2, pCR312 | This study |
| AT240 | *ubc13Δspn1*$^{141-305}$ | *ubc13::*KANMX + *spn1*::LUE2, pCR344 | This study |
| CR58A | *rad6Δ SPN1* | *rad6::*KANMX + *spn1*::LUE2, pCR311 | This study |
| CR58B | *rad6Δ spn1*$^{K192N}$ | *rad6::*KANMX + *spn1*::LUE2, pCR312 | This study |
| CR58C | *rad6Δ spn1*$^{141-305}$ | *rad6::*KANMX + *spn1*::LUE2, pCR344 | This study |
| CR60A | *rad9Δ SPN1* | *rad9::*KANMX + *spn1*::LUE2, pCR311 | This study |
| CR60B | *rad9Δ spn1*$^{K192N}$ | *rad9::*KANMX + *spn1*::LUE2, pCR312 | This study |
| CR60C | *rad9Δ spn1*$^{141-305}$ | *rad9::*KANMX + *spn1*::LUE2, pCR344 | This study |
| CR77A | *rad17Δ SPN1* | *rad17::*KANMX + *spn1*::LUE2, pCR311 | This study |
| CR77B | *rad17Δ spn1*$^{K192N}$ | *rad17::*KANMX + *spn1*::LUE2, pCR312 | This study |
| CR77C | *rad17Δ spn1*$^{141-305}$ | *rad17::*KANMX + *spn1*::LUE2, pCR344 | This study |

| | | | |
|---|---|---|---|
| CR80A | mre11Δ *SPN1* | *mre11*::KANMX + *spn1*::LUE2, pCR311 | This study |
| CR80B | *mre11Δ spn1*$^{K192N}$ | *mre11::*KANMX + *spn1*::LUE2, pCR312 | This study |
| CR80C | *mre11Δ spn1*$^{141-305}$ | *mre11::*KANMX + *spn1*::LUE2, pCR344 | This study |
| CR81A | xrs2Δ *SPN1* | *xrs2::*KANMX + *spn1*::LUE2, pCR311 | This study |
| CR81B | *xrs2Δ spn1*$^{K192N}$ | *xrs2::*KANMX + *spn1*::LUE2, pCR312 | This study |
| CR81C | *xrs2Δ spn1*$^{141-305}$ | *xrs2::*KANMX + *spn1*::LUE2, pCR344 | This study |
| CR82 | CR82 | *sgs1Δ* + *spn1*::LUE2, pRS316-*SPN1* (*URA3*) | |
| CR82A | sgs1Δ *SPN1* | *sgs1::*KANMX + *spn1*::LUE2, pCR311 | This study |
| CR82B | *sgs1Δ spn1*$^{K192N}$ | *sgs1::*KANMX + *spn1*::LUE2, pCR312 | This study |
| CR82C | *sgs1Δ spn1*$^{141-305}$ | *sgs1::*KANMX + *spn1*::LUE2, pCR344 | This study |
| CR86A | *rad24Δ SPN1* | *rad24::*KANMX + *spn1*::LUE2, pCR311 | This study |
| CR86B | *rad24Δ spn1*$^{K192N}$ | *rad24::*KANMX + *spn1*::LUE2, pCR312 | This study |
| CR86C | *rad24Δ spn1*$^{141-305}$ | *rad24::*KANMX + *spn1*::LUE2, pCR344 | This study |
| CR61A | *pol4ΔSPN1* | *pol4::*KANMX + *spn1*::LUE2, pCR311 | This study |
| CR61B | *pol4Δspn1*$^{K192N}$ | *pol4:*KANMX + *spn1*::LUE2, pCR312 | This study |
| CR61C | *pol4Δspn1*$^{141-305}$ | *pol4::*KANMX + *spn1*::LUE2, pCR344 | This study |
| CR31A | *rtt109ΔSPN1* | *rtt109::*KANMX + *spn1*::LUE2, pCR311 | This study |
| CR31B | *rtt109Δspn1*$^{K192N}$ | *rtt109:*KANMX + *spn1*::LUE2, pCR312 | This study |
| CR31C | *rtt109Δspn1*$^{141-305}$ | *rtt109::*KANMX + *spn1*::LUE2, pCR344 | This study |
| AT241 | *spn1*$^{S23A}$ | LZ0 + pAT101, lacking pRS316-SPN1 (URA3) | This study |
| AT242 | *spn1*$^{S23D}$ | LZ0 + pAT102, lacking pRS316-SPN1 (URA3) | This study |
| AT243 | *spn1*$^{S22AS23A}$ | LZ0 + pAT103, lacking pRS316-SPN1 (URA3) | This study |
| AT244 | *spn1*$^{S22AS23D}$ | LZ0 + pAT104, lacking pRS316-SPN1 (URA3) | This study |
| AT245 | *spn1*$^{S22DS23D}$ | LZ0 + pAT105, lacking pRS316-SPN1 (URA3) | This study |
| AT246 | *mms2Δ spn1*$^{S22AS23A}$ | *mms2*::KANMX + *spn1*::LUE2, pAT103 | This study |
| AT247 | *mms2Δ spn1*$^{S22AS23D}$ | *mms2*::KANMX + *spn1*::LUE2, pAT104 | This study |
| AT248 | *mms2Δ spn1*$^{S22DS23D}$ | *mms2*::KANMX + *spn1*::LUE2, pAT105 | This study |
| AT249 | *sgs1Δ spn1*$^{S22AS23A}$ | *sgs1*::KANMX + *spn1*::LUE2, pAT103 | This study |
| AT250 | *sgs1Δ spn1*$^{S22AS23D}$ | *sgs1*::KANMX + *spn1*::LUE2, pAT104 | This study |
| AT251 | *sgs1Δ spn1*$^{S22DS23D}$ | *sgs1*::KANMX + *spn1*::LUE2, pAT105 | This study |
| AT252 | *SPN1 SPN1* | MATa his3Δ1 leu2Δ0 met15Δ0 ura3Δ0, pCR311 (HIS) | This study |
| AT253 | *SPN1 spn1*$^{K192N}$ | MATa his3Δ1 leu2Δ0 met15Δ0 ura3Δ0, pCR312 (HIS) | This study |
| AT254 | *SPN1 spn1*$^{141-305}$ | MATa his3Δ1 leu2Δ0 met15Δ0 ura3Δ0, pCR344 (HIS) | This study |
| AT255 | *LOH_1* | BY4741 + *spn1*::LUE2, *can1::NAT1* pRS316-*SPN1* (*URA3*) | This study |
| AT256 | *LOH_2* | BY4742 + *spn1*::LUE2, pRS316-*SPN1* (*URA3*) | This study |

| | | | |
|---|---|---|---|
| AT257 | *LOH_3* | BY4741/BY4742 + *spn1*::LUE2/spn1::LUE2 *can1::natMX4/CAN1* pRS316-*SPN1* (*URA3*) | This study |
| AT258 | *LOH_SPN1* | BY4741/BY4742 + *spn1*::LUE2/spn1::LUE2 *can1::natMX4/CAN1* pCR311 | This study |
| AT259 | *LOH_SPN1*$^{K192N}$ | BY4741/BY4742 + *spn1*::LUE2/spn1::LUE2 *can1::natMX4/CAN1* pCR312 | This study |
| AT260 | *LOH_SPN1*$^{141-305}$ | BY4741/BY4742 + *spn1*::LUE2/spn1::LUE2 *can1::natMX4/CAN1* pCR344 | This study |
| W303-1B | W303-1B | *MATα leu2-3,112 trp1-1 can1-100 ura3-1 ade2-1 his3-11,15* | Li, 2018 |
| HHY168 | HHY168 | Isogenic to W303-1B except tor11 fpr1::NAT rpl13A-2×FKBP12::TRP1 | Li, 2018 |
| Spn1_AA | *Spn1_AA* | HHY168 + SPN1-FRB His3MX6 | Li, 2018 |
| Spn1_DAmP_GE | Spn1_DAmP_GE | MATa his3Δ1 leu2Δ0 met15Δ0 ura3Δ0 *SPN1-KANMX6* | Dharmacon |
| Spn1_DAmP_LAS | Spn1_DAmP_LAS | MATa his3Δ1 leu2Δ0 met15Δ0 ura3Δ0 *SPN1-KANMX6* | This study |
| Spt6_DAmP_GE | Spt6_DAmP_GE | MATa his3Δ1 leu2Δ0 met15Δ0 ura3Δ0 *SPT6-KANMX6* | Dharmacon |

Table 2.2 Plasmids

| Plasmids | Description |
|---|---|
| pCR 311 | Full length wild type SPN1 with 403 bp of upstream sequence and 116bp of downstream sequence, myc2 tagged at the amino terminus, pRS313 (CEN, HIS3) |
| pCR 312 | spn1$^{K192N}$ with 403 bp of upstream sequence and 116bp of downstream sequence, myc2 tagged at the amino terminus, pRS313 (CEN, HIS3) |
| pAA 344 | spn1$^{141-305}$ with 403 bp of upstream sequence and 116bp of downstream sequence, myc2 tagged at the amino terminus, pRS313 (CEN, HIS3) |
| pAA 317 | spn1$^{1-305}$ with 403 bp of upstream sequence and 116bp of downstream sequence, myc2 tagged at the amino terminus, pRS313 (CEN, HIS3) |
| pAA 342 | spn1$^{141-410}$ with 403 bp of upstream sequence and 116bp of downstream sequence, myc2 tagged at the amino terminus, pRS313 (CEN, HIS3) |
| pAT 101 | spn1$^{S23A}$ with 403 bp of upstream sequence and 116bp of downstream sequence, myc2 tagged at the amino terminus, pRS313 (CEN, HIS3) |
| pAT 102 | spn1$^{S23D}$ with 403 bp of upstream sequence and 116bp of downstream sequence, myc2 tagged at the amino terminus, pRS313 (CEN, HIS3) |
| pAT 103 | spn1$^{S22AS23A}$ with 403 bp of upstream sequence and 116bp of downstream sequence, myc2 tagged at the amino terminus, pRS313 (CEN, HIS3) |
| pAT 104 | spn1$^{S22AS23D}$ with 403 bp of upstream sequence and 116bp of downstream sequence, myc2 tagged at the amino terminus, pRS313 (CEN, HIS3) |
| pAT 105 | spn1$^{S22DS23D}$ with 403 bp of upstream sequence and 116bp of downstream sequence, myc2 tagged at the amino terminus, pRS313 (CEN, HIS3) |
| pAG25 | natMX4 |

Table 2.3 Primers

| Name | Primer Sequence | Description |
|---|---|---|
| STA238 | CTGAAGTATATATAGAGG | 57 BP up stream of Spn1 start codon |
| STA763 | GTTTATAGTTGACTTTTGGGCGGAAGCTGTCCCATCTTC | Spn1 S23A reverse |
| STA764 | GAAGATGGGACAGCTTCCGCCCAAAAGTCAACTATAAAC | Spn1 S23A forward |
| STA765 | CGTTTATAGTTGACTTTTGGTCGGAAGCTGTCCCATCTTCTG | Spn1 S23D reverse |
| STA766 | CAGAAGATGGGACAGCTTCCGACCAAAAGTCAACTATAAACG | Spn1 S23D forward |
| STA778 | CTTTTGGGCGGCAGCTGTCCCATCTTCTGGTG | Spn1 S22AS23A reverse |
| STA779 | CACCAGAAGATGGGACAGCTGCCGCCCAAAAG | Spn1 S22AS23A forward |
| STA780 | TTGACTTTTGGTCGGCAGCTGTCCCATCTTCTGG | Spn1 S22AS23D reverse |
| STA781 | CCAGAAGATGGGACAGCTGCCGACCAAAAGTCAA | Spn1 S22AS23D forward |
| STA782 | ATAGTTGACTTTTGGTCGTCAGCTGTCCCATCTTCTGGTG | Spn1 S22DS23D reverse |
| STA783 | CACCAGAAGATGGGACAGCTGACGACCAAAAGTCAACTAT | Spn1 S22DS23D forward |
| M13R | CAGGAAACAGCTATGAC | M13 reverse (Addgene) |
| JAO271 | gcgaaatggcgtggaaatgtgatcaaaggtaataaaacgtcatatAATTAAGGCGCGCCAGATCTG | CAN1 deletion with NAT1 forward |
| JAO272 | atcgaaagtttatttcagagttcttcagacttcttaactcctgtaGCATAGGCCACTAGTGGAT | CAN1 deletion with NAT1 reverse |
| STA691 | CCAGATCATTGGGGAAACCC | forward primer anneals 468bp upstream of SPN1 ATG, for Spn1 K.O. |
| STA692 | CGCCAAGGGTATTGTCTTGG | reverse primer anneals 485bp downstream of SPN1 UAA, for Spn1 K.O. |
| STA863 | GAAGAGTGGTTGCGAACAGAG | upstream *CAN1* forward |
| STA864 | GGTCTGAAGGAGTTTCAAATGC | downstream *CAN1* reverse |

# CHAPTER 3. SPN1 CONTRIBUTES TO GENOME INSTABILITY[1]

## 3.1 Summary

Cells expend a large amount of energy to maintain the DNA sequence. Chromatin architecture contributes to maintaining genome stability by providing physical protection of the DNA and DNA processing pathway regulation. Thus, many chromatin architecture proteins have been shown to aid in the regulation of genome stability. Expression of a mutant allele of the chromatin binding and elongation factor *SPN1*, results in cellular resistance to the DNA damaging agent, methyl methanesulfonate, lower spontaneous and lower damage induced mutation rates, along with increased chronological longevity. We attribute these effects to an increased usage of the error free branch of DNA damage tolerance pathway in the *spn1* strain. This provides evidence for a role of Spn1 in promoting genome instability in wildtype cells as well as ties to overcoming replication stress and contributions to chronological aging.

## 3.2 Introduction

Maintaining the genome is the most important function of a cell. Lack of genome integrity can cause disease states, including cancer. Overlapping conserved DNA repair pathways, damage cell cycle checkpoints, proofreading polymerases, and chromatin structure are all ways in which the cell minimizes changes to the genome (KAWASAKI and SUGINO 2001; AGUILERA and GARCIA-MUSE 2013; POLO and ALMOUZNI 2015; CHATTERJEE and WALKER 2017). However, some level of genome instability (mutation, deletion, insertion, amplification) is tolerated by the cell and in

[1] This chapter is a manuscript in preparation. Authors are Alison K Thurston, Catherine A Radebaugh, Adam R Almeida, Juan Lucas Argueso and Laurie A Stargell. Catherine Radebaugh performed the original phenotype analysis of the *spn1*$^{141\text{-}305}$ strain on MMS, contributed to strain creation and testing of the *RAD6*, *RAD9* and *SGS1* strains. Adam Almeida performed the chronological aging assays. Juan Lucas Argueso provided instruction for the forward spontaneous mutation rate analysis, the damage induced mutation rate analysis, and the loss of heterozygosity assay. Additionally, he provided instruction and reagents for strain creation used in the loss of heterozygosity assay.

fact can be beneficial for adaptation (SKONECZNA *et al.* 2015). DNA lesions, DNA breaks, DNA helix distortion, and DNA associated proteins can be an obstacle for the replication machinery (HUSTEDT *et al.* 2013; BRAMBATI *et al.* 2015; CHATTERJEE and WALKER 2017). The DNA damage tolerance (DDT) pathway provides mechanisms for the cells to circumnavigate blocks to the DNA replication fork. Prolonged replication fork stalling at distorted DNA can result in genome instability or cell death. DDT is different from other repair pathways as the initial damage is not repaired. Intermediate steps of the DNA damage repair pathways can be detrimental to the cell if performed downstream of the replication fork. The cleavage of the phosphate backbone in the ssDNA template would result in a double strand break, further increasing the risk of aberrant recombination. The DNA damage tolerance pathway incorporates two sub-pathways, TLS (error prone branch) and template switch (error free branch) (LEE and MYUNG 2008; XU *et al.* 2015; BRANZEI and SZAKAL 2016).

Translesion synthesis (TLS) utilizes polymerase switching to overcome replication blocks using the lower fidelity polymerases POL ζ (Rev3/Rev7) with Rev1 (Prakash 2005). The TLS branch is considered error prone since it can potentially introduce a miss-matched dNTP via the low fidelity polymerase. TLS can contribute to over half the point mutations accumulated in a cell (STONE *et al.* 2012). The error free sub-pathway utilizes the newly synthesized sister strand as a template for DNA synthesis past the obstruction. This requires homologous recombination factors for strand invasion and downstream DNA processing factors to resolve recombination intermediates. The error free pathway has been determined to be different from traditional recombination repair pathways through epigenetic studies (BRANZEI and SZAKAL 2016). How the cell determines which pathway to use is still under investigation. The post translational modification of PCNA, cell cycle phase, DNA structure, and histone modification have all been shown to influence pathway choice (DAIGAKU *et al.* 2010; GONZALEZ-HUICI *et al.* 2014; MEAS *et al.* 2015; XU *et al.* 2015; BRANZEI and SZAKAL 2016; HUNG *et al.* 2017).

Spn1 (Suppresses post-recruitment gene number 1) is a transcription elongation and chromatin binding factor (FISCHBECK *et al.* 2002; KROGAN *et al.* 2002; LI *et al.* 2017). Spn1 is essential and conserved (FISCHBECK *et al.* 2002; LIU *et al.* 2007; PUJARI *et al.* 2010). The intrinsically disordered tails of Spn1 are responsible for histone, DNA and nucleosome binding (LI *et al.* 2017), while the ordered core region (amino acids 141-305) binds to RNA Polymerase II (RNAPII) and the histone chaperone, Spt6 (DIEBOLD *et al.* 2010; MCDONALD *et al.* 2010; PUJARI *et al.* 2010; LI *et al.* 2017). Loss of the DNA, histone and nucleosome binding (spn1$^{141-305}$) is not detrimental to cell growth under rich media conditions (FISCHBECK *et al.* 2002; LI *et al.* 2017). However, expression of spn1$^{141-305}$ in transcription elongation and histone chaperone deletion background strains result in defective cell growth (LI *et al.* 2017). Spn1 genetically and physically interacts with ATPase remodelers, INO80 (COSTANZO *et al.* 2016) and SWR-C/SWR1 (COLLINS *et al.* 2007) both of which are involved in replication (SHIMADA *et al.* 2008; VAN *et al.* 2015) and double strand break repair (VAN ATTIKUM *et al.* 2007). Additionally, *SPN1* genetically interacts with replicative histone chaperones *CAF-1*, *ASF1* and *FACT* (LI *et al.* 2017) (Radebaugh, unpublished). The chromatin assembly functions of CAF-1, Asf1 and FACT are important for DNA repair (KIM and HABER 2009; DINANT *et al.* 2013). This raises the question whether Spn1 could also function in these pathways.

In this study, we examined a role for Spn1 in DNA repair. Expression of the mutant protein, spn1$^{141-305}$, revealed a resistance to the DNA damaging agent, methyl methanesulfonate (MMS) not observed in the *SPN1 strain*. Methyl methanesulfonate is an alkylating agent used to study both DNA damage repair and damage induced genome instability. We tested genetic interactions between *SPN1* and genes involved in base excision repair (BER), nucleotide excision repair (NER), homologous recombination (HR), and the DNA damage tolerance (DDT) pathway. Through these genetic interactions we determined the resistance to MMS observed in the *spn1$^{141-305}$* strain is dependent on DDT and HR. Furthermore, truncation of Spn1 displayed decreased spontaneous and damage induced mutation rates and increased chronological longevity.

Through genetic interaction analysis, and mutation rate analysis we have revealed a role for Spn1 in promoting genome instability by influencing DNA damage tolerance pathway selection.

## 3.3 Results

### *3.3.1 Expression of* spn1$^{141-305}$ *results in cellular resistance to methyl methanesulfonate*

*SPN1* genetically interacts with genes whose protein products are involved in DNA repair such as Rad23, Polε, the CAF complex, and the SWI/SNF complex (COLLINS *et al.* 2007; ZHANG *et al.* 2008; DUBARRY *et al.* 2015; LI *et al.* 2017). Thus, we were interested if Spn1 could function in DNA repair. Cells expressing spn1$^{141-305}$ were grown on media containing various DNA damaging agents (Figure 3.1A). Interestingly, the *spn1$^{141-305}$* strain displayed resistance to MMS (Figure 3.1B). The observed resistance appears specific to the DNA damaging agent MMS as sensitivity to the other tested DNA damaging agents was not observed**.** We investigated if the MMS resistance phenotype due to *spn1$^{141-305}$* is dominant. Merodiploid strains expressing endogenous Spn1 and plasmid bound Spn1 or spn1$^{141-305}$ were created (Table 2.1). Co-expression of spn1$^{141-305}$ and endogenous Spn1 did not result in increased resistance to MMS (Figure 3.2A), indicating that *spn1$^{141-305}$* is recessive.

To verify that cells expressing spn1$^{141-305}$ are accumulating DNA damage after exposure to MMS, the H2A serine 129 phosphorylation (H2A S129Ph) levels in *SPN1* and *spn1$^{141-305}$* cells were examined by western blot analysis. H2A S129 is phosphorylated in response to DNA damage (DOWNS *et al.* 2000; FOSTER and DOWNS 2005). A large increase in the amount of H2A S129Ph after MMS exposure was observed in both *SPN1* and *spn1$^{141-305}$* strains. The levels of H2A S129Ph were similar the two strains (Figure 3.1B).

As DNA damage occurs in both strains, we reasoned if cells expressing spn1$^{141-305}$ lacked a DNA damage cell cycle checkpoint then we would observe differences in the cell cycle phase distributions between strains expressing Spn1 and spn1$^{141-305}$. However, no difference in the cell

cycle phase distribution was observed (Figure 3.2B). This suggests that the resistance to MMS in the *spn1*$^{141-305}$ strain is not due to loss of DNA damage checkpoints.

To further investigate DNA damage response, genetic interactions between *SPN1* and *TEL1* and *RAD9* were examined. Tel1 is an evolutionarily conserved phosphatidylinositol-3 kinase related protein kinases (PIKKs). Tel1 along with Mec1 transduce a kinase cascade after sensor proteins detect DNA damage. PIKKs activate adapter proteins such as Rad9 and transducer kinases, such as Rad53 and Dun1, which activate effectors proteins. Effector proteins carry out DNA damage repair, cell cycle arrest, transcription programs, dNTP synthesis, and replication fork stabilization as a response to the cellular stress (CRAVEN *et al.* 2002; TOH and LOWNDES 2003; ENSERINK 2011). Loss of the MMS resistance is observed when spn1$^{141-305}$ is expressed in *tel1Δ* and *rad9Δ* strains (Figure 3.1D). This indicates that MMS resistance observed in the *spn1*$^{141-305}$ strain is dependent on Tel1 and Rad9 activity.

Spn1 S23 is phosphorylated in response to exposure to MMS and HU in a Mec1 and Tel1 dependent manner (CHEN *et al.* 2010; BASTOS DE OLIVEIRA *et al.* 2015). As resistance to MMS in the *spn1*$^{141-305}$ strain is dependent on Tel1 kinase activity, we investigated if the loss of phosphorylation on S23 would be sufficient for resistance. Phospho-mimetic (*spn1*$^{S23D}$) and phospho-deficient (*spn1*$^{S23A}$) strains were created and grown on MMS (Figure 3.2C). We did not observe any mutant growth phenotypes with the S23 mutants, suggesting that loss of phosphorylation at S23 is not sufficient to cause resistance to MMS.

### *3.3.2 Removal of methyl lesions through Mag1 glycosylase is necessary for resistance.*

To investigate if the resistance to MMS could be due to more efficient DNA repair, the genetic interactions between *SPN1* and genes involved in the base excision repair pathway (BER) were examined. BER is the primary repair pathway for damage caused by MMS (MEMISOGLU and SAMSON 2000). Mag1 is the DNA glycosylase responsible for the removal of the toxic N3- methyl adenine adducts resulting in an abasic site (PRAKASH and PRAKASH 1977; CHEN *et al.* 1989).

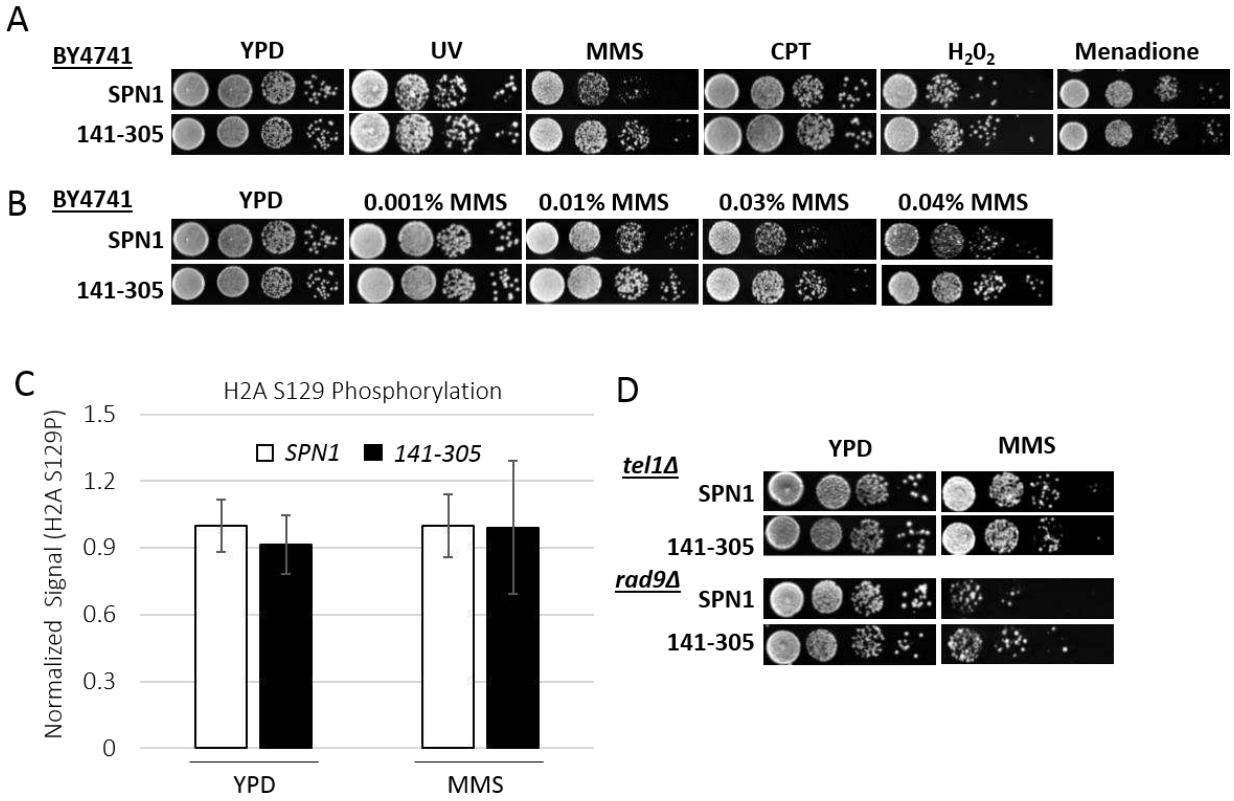


**Figure 3.1. Expression of spn1$^{141\text{-}305}$ suppresses sensitivity to the DNA damaging agent, methyl methanesulfonate.** A) Ten-fold serial dilutions of cells expressing Spn1 or spn1$^{141\text{-}305}$ were exposed to DNA damaging agents: 50 J/m2 UV, 0.03% MMS, 50 µg/ml camptothecin (CPT), 3.0% hydrogen peroxide ($H_2O_2$) and 70 µM menadione. B) Ten-fold serial dilutions of cells expressing Spn1 or spn1$^{141\text{-}305}$ were grown on increasing concentrations of MMS. C) Quantification of western blot showing H2A S129 phosphorylation levels before and after exposure to 0.1% MMS in cells expressing Spn1 or spn1$^{141\text{-}305}$. H2A S129 Phosphorylation signal is normalized to TBP. Spn1 ratio is set to 1. Standard deviation is calculated from 4-5 biological replicates. D) Ten-fold serial dilutions of cells expressing Spn1 or spn1$^{141\text{-}305}$ in *tel1Δ* and *rad9Δ* strains. Due to background strain sensitivity to MMS, cells were grown on YPD and 0.03% MMS and 0.01% MMS, respectively.

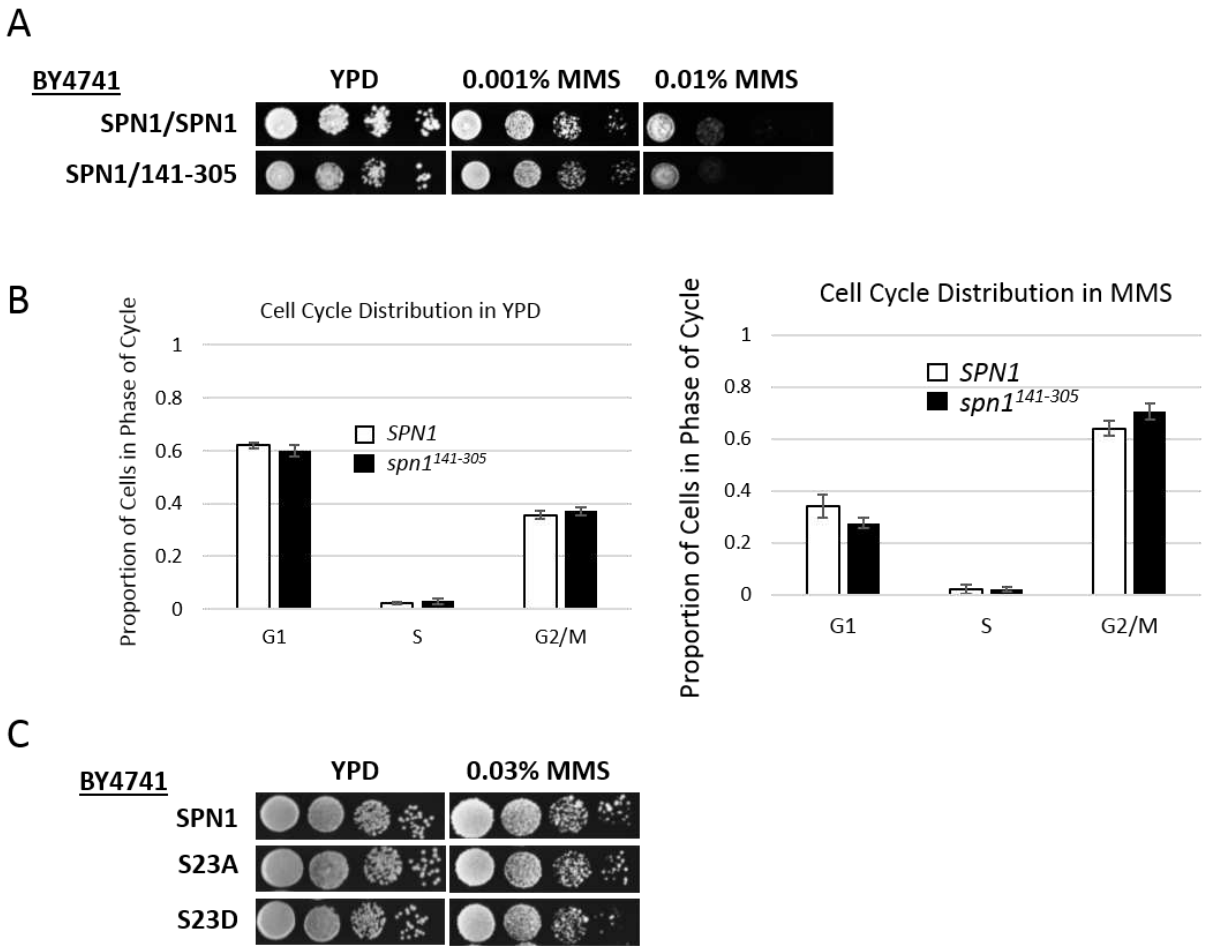


**Figure 3.2. *spn1*$^{141\text{-}305}$ is a recessive allele.** A) Ten-fold serial dilutions of cells expressing endogenous Spn1 and plasmid bound Spn1 or spn1$^{141\text{-}305.}$ Cells were grown on increasing concentrations of MMS. (B) Logarithmically growing cells in YPD or MMS were fixed and examined by microscopy for cell cycle distribution by budding index. C) Ten-fold serial dilutions of cells expressing Spn1, spn1$^{S23A}$, or spn1$^{S23D}$ were grown on YPD and 0.03% MMS plates.

Apn1 is the major endonuclease responsible for cleaving the phosphate backbone at the abasic site, which is subsequently repaired through long or short patch BER (MEMISOGLU and SAMSON 2000; ODELL *et al.* 2013b). Cells expressing either Spn1 or spn1$^{141-305}$ in the *mag1*Δ background were sensitive to MMS (Figure 3.3). In contrast, cells expressing spn1$^{141-305}$ in the *apn1*Δ background were resistant to MMS (Figure 3.3). This suggests that cells are able to retain resistance with a defective BER pathway if the damaging lesion can be processed by Mag1.

### *3.3.3 Resistance to MMS is independent of the nucleotide excision repair pathway*

As Spn1 is involved in transcription and mRNA processing (FISCHBECK *et al.* 2002; KROGAN *et al.* 2002; YOH *et al.* 2007; YOH *et al.* 2008) we predicted that Spn1 could be functioning in transcription coupled nucleotide excision repair (TC-NER). NER can be used as an alternative to BER (BAUER *et al.* 2015). Genetic interactions were examined with introduction of *spn1$^{141-305}$* into the *rad26*Δ and *rad14*Δ backgrounds. *RAD26* encodes for a DNA-dependent ATPase involved in TC-NER (GUZDER *et al.* 1996a; PRAKASH and PRAKASH 2000). Rad14 is a subunit of the nucleotide excision repair factor 1 (NEF1) and is required for TC-NER and global genomic (GG-NER) (GUZDER *et al.* 1996b; PRAKASH and PRAKASH 2000). Resistance was observed in cells expressing spn1$^{141-305}$ in both *rad26*Δ and *rad14Δ* strains when cells were exposed to MMS but not UV (Figure 3.4A). Furthermore, exposing cells to increasing amounts of UV in the wildtype background did not produce the resistant mutant phenotype (Figure 3.4B), indicating that the observed resistance to MMS is not dependent on either NER pathway.

### *3.3.4 Resistance is dependent on the error free sub-pathway of the DNA damage tolerance pathway*

The DNA damage tolerance (DDT) pathway provides a mechanism for cells to circumnavigate blocks to the DNA replication fork, including lesions caused by exposure to MMS. The primary signal for entry into the TLS sub pathway of DDT is dependent on the mono-ubiquitination of PCNA through the actions of the Rad18 and Rad6 complex. Further poly-ubiquitination through the actions of the Rad5, Ubc13 and Mms2 complex is the primary signal for error free bypass

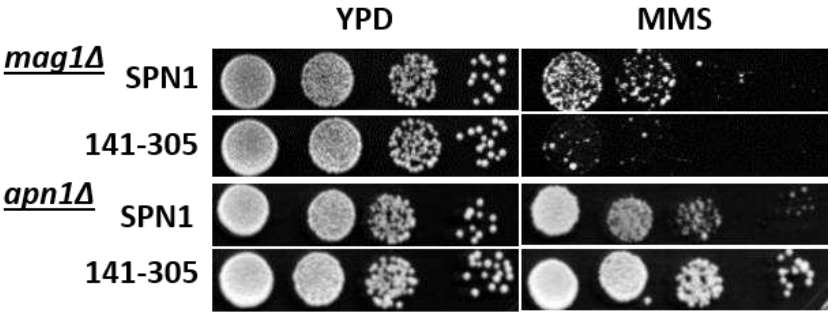


**Figure 3.3. *spn1*$^{141\text{-}305}$ resistance is dependent on a functional BER pathway**. Ten-fold serial dilutions of cells expressing Spn1 or spn1$^{141\text{-}305}$ in *mag1Δ* and *apn1Δ* backgrounds. Cells were grown on YPD and 0.01% MMS.

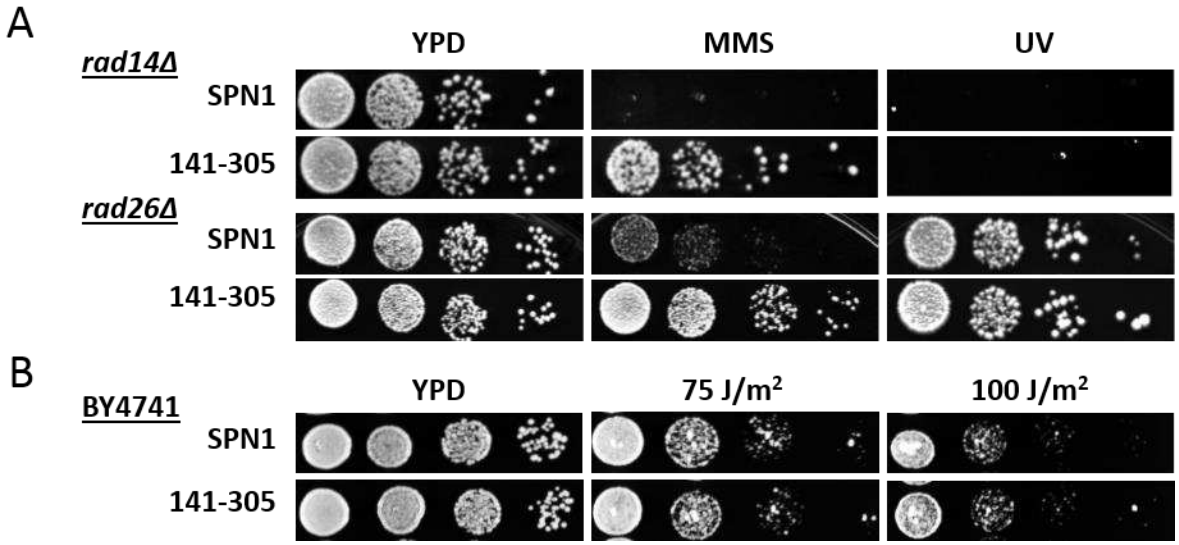


**Figure 3.4. *spn1*$^{141\text{-}305}$ resistance is independent of NER**. Ten-fold serial dilutions of cells expressing Spn1 or spn1$^{141\text{-}305}$ in *rad14Δ* and *rad26Δ* backgrounds. Cells were grown on YPD and 0.03% MMS. Cells were exposed to 75 J/m$^2$ B) Ten-fold serial dilutions of cells expressing Spn1 or spn1$^{141\text{-}305}$ in increasing exposure to UV.

(Figure 3.5). Abolishment of the DDT pathway results in extreme sensitivity to MMS (Huang, et al 2013). Since we observe resistance to MMS in the *spn1*$^{141-305}$ strain we predicted that the DDT pathway must be functional. Consistent with this, deletion of *RAD6* or *RAD18* result in the loss of resistance with the expression of spn1$^{141-305}$ when grown on MMS (Figure 3.6A).

MMS resistance is correlated to the loss of inhibition of the TLS branch of DDT (CONDE and SAN-SEGUNDO 2008; CONDE *et al.* 2010). Thus we predicted that if Spn1 inhibits TLS, then the *spn1*$^{141-305}$ strain has loss this function. The genetic interactions of *SPN1* with the subunits of the POLζ (*REV3/REV7/REV1*), a TLS polymerase, and *RAD5/MMS2/UBC13*, a complex responsible for error free sub-pathway signaling, were examined. Interestingly, cells expressing spn1$^{141-305}$ retained resistance to MMS in the TLS gene deletion backgrounds (Fig 3.7A). Likewise, a loss of resistance in the error-free deletion strains was observed (Fig 3.7B). These data suggest cells expressing Spn1 are utilizing the TLS branch; where cells expressing spn1$^{141-305}$ are not dependent on TLS. The error-free branch preferentially occurs during S-phase of the cell cycle, while TLS functions during G2 (BRANZEI and SZAKAL 2016). The *spn1*$^{141-305}$ strain displays a slight sensitive to HU. This phenotype is exacerbated in the DDT deletion strains (Figure 3.8). This demonstrates an important role for Spn1 in overcoming replication stress caused by HU, which spn1$^{141-305}$ cannot overcome in DDT deficient strains.

### *3.3.5* Spn1 *contributes to spontaneous and damage induced genome instability.*

The TLS polymerases can cause upward of 50% of mutations in a genome (STONE *et al.* 2012). Thus, we predicted that if the *spn1*$^{141-305}$ strain is not utilizing the TLS sub-pathway then we would observe a difference in the damage induced mutation rates between the *SPN1* and *spn1*$^{141-305}$ strains. To detect levels of damage induced mutations, a fluctuation assay looking at mutations occurring within the *CAN1* locus was performed. Cells expressing spn1$^{141-305}$ had a significant decrease in the damage induced mutation rate compared to WT cells (Table 3.1). Surprisingly, the *spn1*$^{141-305}$ strain also displayed a decrease in the forward spontaneous mutation rate

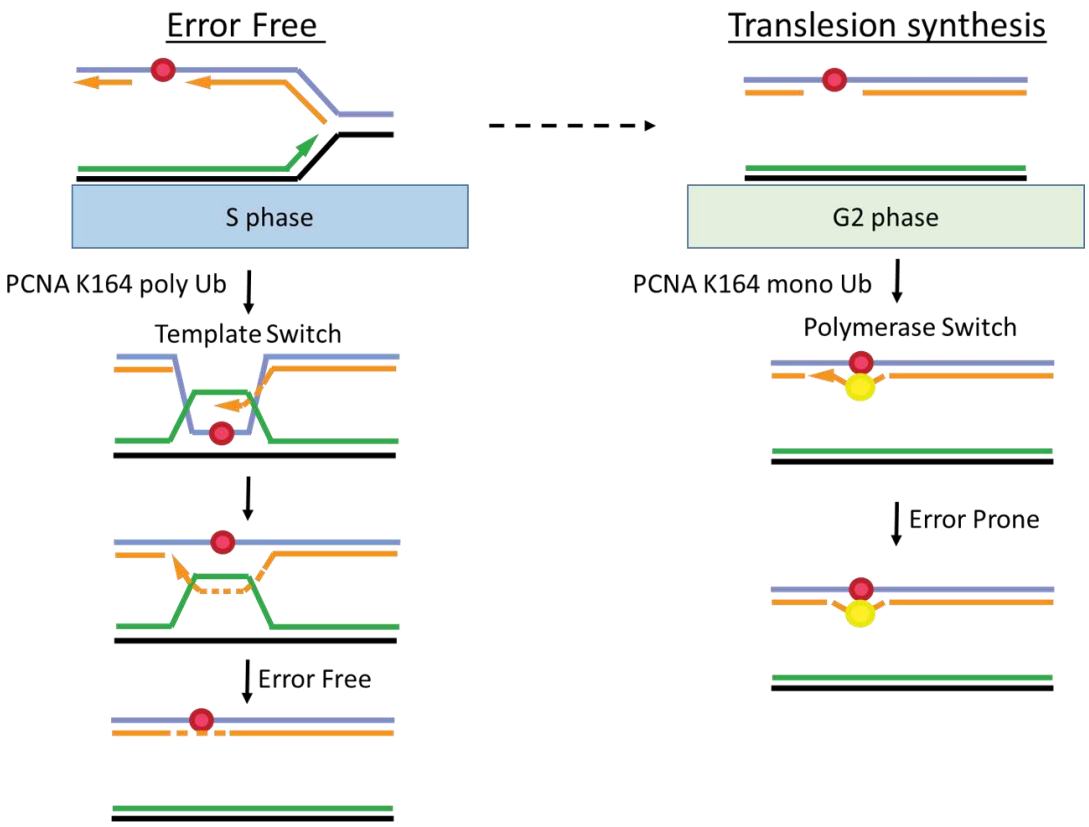


**Figure 3.5. Diagram depicting the DNA damage tolerance pathway.** The DNA damage tolerance pathway consists of two branches, error free and translesion synthesis. Image adapted from (BRANZEI and PSAKHYE 2016).

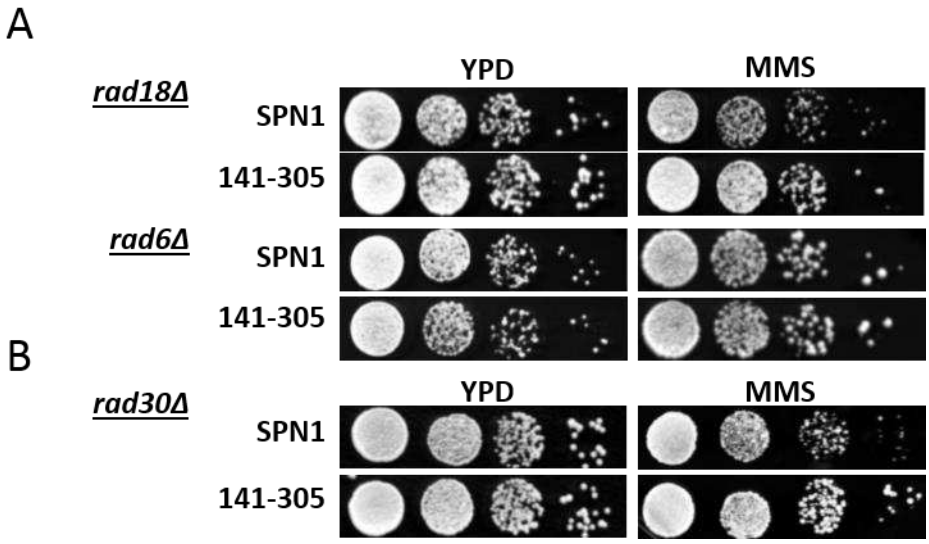


**Figure 3.6 DDT is functional in the cell expressing spn1$^{141-305}$.** Ten-fold serial dilutions of cells expressing Spn1 or spn1$^{141-305}$ in A) *rad18Δ* and *rad6Δ* strains and B) *rad30Δ*. Cells were grown on YPD and 0.00025%, 0.01% and 0.03% MMS plates

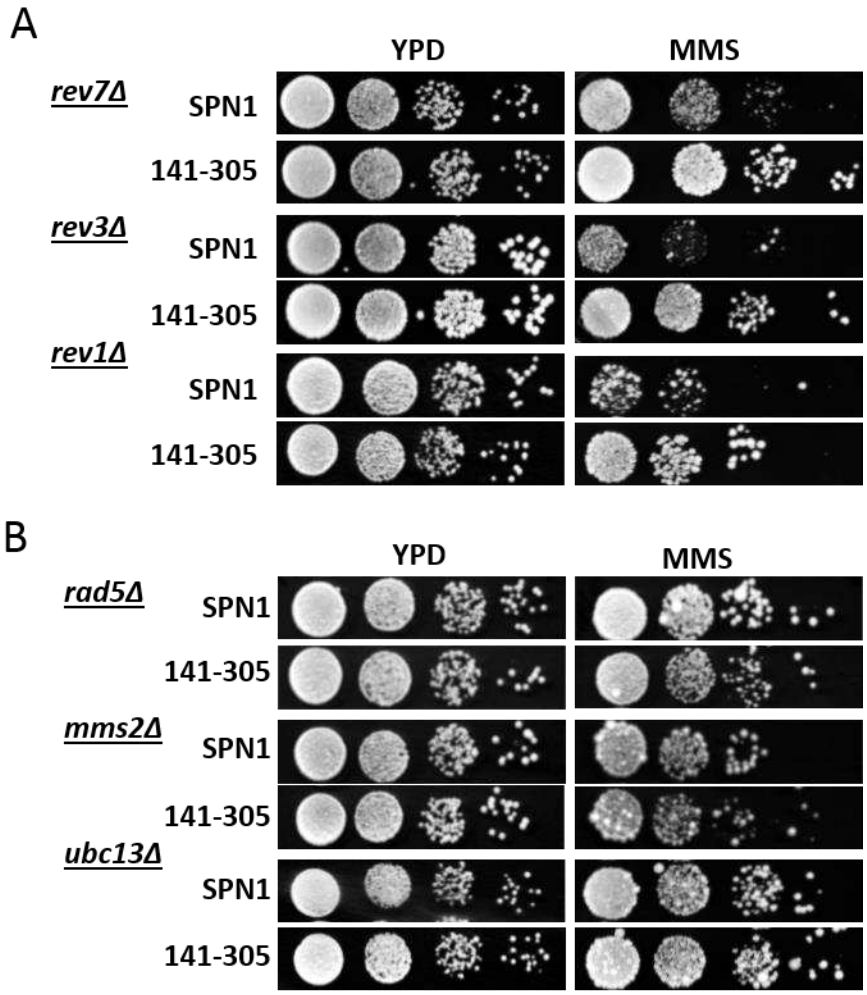


**Figure 3.7. *spn1*$^{141\text{-}305}$ resistance is dependent on the error free sub-pathway of DNA damage tolerance pathway.** Ten-fold serial dilutions of cells expressing Spn1 or spn1$^{141\text{-}305}$ in A) TLS deletion background and B) error free deletion background strains. Strains were grown on the following MMS concentrations listed in order: A) 0.02%, 0.015%, 0.03% and B) 0.001%, 0.01%, 0.01%.

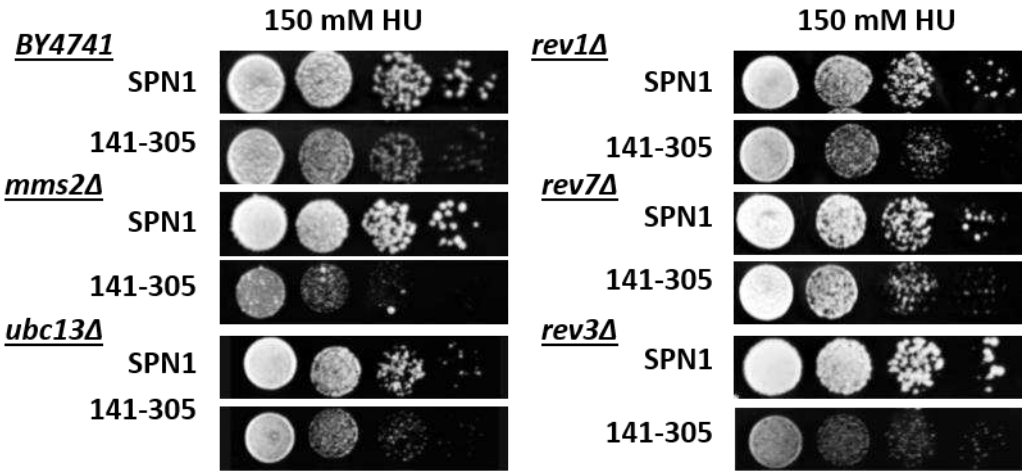


**Figure 3.8. HU sensitivity in DDT strains.** Ten-fold dilutions of cells expressing Spn1 or spn1$^{141\text{-}305}$ in DDT deletion backgrounds. Strains were grown on plates containing 150 mM hydroxyurea (HU).

Table 3.1 Spontaneous and damage induced mutation rates of strains expressing Spn1 and spn1$^{141\text{-}305}$

| Spontaneous Mutation Rate | | | | | |
|---|---|---|---|---|---|
| **Strain** | **Mutation Rate x10^-7** | **Upper Difference** | **Lower Difference** | **Number of Replicates** | **Significant** |
| *SPN1* | 1.20 | 0.39 | 0.24 | 21 | |
| *spn1*$^{141\text{-}305}$ | 0.64 | 0.20 | 0.20 | 21 | <0.0001 |
| *rev3Δ* | 2.02 | 0.47 | 0.66 | 7 | |
| *rev3Δspn1*$^{141\text{-}305}$ | 0.95 | 2.62 | 0.30 | 7 | <0.05 |
| *mms2Δ* | 25.56 | 6.32 | 2.60 | 14 | |
| *mms2Δspn1*$^{141\text{-}305}$ | 23.08 | 7.23 | 9.08 | 12 | |
| **Damage Induced Mutation Rat** | | | | | |
| **Strain** | **Mutation Rate x10^-7** | **Upper Difference** | **Lower Difference** | **Number of Replicates** | **Significant** |
| *SPN1* | 22.76 | 3.07 | 3.64 | 21 | |
| *spn1*$^{141\text{-}305}$ | 15.46 | 0.52 | 3.06 | 21 | <0.0001 |
| *rev3Δ* | 11.43 | 3.66 | 3.80 | 20 | |
| *rev3Δspn1*$^{141\text{-}305}$ | 4.72 | 4.59 | 1.46 | 21 | <0.01 |
| *mms2Δ* | 289.63 | 101.42 | 39.39 | 21 | |
| *mms2Δspn1*$^{141\text{-}305}$ | 240.62 | 93.54 | 59.72 | 20 | |

(Table 3.1). This indicates that Spn1 contributes to genome instability experienced by cells as they progresses through the cell cycle.

To test if the decreased mutation rate observed in the *spn1*$^{141-305}$ strain is dependent on the error free sub-pathway, damage induced mutation rates in the *rev3*Δ and *mms2*Δ strains were examined. We predicted that deletion of *MMS2* would result in the *spn1*$^{141-305}$ strain mutation rate returning to WT levels. As predicted, the deletion of *MMS2* resulted in WT damaged induced mutation rate levels (Table 3.1). This indicates that the mutation rate decrease in the *spn1*$^{141-305}$ strain is dependent on error free sub-pathway.

The deletion of the histone methyl transferase Dot1 results in resistance to MMS through the inhibition of the TLS sub-pathway (CONDE and SAN-SEGUNDO 2008). The resistance in the *spn1*$^{141-305}$ strain is due to use of the error free sub-pathway and thus we predicted that Spn1 and Dot1 are acting in parallel pathways. To test this, a genetic analysis between the *SPN1* and *DOT1* strains was performed. Interestingly, the deletion of *DOT1* with *spn1*$^{141-305}$ resulted in increased growth compared to *dot1*Δ alone on YPD (Figure 3.9A). The increased growth is exacerbated when cells are grown on plates containing MMS. Expression of spn1$^{141-305}$ in the *dot1*Δ strain results in significant decreased mutation rates, although we observe higher levels of overall damage induced mutation rates in *dot1*Δ which is consistent with previously reported data (Figure 3.9B) (CONDE and SAN-SEGUNDO 2008). The mutant growth phenotype observed in the *dot1*Δ *spn1*$^{141-305}$ strain suggests a deregulation of both sub pathways of DDT. The opposing effects on genome instability in these two strains suggest that MMS resistance is related to genome instability but is not predictive.

### *3.3.6 Resistance to MMS is dependent on homologous recombination machinery*

The template switching mechanism utilized in the error free sub-pathway requires many of the factors involved in homologous recombination (BRANZEI and SZAKAL 2016; HANAMSHET *et al.* 2016), thus we predicted MMS resistance would require various HR factors. During DDT, Rad51

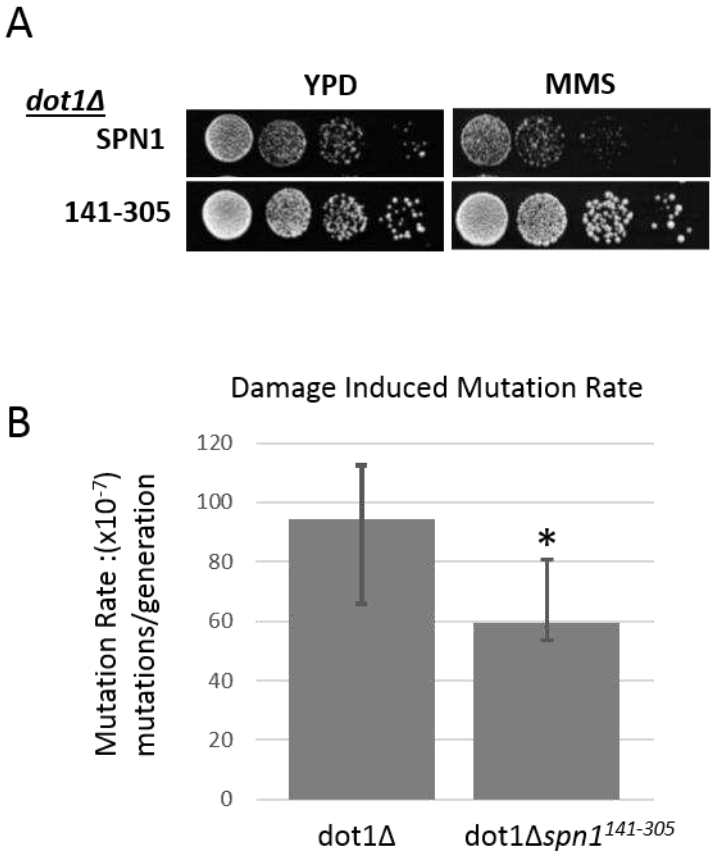


**Figure 3.9. Deletion of *DOT1* in *SPN1* and *spn1*$^{141\text{-}305}$ strains**. A) Ten-fold serial dilutions of cells expressing Spn1 or spn1$^{141\text{-}305}$ in *dot1Δ* background. Cells were grown on YPD and 0.03% MMS. We do note that we did not observe the reported increased MMS resistance in the *dot1Δ* strain as previously reported. We verified the deletion of *DOT1* in our strain by PCR (data not shown). B) Damage induced mutation rate of strains expressing Spn1 and spn1$^{141\text{-}305}$ in *dot1*Δ. Mutation rates were calculated by the Lea-Coulson method of the median using the FALCOR program. Significance was determined using the Mann-Whitney nonparametric t-test on GraphPad. Fluctuation assay was performed twice with 7 replicates. P value is <0.001.

binds ssDNA that results from re-priming of the replication fork. Rad51 is required for DNA damage tolerance (SYMINGTON *et al.* 2014). Rad55 and Rad57 work as a heterodimer to stabilize the association of Rad51 with the ssDNA (SYMINGTON *et al.* 2014). Deletion of *RAD51*, *RAD55* or *RAD57* combined with *spn1*$^{141\text{-}305}$ resulted in loss of resistance after exposure to MMS (Figure 3.10A). We do note that the *rad51*Δ*spn1*$^{141\text{-}305}$ strain appears slightly more sensitive than *rad51*Δ, although this is not further investigated at this time. To investigate the effect of expression of spn1$^{141\text{-}305}$ on DNA recombination events, loss of heterozygosity (LOH) was measured at the *CAN1* locus (ACUNA *et al.* 1994; ANDERSEN *et al.* 2008). A significant decrease in LOH events was observed in strains expressing spn1$^{141\text{-}305}$ (Figure 3.10B), indicating the observed resistance to MMS is dependent on functional HR factors.

### *3.3.7 DNA intermediates are processed through* **Sgs1** *and* **Rmi1** *in spn1*$^{141\text{-}305}$

During error free DDT and HR, DNA crossover intermediates are a result of strand invasion. The functions of topoisomerases, helicases, and exonucleases aid in resolving these intermediates (MITCHEL *et al.* 2013; CAMPOS-DOERFLER *et al.* 2018). Sgs1, Rmi1 and Top3 work in complex to aid in resolving holiday junctions that result after strand cross over (MULLEN *et al.* 2005; BERNSTEIN *et al.* 2009). Genetic analysis revealed that the deletion of *SGS1* or *RMI1* is synthetically lethal with *spn1*$^{141\text{-}305}$ on MMS and HU (Figure 3.11). Furthermore, *spn1*$^{141\text{-}305}$ cells remain resistant to MMS and HU in *exo1*Δ strains. The resectioning activity of Sgs1/Dna2 and Exo1 are thought to be redundant (MIMITOU and SYMINGTON 2008) (CAMPOS-DOERFLER *et al.* 2018). This suggests that cells expressing spn1$^{141\text{-}305}$ are utilizing recombination pathways that require a functional Sgs1/Rmi1 complex to resolve crossover intermediates.

### *3.3.8* **Spn1**$^{141\text{-}305}$ *expression results in increased chronological longevity.*

Decreased mutation rates have been linked to chronological aging (LONGO and FABRIZIO 2012). Increased chronological longevity has been associated with the inactivation of the TLS pathway (LONGO and FABRIZIO 2012). Since decreased mutation rates in cells expressing spn1$^{141\text{-}305}$ were

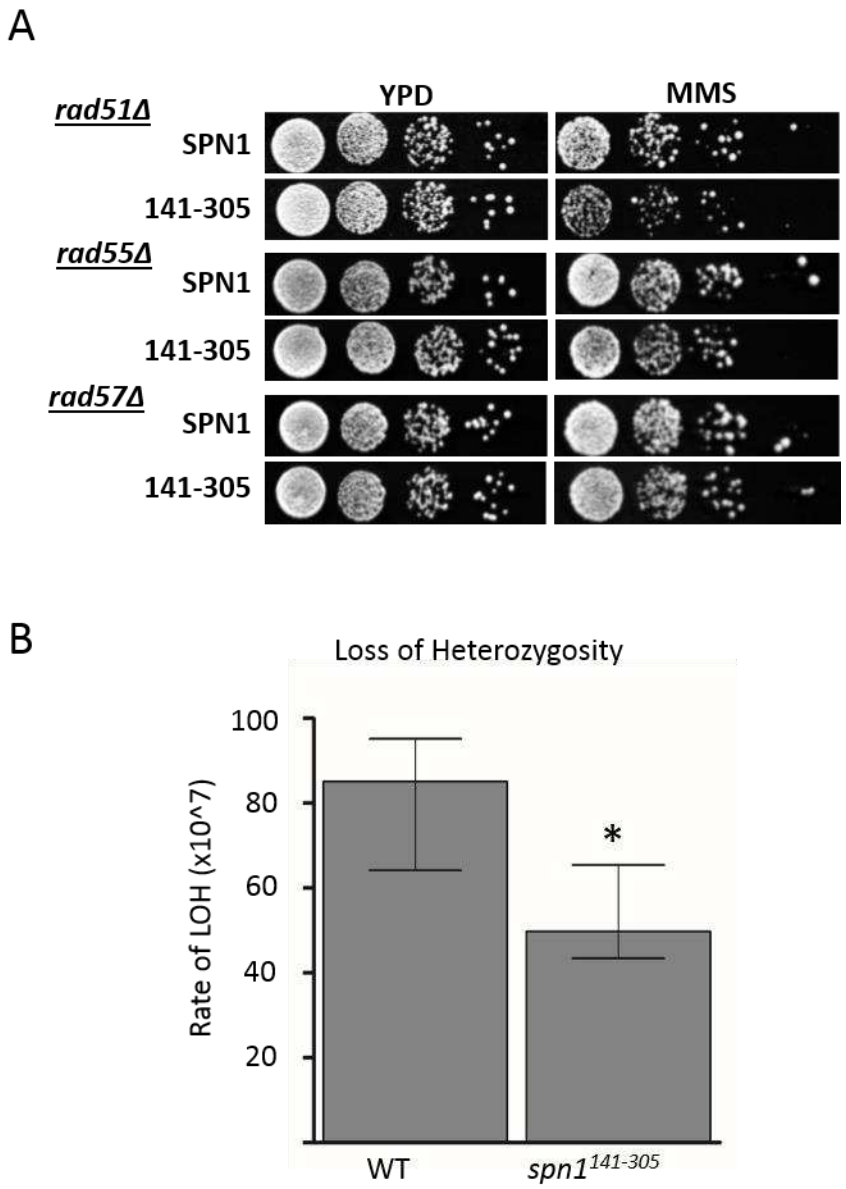


**Figure 3.10. *spn1*$^{141\text{-}305}$ resistance is dependent on the homologous recombination factors.** Ten-fold serial dilutions of cells expressing Spn1 or spn1$^{141\text{-}305}$ in homologous recombination deletion background strains grown on 0.01% MMS. B) Loss of heterozygosity rates of diploid cells expressing Spn1 or spn1$^{141\text{-}305}$. Rates were calculated by the Lea-Coulson method of the median using the FALCOR program. Significance was determined using the Mann-Whitney nonparametric t-test on GraphPad. 27 replicates were performed for each strain. P-value is < 0.01.

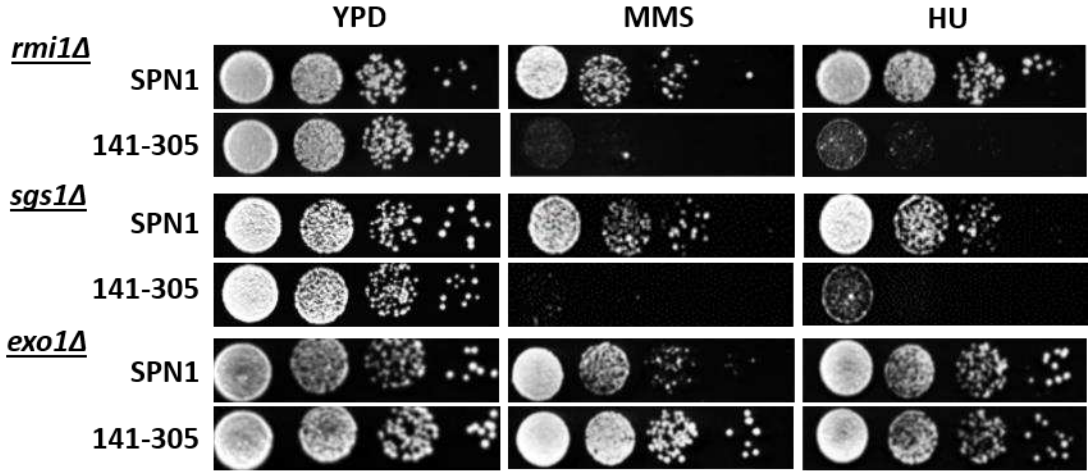


**Figure 3.11. Expression of spn1$^{141-305}$ is lethal in *sgs1*Δ and *rmi1*Δ strains.** Ten-fold serial dilutions of cells expressing Spn1 or spn1$^{141-305}$ in DNA processing gene deletion background, *sgs1Δ*, *rmi1Δ* and *exo1Δ.* Strains are grown on 0.01%MMS, 0.01%MMS and 0.03% MMS and 50mM HU, 25mM HU and 150mM HU. Concentrations of MMS and HU are listed in order.

observed, we predicted that we would also observe an increase in chronological lifespan. A dramatic difference in the chronological lifespan between cells expressing Spn1 and spn1$^{141-305}$ was observed. At the termination of the assay (19 days) the *spn1$^{141-305}$* culture maintained 85% viability, while *SPN1* culture was close to zero (Figure 3.12). The wildtype culture had 50% viability at day 10. This suggests a link between Spn1, genome instability and chronological aging.

### 3.4 Discussion

Here we have investigated the role of the chromatin binding factor Spn1 in DNA damage response and genome instability. Expression of spn1$^{141-305}$ covers wildtype functions when cells are grown in rich culturing conditions (LI *et al.* 2017). Upon exposure to the DNA damaging agent MMS, we observed resistance in cells expressing spn1$^{141-305}$. MMS results in the addition of methyl groups on single and double strand DNA (YANG *et al.* 2010). The methyl group is primarily transferred to a double bonded nitrogen on adenine, cytosine and guanine with varying frequencies (WYATT and PITTMAN 2006). While not all methyl lesions are toxic, N3-Methyladenine creates a barrier for replication machinery (CHANG *et al.* 2002). Activation of DNA damage response was detected by H2A S129 phosphorylation in both the wildtype and mutant strains after exposure to MMS. MMS is primarily repaired through BER although other repair pathways such as NER can partially compensate (BAUER *et al.* 2015). Deletion of *MAG1*, the DNA glycosylase responsible for the recognition and removal of the toxic N3-methyladenine results in cell sensitivity to MMS (PRAKASH and PRAKASH 1977). Expression of spn1$^{141-305}$ in the *mag1Δ* strain could not suppress the MMS sensitivity observed in the *mag1Δ* strain meaning this activity is necessary for resistance to MMS. Interestingly, cells expressing spn1$^{141-305}$ retain resistance in the *apn1Δ* strain. We reasoned that the initial removal of the methylated base is necessary for MMS resistance. Once Mag1 removes the affected base, the resulting abasic site could be processed by other endonucleases in BER or overlapping DNA repair pathways.

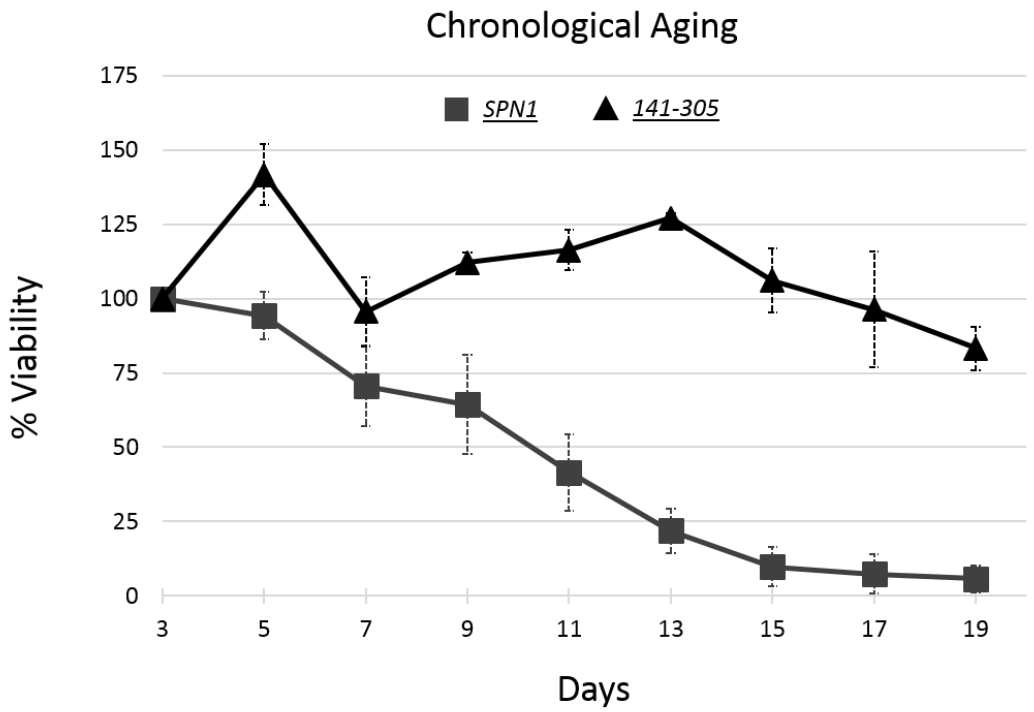


**Figure 3.12. Expression of spn1$^{141\text{-}305}$ increases chronological lifespan.** Representation of the average viability of multiple replicates for the wild type (n=5) and spn1$^{141\text{-}305}$ (n=4) strains

One such pathway is the NER. It appeared very plausible that Spn1 could function in NER. Spn1 has been shown to function as a transcription elongation factor and has physical and genetic interactions with transcription factors and RNA Polymerase II (FISCHBECK *et al.* 2002; KROGAN *et al.* 2002; PUJARI *et al.* 2010). We wondered if expression of spn1$^{141\text{-}305}$ could enhance NER. The expression of spn1$^{141\text{-}305}$ suppresses cell death as a result of the loss of Rad14 when grown on MMS; however expression of spn1$^{141\text{-}305}$ could not rescue lethality due to any amount of UV exposure. Additionally, the *spn1$^{141\text{-}305}$* strain revealed no mutant UV phenotype, indicating that expression of spn1$^{141\text{-}305}$ was not enhancing NER repair.

Further genetic analysis revealed that the resistance observed in the *spn1$^{141\text{-}305}$* strain was dependent on the error free sub-pathway of DDT. MMS resistance remained when any of the Polζ genes (*REV3/REV7/REV1*) were deleted suggesting that the TLS sub-pathway is not necessary for the resistant mutant phenotype. Resistance was lost upon deletion of any of the genes responsible for poly-ubiquitination of PCNA (*RAD5/MMS2/UBC13*), the major signal for entry into the error free sub-pathway. Error free bypass utilizes HR factors for template switching (BRANZEI and SZAKAL 2016; HANAMSHET *et al.* 2016). We observe loss of resistance in all genes tested in the *RAD51* group (*RAD51/RAD55/RAD57*). Template switching requires factors to resolve DNA intermediates. Introduction of *spn1$^{141\text{-}305}$* into the *sgs1Δ* or *rmi1Δ* strain is synthetically lethal when grown on MMS and HU. Lethality is not observed in the *exo1Δ* strain. We conclude that expression of spn1$^{141\text{-}305}$ shifts the regulation of DDT towards the error free sub-pathway (Figure 3.13) and resolution of the resulting DNA intermediates is dependent on the function of the Sgs1/Rmi1/Top3 complex (BERNSTEIN *et al.* 2009). This shift in the pathway results in significant decreases in genome instability. This indicates a role for wild type Spn1 in overcoming replication stress and promoting TLS, resulting in tolerable levels of genome instability in the cell (Figure 3.13).

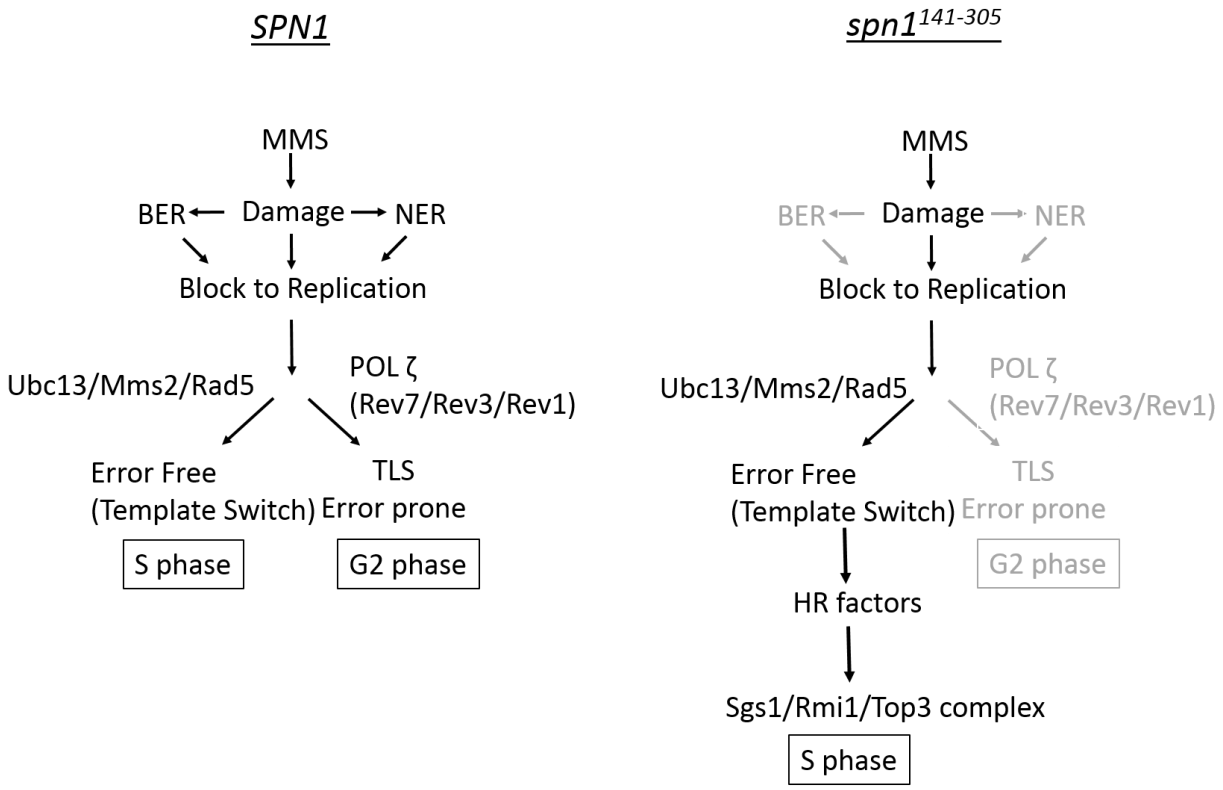


**Figure 3.13. Spn1 influences DNA damage tolerance sub-pathway selection.** WT cells tightly regulate the balance between error free and error prone DDT allowing for a small amount of genome instability each generation. Expression of spn1$^{141\text{-}305}$ alters the balance resulting in a MMS resistance dependence on a functional error free sub-pathway and decreased levels of spontaneous and damage induced mutation rates.

The significant decrease in genome instability is intriguing. Very few studies have identified or spent much time discussing this phenotype with the exception of the TLS polymerases. Deletion of any of the components of POLζ results in a 50-80% decrease in spontaneous mutation rate (STONE *et al.* 2012). We observed a significant decrease in both spontaneous and damage induced mutation rates in the *spn1*$^{141-305}$ strain. The decrease in mutation rate is lost upon deletion of *MMS2* but not *REV3*. The error free sub-pathway occurs predominantly during S phase of the cell cycle (BRANZEI and SZAKAL 2016). If an increase in S phase error free bypass was utilized in the *spn1*$^{141-305}$ cells, this could explain a decrease in detectable LOH events. During S phase, the newly replicated sister chromatid would be available as a template for bypass (HUANG *et al.* 2013) and would not result in loss of heterozygosity. In contrast, in *SPN1* cells, damage bypass may be occurring in G2 where the TLS, error free bypass, or the savage pathway could be utilized. This could result in an increase of detectable LOH events using the heteroallele as a template. We have demonstrated three types of decreased genome instability as a result of *spn1*$^{141-305}$. As yeast age, the frequency of all types of mutations increases (MADIA *et al.* 2007; LONGO and FABRIZIO 2012). Decreases in mutation rates are linked to a cell's ability to process damaged DNA (primarily oxidative damage), decrease activity of the TLS polymerases, control over mitotic recombination rates and regulate metabolism (MADIA *et al.* 2009). Aging is influenced by chromatin structure, DNA processing, and cellular metabolism. As we have now provided a connection between Spn1 and aging phenotypes, further investigations should be pursued for a mechanistic understanding. Perhaps this function of Spn1 is conserved in its human homolog.

The question remains; how does Spn1 influence the DDT pathway. Spn1 has been shown to promote repressive chromatin states. At *CYC1,* Spn1 prevents the chromatin remodeler SWI/SNF from being recruited (ZHANG *et al.* 2008). Additionally, human Spn1 along with human Spt6 and LEDGE/p27 maintain a repressive chromatin state of HIV post integration (GERARD *et al.* 2015). We previously have shown resistance to MNase digestion at *CYC1* during active

transcription in cells expressing spn1$^{141-305}$. This suggests local chromatin changes due to the truncation of Spn1 (LI *et al.* 2017). The loss of Spn1's ability to interact with chromatin could alter the chromatin architecture. Chromatin structure, histone tails modification, DNA topography, and DNA sequence all influence DDT pathway selection (GONZALEZ-HUICI *et al.* 2014; MEAS *et al.* 2015; HUNG *et al.* 2017). It is presumable that under replication stress or damage conditions, the *spn1$^{141-305}$* strain could not undergo the necessary chromatin changes, which affect the overall outcome of genome stability.

During replication, chromatin structure is completely disrupted to allow for semi-conservative DNA synthesis. The DNA double helix must re-associate with histone octamers to form the chromatin structure of the newly synthesized sister chromatids. Human Spn1 was detected within the chromatin fraction of replicated DNA, although it was not detected through a direct interaction with the replisome (ALABERT *et al.* 2014). Spn1 genetically and physically interacts with ATPase remodelers, INO80 (COSTANZO *et al.* 2016) and SWR-C/SWR1 (COLLINS *et al.* 2007) , both of which are involved in replication (SHIMADA *et al.* 2008; VAN *et al.* 2015) and double strand break repair (VAN ATTIKUM *et al.* 2007). *SPN1* genetically interacts with replicative histone chaperones CAF-1 and FACT (LI *et al.* 2017). The histone chaperone CAF-1 has been showed to localize to the replication fork through interactions with PCNA (SHIBAHARA and STILLMAN 1999). CAF-1 along with histone chaperone Asf1 aid in the proper assemble of newly formed chromatin after DNA synthesis (MACALPINE and ALMOUZNI 2013). All suggest a chromatin role for Spn1 during replication. Additionally, *spn1$^{141-305}$* displays moderate sensitivity to HU. This is exacerbated in the DDT deletion backgrounds, suggesting a role for Spn1 in overcoming replication stress. Further investigation into location and timing of Spn1's association with chromatin and other chromatin factors during replication and DNA damage could give a clearer picture on how Spn1 is influencing genome stability within the cell.

# CHAPTER 4: MUTANT PHENOTYPES OF DIFFERENT *SPN1* STRAINS ARE PREDOMINANTLY ALLELE SPECIFIC

## 4.1 Introduction

The yeast model system is a powerful tool to study biological processes and model human disease. Processes such as transcription, translation, DNA replication, DNA repair, cell cycle, cell signaling, cell trafficking, and apoptosis have all been studied using the yeast model system (DUINA *et al.* 2014; LAURENT *et al.* 2016). Comparison studies have shown over 30% of yeast genes have human orthologs (O'BRIEN *et al.* 2005; LAURENT *et al.* 2016). The ability to manipulate the genome, availability of replicating plasmids, auxotrophic markers, inexpensive cost, ease of culturing and fast generation time all make *S. cerevisiae* a competitive choice when considering model organisms (DUINA *et al.* 2014).

Although *S. cerevisiae* is a simple eukaryotic system, the study of essential genes is still challenging. Of the 6000 genes in the genome of *Saccharomyces cerevisiae* around 20% are essential (ZHANG and REN 2015). Many systems have been developed in order to study essential genes including the anchor away technique, which depletes nuclear proteins to the cytoplasm through a tethering system (HARUKI *et al.* 2008), the decreased abundance of mRNA perturbation (DAmP) approach, which creates hypomorphic alleles through the destabilization of the mRNA (SCHULDINER *et al.* 2005; BRESLOW *et al.* 2008) and the creation of conditional alleles.

Since *SPN1* is essential, deleting the endogenous gene for cellular study is not an option. Thus, truncations, point mutants and conditional alleles were engineered for the study of Spn1. In the previous chapter, the *spn1* allele, *spn1*$^{141\text{-}305}$ is studied to reveal a role for Spn1 in promoting genome instability and overcoming replication stress. The mutant protein, spn1$^{141\text{-}305}$ is defective for nucleic acid binding, histone binding, nucleosome binding and nucleosome assembly but still

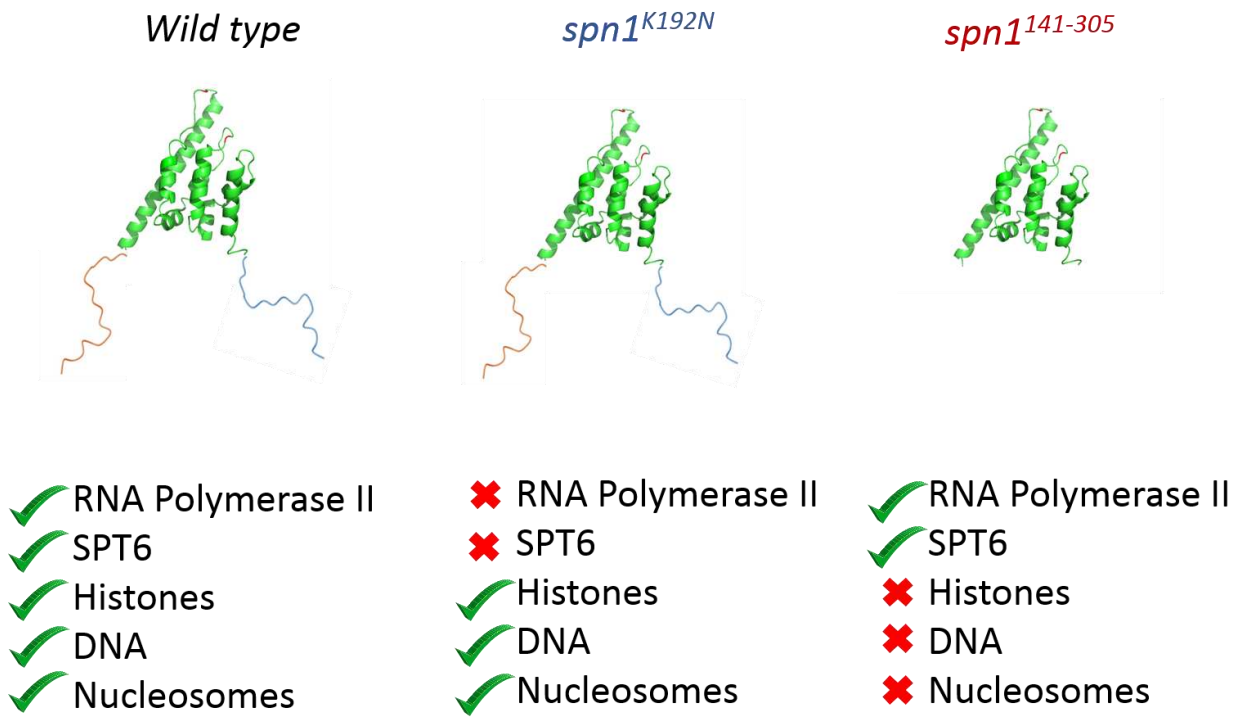


**Figure 4.1. Comparison of experimental determined interactions between Spn1, spn1$^{K192N}$ and spn1$^{141-305}$.** PDB#: 3NFQ

retains protein interactions through the core domain, potentially masking important information (Figure 4.1) (LI *et al.* 2017; LI 2018). In addition to investigating growth defects due to *spn1*$^{141-305}$, another *spn1* allele, *spn1*$^{K192N}$ has been studied. The affected residue in spn1$^{K192N}$ sits in the bottom of a cavity formed on the surface of Spn1 (PUJARI *et al.* 2010). Residue K192 is conserved from yeast to humans, and mutation causes temperature sensitivity and loss of protein-protein interactions with Spt6 and RNA polymerase II, while retaining chromatin related interactions (FISCHBECK *et al.* 2002; LI *et al.* 2017) (Figure 4.1).

In this chapter, a comparison is done between two *spn1* alleles, to investigate how they affect transcriptional profiles, genetic interactions, and spontaneous mutation rates. The two mutant alleles are dissimilar structurally and do not retain the same binding partners. spn1$^{141-305}$ is defective for chromatin related binding while retains interactions with RNAPII and Spt6. spn1$^{K192N}$ has lost the ability to interact with RNAPII and Spt6 while still retains DNA, histone and nucleosome interactions. By using alleles defective for specific interactions we hope to learn when, where and how these interactions are important for Spn1 function. The experimental outcome due to expression of either spn1 protein at times can show similarity and at others disagreement. Determining the biological implications can be quite challenging and often requires reinterpretation of preexisting ideas about Spn1.

## 4.2 Results

### *4.2.1 Expression of* spn1$^{K192N}$ *or* spn1$^{141-305}$ *result in dissimilar transcriptional profiles*

The role of Spn1 in transcription at the poised promoter of *CYC1* has been extensively studied (FISCHBECK *et al.* 2002; ZHANG *et al.* 2008; YEARLING *et al.* 2011; LI *et al.* 2017). Spn1 regulates the recruitment of Spt6 and Swi/Snf to *CYC1* (ZHANG *et al.* 2008). Expression of spn1$^{K192N}$ results in increased expression of CYC1, while expression of spn1$^{141-305}$ results in chromatin changes after *CYC1* activation in ethanol visualized by microccocal nuclease digestion (MNase); and decreased abundance at the promoter prior to activation, independent of RNAPII (LI *et al.* 2017).

Additionally, Spn1 co-localizes throughout the genome with RNAPII (MAYER *et al.* 2010). We were interested if expression of the mutant alleles of Spn1 affect transcription globally. Whole genome RNA sequencing was previously performed by Lillian Huang. Messenger RNA (mRNA) was collected from *SPN1*, *spn1*$^{K192N}$ and *spn1*$^{141-305}$ strains grown in YPD in duplicate. RNA-sequencing was performed using the Ilumina platform. In total there are 684 (191 up and 493 down) genes that were differentially expressed in cells expressing spn1$^{141-305}$ and 389 genes (181 up and 208 down) differentially expressed in cells expressing spn1$^{K192N}$. Genes that have a 2 fold change were submitted for gene ontology (GO) term enrichment analysis. Redundant GO-terms were removed by utilizing REVIGO (reduce and visualize gene ontology) (SUPEK *et al.* 2011). Interestingly, cells expressing spn1$^{K192N}$ resulted in more processes being up regulated than down regulated (Figure 4.2). In contrast, cells expressing spn1$^{141-305}$ had both an increase and decrease of GO-term processes (Figure 4.2). Only two GO-terms appeared in both strains. Alpha-amino acid metabolic process and nitrogen cycle metabolic process are both up regulated in the two *spn1* strains compared to WT. While transcription is affected in both of these strains, the transcriptional profiles that result are different.

### *4.2.2 Genetic comparison of spn1$^{K192N}$ and spn1$^{141-305}$*

Many genetic interaction analyses have been performed using the *spn1* alleles. Process and media depending, the alleles can result in similar or dissimilar growth behaviors. Interpreting these genetic interactions can be quite challenging. As an alternative to comparing growth of a mutant strain to the wildtype, a more global method was utilized to compare the two *spn1* alleles. First, the growth effects of the two alleles were compared on all the tested media. Second, the growth effects of the two alleles were compared on the individual media. Both of these analyses are pathway independent. Cell growth of strains containing *spn1*$^{K192N}$ or *spn1*$^{141-305}$ in deletion strains were grouped as either sensitive, no change or resistant compared to *SPN1* in the

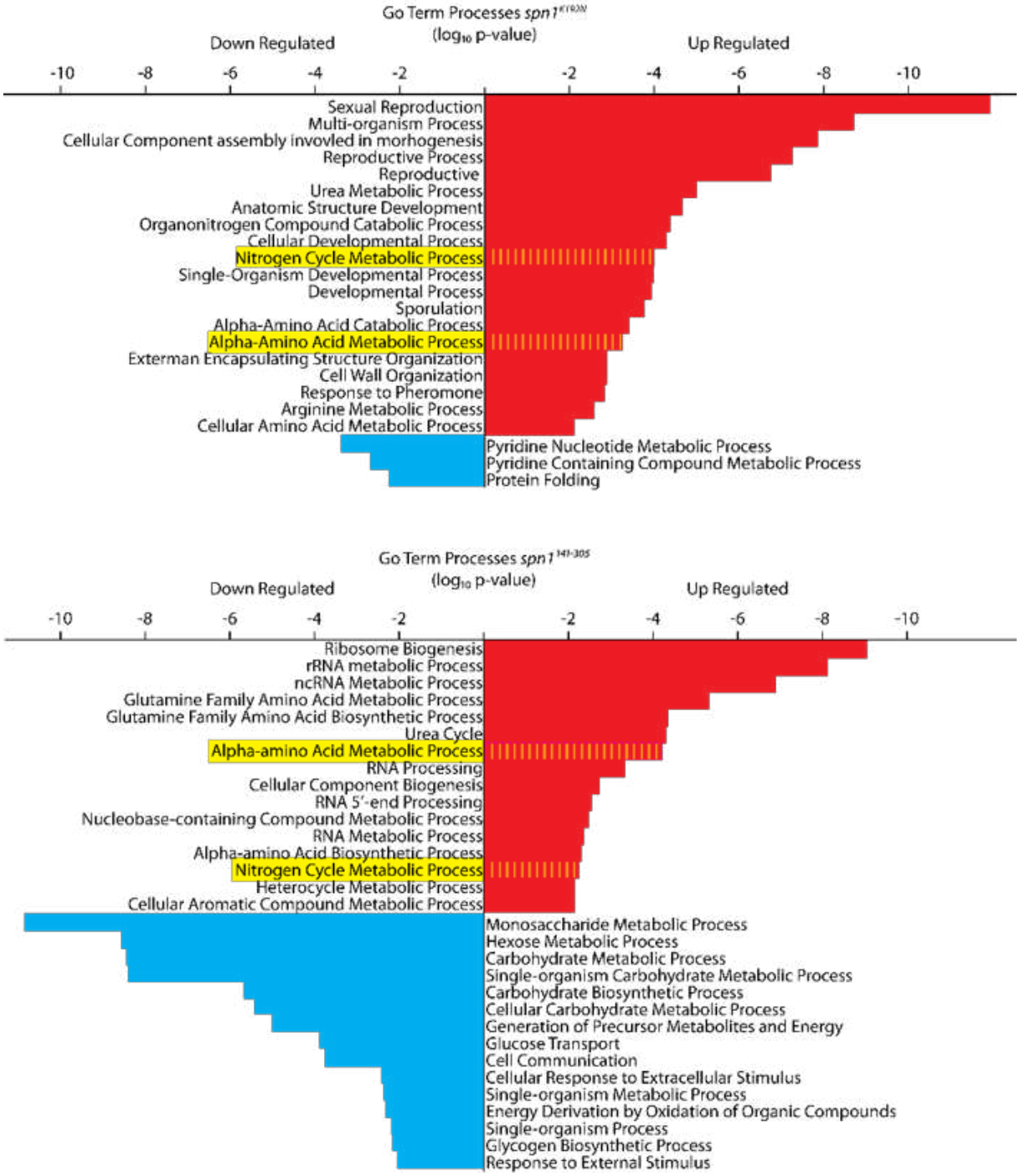


**Figure 4.2. Cellular processes affected by changes in the transcriptional profiles in the *spn1* strains are dissimilar.** Charts show processes that are up regulated or down regulated in the *spn1*$^{K192N}$ and *spn1*$^{141-305}$ strains compared to wildtype cells cultured in YPD.

respective deletion background (Table 4.1). Visual interpretations of the groupings allowed for similarities and differences to be discerned between the alleles on the tested media independent of the strain background. Discussed below are a few general observations. The pie charts depicting cellular sensitivity and resistance look dissimilar between the two *spn1* alleles. The majority of resistant growth phenotypes occur on MMS in both alleles. This suggests a role in cellular response to MMS. Expression of spn1$^{K192N}$ results in temperature sensitivity when strains are grown on YPD plates at 39°C. In fact, there were no tested genetic interactions which resulted in suppression of the temperature sensitivity due to expression of spn1$^{K192N}$ (Figure 4.3 and Figure 4.4). Interestingly, a fair number of strains became temperature sensitive with the introduction of *spn1*$^{141-305}$ (Figure 4.3). Expression of spn1$^{141-305}$ appears to increase the sensitivity of cells to HU and caffeine. A number of strains became sensitive to HU with the introduction of *spn1*$^{k192N}$ although no caffeine sensitivities were observed. This suggests a role for Spn1 in cell cycle progression, specifically through replication. This role appears important to overcoming replication stress, which spn1$^{141-305}$ is defective. Interestingly, resistance in only observed in cells expressing spn1$^{k192N}$ when grown on HU, caffeine and MMS. Further indicating roles for Spn1 in DNA repair and replication. In contrast, the introduction of *spn1*$^{141-305}$ appears to give resistance on a wider variety of media (Figure 4.3). This is a bit misleading; the observed resistance is due to expression of spn1$^{141-305}$ in the *dot1Δ* strain, which provides increased growth even on YPD (Figure 3.9A).

To further analyze the *spn1* alleles, cellular growth was compared on each media type. The two alleles appear to behave similarly when grown on YPD, rapamycin, and exposed to UV (Figure 4.4). Large differences in growth are observed between the two alleles when cells are grown at 39°C, exposed to MMS, HU, and caffeine (Figure 4.4). From this analysis allele specific traits are more easily observable than when looking at specific genetic interactions or pathways. By combining these analyses with other data we can tease out further avenues of inquiry.

Table 4.1 Comparison of genetic interactions of *spn1*$^{K192N}$ and *spn1*$^{141-305}$ in deletion strains

| | ***spn1*$^{K192N}$** | | | ***spn1*$^{141-305}$** | | |
|---|---|---|---|---|---|---|
| | **Sensitive** | **No Change** | **Resistant** | **Sensitive** | **No Change** | **Resistant** |
| **YPD** | *rad6* | *BY4741, apn1, apn2, clb1, cln3, dot1, exo1, hfm1, isw1, mag1, mms2, msn2, msn4, mre11, ntg1, pol4, rad5, rad9, rad14, rad17, rad18, rad23, rad24, rad26, rad30, rad51, rad55, rad57, rev1, rev3, rev7, rmi1, rtt109, sae2, sgs1, siz1, srs2, tel1, top3, ubc13, xrs2* | | | *BY4741, apn1, apn2, clb1, cln3, exo1, hfm1, isw1, mag1, mms2, msn2, msn4, mre11, ntg1, pol4, rad5, rad6, rad9, rad14, rad17, rad18, rad23, rad24, rad26, rad30, rad51, rad55, rad57, rev1, rev3, rev7, rmi1, rtt109, sae2, sgs1, siz1, srs2, tel1, top3, ubc13, xrs2* | *dot1* |
| **39°C** | No growth in all backgrounds | | | *apn1, clb1, cln3, exo1, rad6, rad9 isw1, msn2, msn4, rad18, rad23, rad55, rad57, rev1,rev3, rmi1, siz1, tel1, ubc13* | *BY4741, hfm1, mms2, mre11, ntg1, pol4, rad5, rad14 (dead), rad17, rad24, rad26, rad30, rad51, rev7, rtt109, sae2, sgs1, srs2, top3, xrs2* | *dot1* |
| **UV** | | *BY4741, apn1, apn2, clb1, cln3, dot1, exo1, hfm1, isw1, mag1, mms2, msn2, msn4, mre11, ntg1, pol4, rad5, rad6, rad9, rad14 (dead), rad17, rad18 (dead), rad23, rad26, rad30, rad51, rad55, rad57, rev1, rev3, rev7, rmi1, rtt109, sae2, sgs1, srs2, tel1, top3, ubc13, xrs2* | | | *BY4741, apn1, apn2, clb1, cln3, exo1, hfm1, isw1, mag1, mms2, msn2, msn4, mre11, ntg1, pol4, rad5 (dead), rad6, rad9, rad14 (dead), rad17, rad18 (dead), rad23, rad26, rad30, rad51, rad55, rad57, rev1, rev3, rev7, rmi1, rtt109, sae2, sgs1, srs2, tel1, top3, ubc13, xrs2* | *dot1* |
| **CPT** | *rad6,rad55, rad57, sae2* | *BY4741, apn1, apn2, clb1, cln3, dot1, exo1, mms2, msn4, mre11, ntg1, pol4, rad5, rad9, rad14, rad18, rad23, rad26, rad51 (dead), rev7, rmi1, rtt109 (dead), srs2, tel1, top3 (dead)* | | *rmi1* | *BY4741, apn1, apn2, clb1, cln3, exo1, mms2, msn4, mre11, ntg1, pol1, rad5, rad6, rad9, rad14, rad18, rad23, rad26, rad51 (dead), rad55, rad57, rev7, rtt109 (dead), srs2, tel1, top3 (dead)* | *dot1, sae2* |

| | ***spn1*$^{K192N}$** | | | ***spn1*$^{141-305}$** | | |
|---|---|---|---|---|---|---|
| | **Sensitive** | **No Change** | **Resistant** | **Sensitive** | **No Change** | **Resistant** |
| **MMS** | | *dot1, rad5, rad6, rad23, rad18, rad17, rad51, rad55, rad57, rtt109, sae2, sgs1, siz1, top3, xrs2, tel1* | *BY4741, apn1, apn2, clb1, cln3, exo1, hfm1, isw1, mag1, mms2, msn2, msn4, mre11, ntg1, pol4, rad9, rad14, rad24, rad26, rad30, rev1, rev3, rev7, rmi1, srs2, ubc13* | *mag1, mms2, rad5, rad51, rmi1, rtt109, sgs1, siz1* | *mre11, rad6, rad9, rad17, rad18, rad23, rad55, rad57, sae2, tel1, top3, ubc13, xrs2* | *BY4741, apn1, apn2, clb1, cln3, dot1, exo1, hfm1, isw1, msn2, msn4, ntg1, pol4, rad14, rad24, rad26, rad30, rev1, rev3, rev7, srs2* |
| **CAF** | | *BY4741, apn1, apn2, clb1, cln3, dot1, exo1, hfm1, isw1, mms2, msn2, msn4, mre11, ntg1, pol4, rad5, rad6, rad9, rad17, rad18, rad23, rad24, rad26, rad30, rad51, rad55, rad57, rev1, rev3, rev7, rmi1, sae2, sgs1, siz1, srs2, tel1, top3, ubc13, xrs2* | *rad14* | *BY4741, clb1, cln3, dot1, exo1, hfm1, isw1, mms2, msn2, msn4, ntg1, pol4, rad6, rad9, rad23, rad26, rad30, rad51, rad55, rev1, rev3, rev7, sae2, siz1, srs2, top3, ubc13* | *apn1, apn2, mre11, rad5, rad14, rad17, rad18, rad24, rad57, rmi1, sgs1, tel1, xrs2* | |
| **HU** | *dot1, rad6, rad23, rad57, tel1, xrs2* | *BY4741, apn1, apn2, clb1, cln3, exo1, hfm1, isw1, mms2, msn2, msn4, mre11, ntg1, pol4, rad5, rad9, rad17, rad18, rad24, rad26, rad30, rad51, rad55(dead), rev1, rev3, rev7, rmi1, sae2, sgs1, siz1, srs2, top3 (dead), ubc13* | *rad14* | *BY4741, apn1, clb1, cln3, isw1, mms2, msn2, msn4,ntg1, pol4, rad6, rad9, rad17, rad23, rad24, rad26, rad30, rev1, rev3, rev7, rmi1, sae2, sgs1, siz1, srs2, tel1, ubc13, rs2* | *apn2, dot1, exo1, hfm1, mre11, rad5, rad51, rad55, rad57, top3 (dead)* | *rad14, rad18* |
| **RAP** | *rad6, rev7* | *BY4741, apn1, apn2, clb1, cln3, dot1, exo1, mms2, msn2, msn4, mre11, pol4, rad5, rad9, rad14, rad17, rad18, rad23, rad24, rad26, rad51, rad55, rad57, rmi1, sae2, sgs1, siz1, srs2, tel1, top3, xrs2* | | *rad14* | *BY4741, apn1, apn2, clb1, cln3, exo1, mms2, msn2, msn4, mre11, pol4, rad5, rad6, rad9, rad17, rad18, rad23, rad24, rad26, rad51, rad55, rad57, rev7, rmi1, sae2, sgs1, siz1, srs2, tel1, top3, xrs2* | *dot1* |

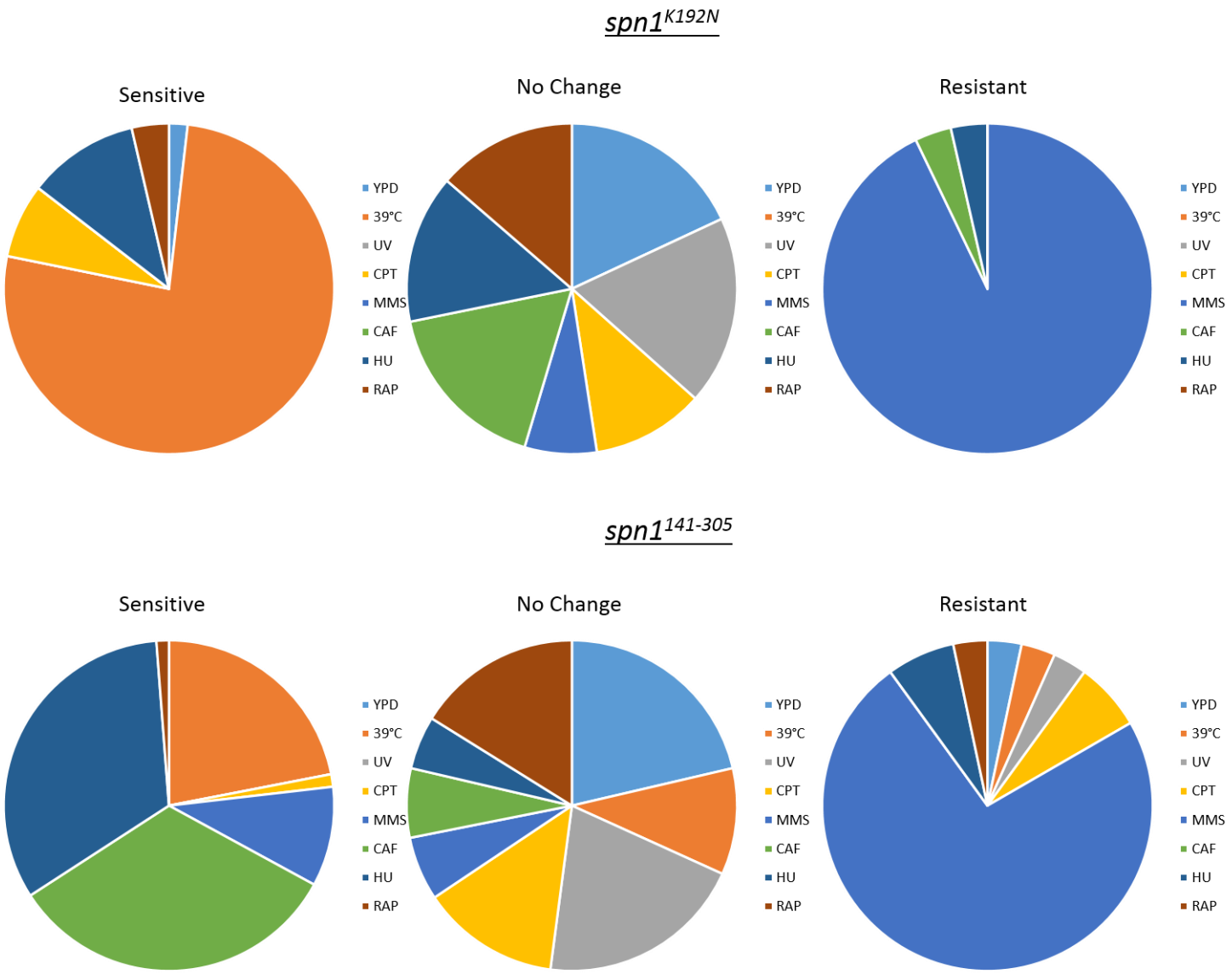


**Figure 4.3. Assessment of growth as a result of expression of spn1.**

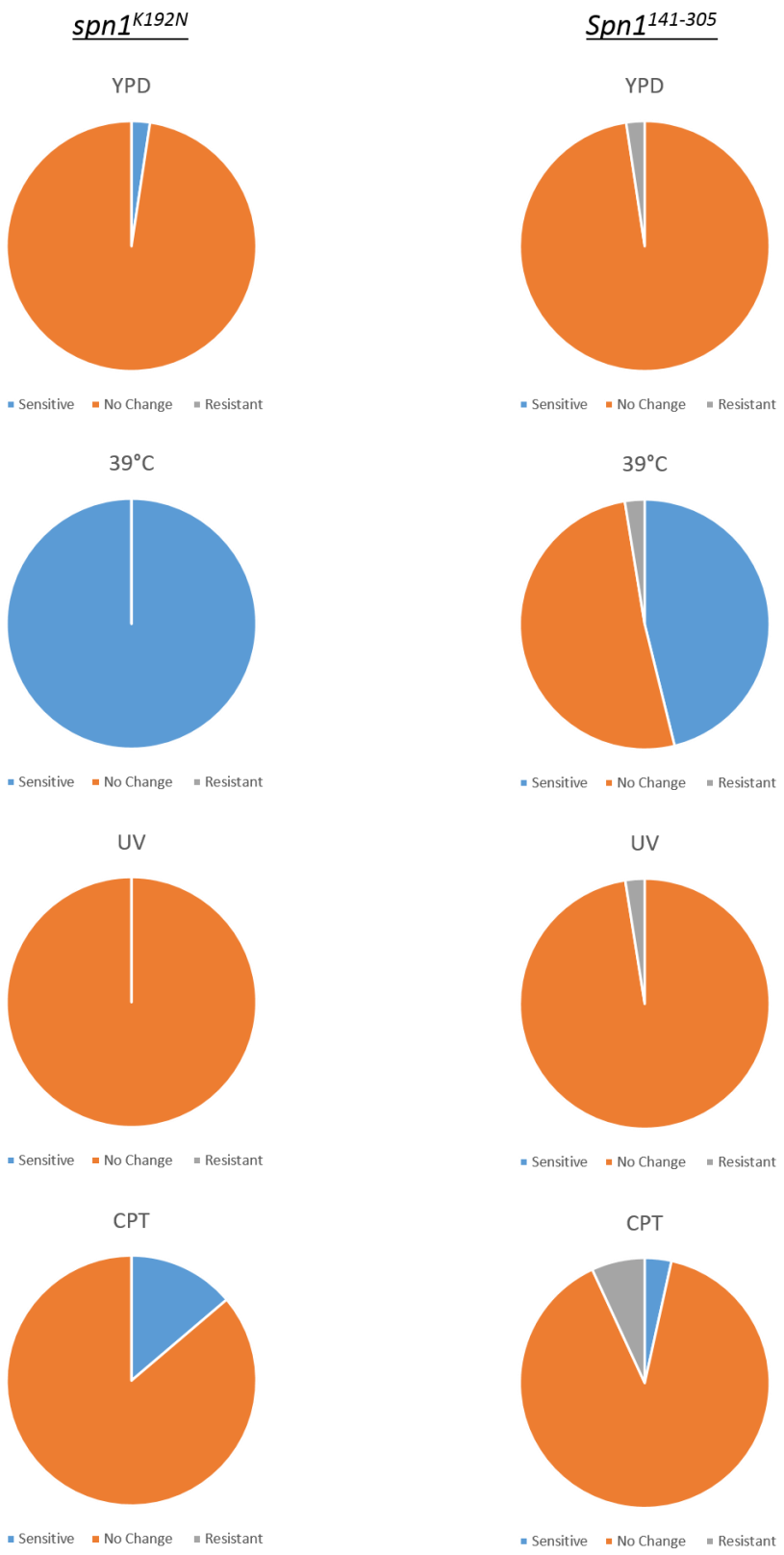


**Figure 4.4. Comparison of *spn1* alleles on tested growth media in deletion strain backgrounds.**

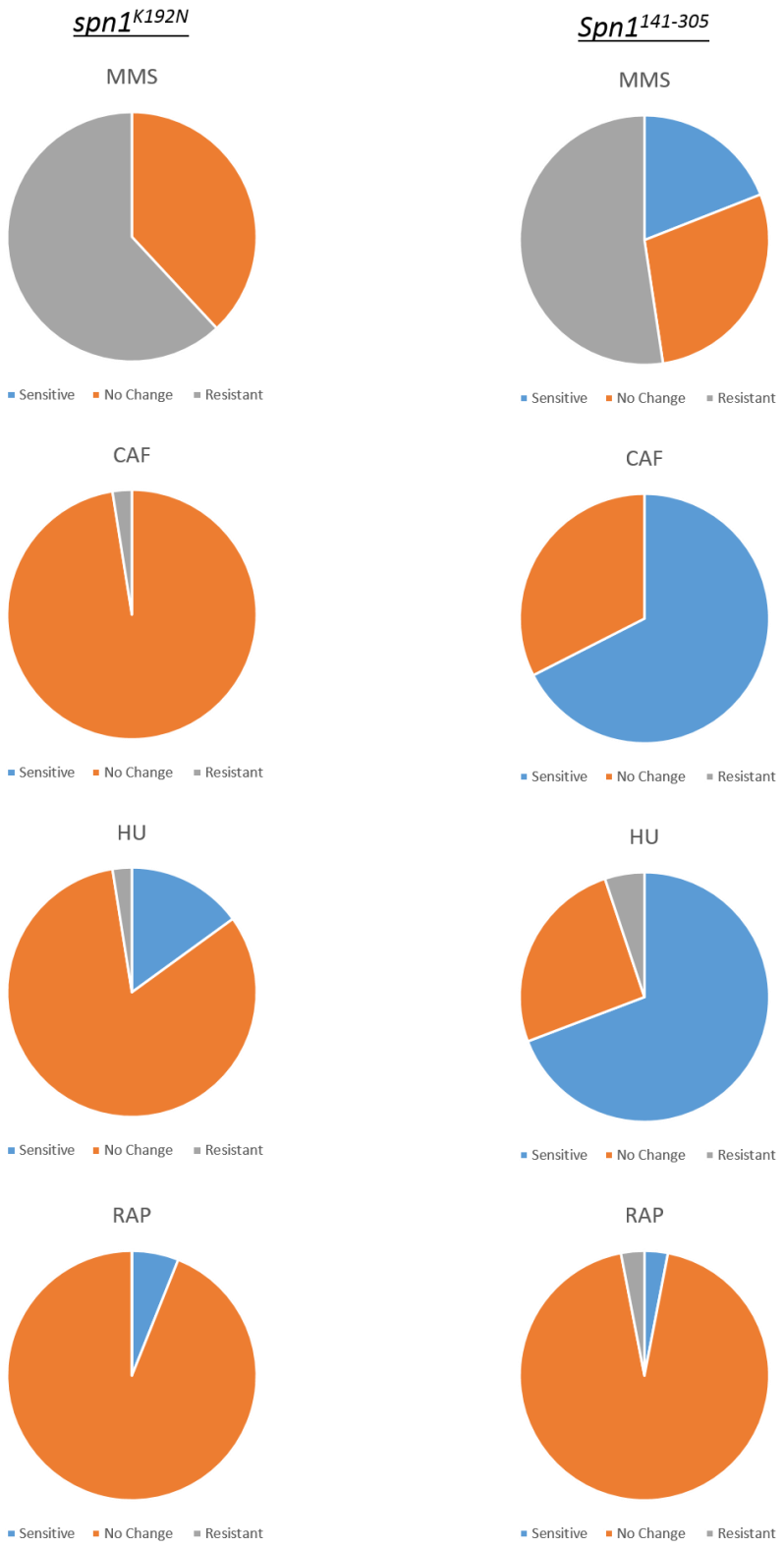


**Figure 4.4. continued.**

### *4.2.3 The spn1$^{k192N}$ strain is resistant to MMS*

Introduction of *spn1$^{k192N}$* and *spn1$^{141-305}$* both result in MMS resistance in BY4741 and a large number of other deletion strains (Figure 4.2A, Figure AI.1 and Table 4.1). MMS resistance is an unusual phenotype and is correlated with the DDT pathway (CONDE and SAN-SEGUNDO 2008; CONDE *et al.* 2010). As the two mutant proteins results in different physical interactions, transcriptional affects, genetic interactions, and chromatin effects, we wanted to investigate if the MMS resistance observed in *spn1$^{K192N}$* cells is also due to DDT regulation alteration. A similar stepwise genetic approach as in Chapter 3 was pursued to analyze how expression of spn1$^{K192N}$ affects cellular growth on MMS. Like *spn1$^{141-305}$*, *spn1$^{K192N}$* is recessive and the DNA damage response is active in the *spn1$^{K192N}$* strain (Figure 4.5B and 4.5C).

### *4.2.4 Resistance in the spn1$^{K192N}$ strain is not dependent on the damage tolerance pathways*

Genetic interactions between the *spn1$^{K192N}$* and genes involved in BER and NER were examined. Unlike the *spn1$^{141-305}$* strain, the resistance to MMS observed in cells expressing spn1$^{K192N}$ is not dependent on *MAG1*. The expression of spn1$^{K192N}$ in *apn1Δ*, *rad14Δ*, and *rad26Δ* retained resistance to MMS (Figure 4.6). This suggests the resistance in cells expressing spn1$^{K192N}$ is not dependent on BER or NER. The MMS resistance observed in the *mag1Δ* background highlights a difference between how these two mutant Spn1 proteins function in the cell (Figure 3.3, Figure 4.6 and Figure AI.1).

Cells expressing spn1$^{K192N}$ were analyzed for genetic interactions with genes involved in DDT and HR. A dependence on the error free sub-pathway in the *spn1$^{141-305}$* strain was observed (Figure 3.6 and 3.7). Interestingly, expression of spn1$^{K192N}$ in either the error free or the TLS sub-pathways promotes resistant growth on MMS, with the exception of the *rad5Δ* strain (Figure 4.7) However, this resistance is lost in HR deletion strain backgrounds (Figure 4.8). These data indicates the MMS resistance in the *spn1$^{K192N}$* strain is not dependent on the DDT pathway as

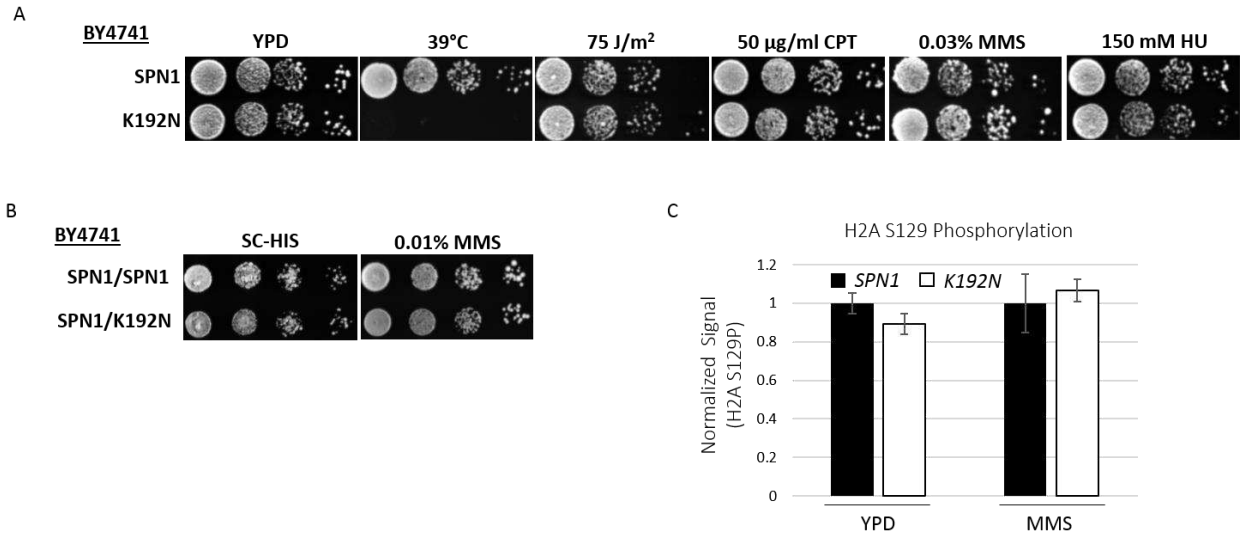


**Figure 4.5. Expression of spn1$^{K192N}$ suppresses sensitivity to the DNA damaging agent, methyl methanesulfonate.** A) Ten-fold serial dilutions of cells expressing Spn1 or spn1$^{k192N}$ B) Ten-fold serial dilutions of cells expressing endogenous Spn1 and plasmid bound Spn1 or spn1$^{K192N}$. C) Quantification of western blot showing H2A S129 phosphorylation levels before and after exposure to 0.1% MMS in cells expressing Spn1 or spn1$^{K192N}$. H2A S129 Phosphorylation signal is normalized to TBP signal. Spn1 ratio is set to 1. Standard deviation is calculated from 4-5 biological replicates.

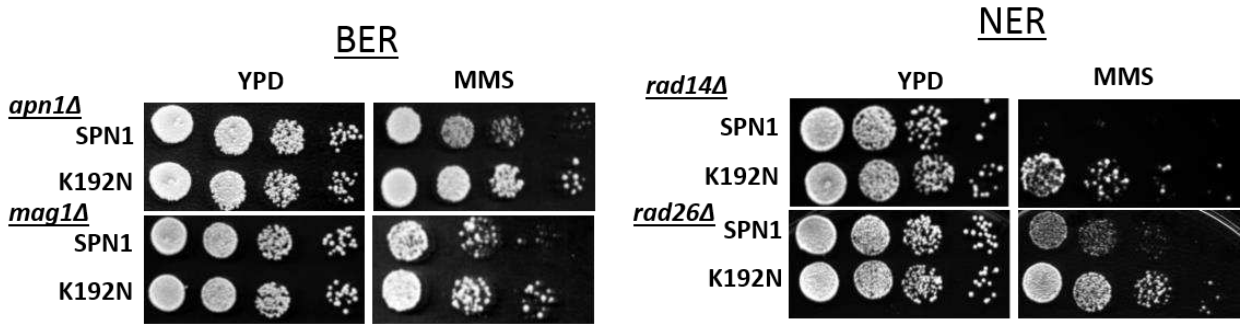


**Figure 4.6. *MMS* resistance in the *spn1$^{K192N}$* strain is independent of BER or NER.** Ten-fold serial dilutions of cells expressing Spn1 or spn1$^{K192N}$ in *apn1Δ*, *mag1Δ*, *rad14Δ* and *rad23Δ* strains. *apn1Δ,* and *mag1Δ* strains were grown on 0.01% MMS, *rad14Δ* and *rad23Δ,* strains were grown on 0.03% MMS.

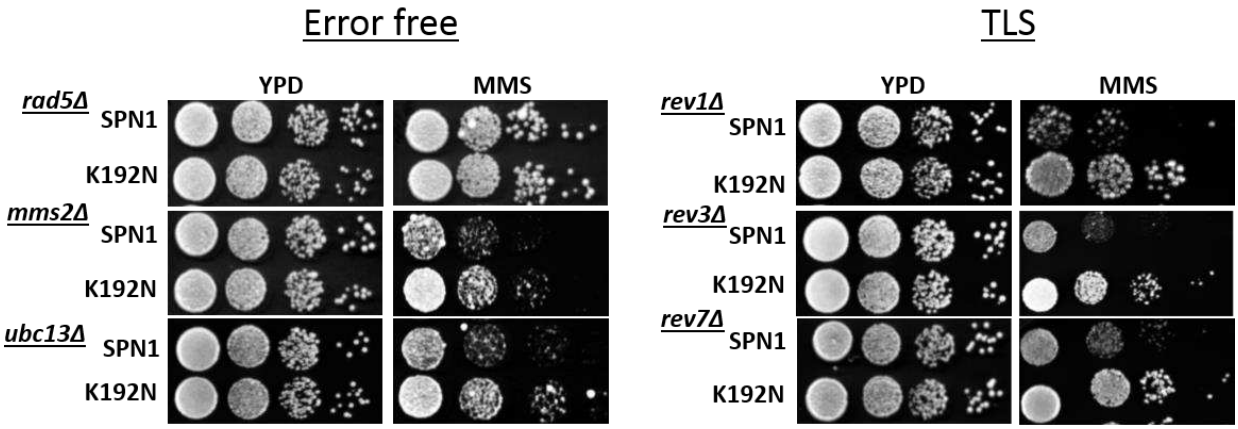


**Figure 4.7. *MMS* resistance in the *spn1$^{K192N}$* strain is independent of DDT.** Ten-fold serial dilutions of cells expressing Spn1 or spn1$^{K192N}$ in *rad5Δ*, *mms2Δ*, *ubc13Δ*, *rev1Δ*, *rev3Δ* and *rev7Δ* strains. *mms2Δ*, and *ubc13Δ* strains were grown on 0.01% MMS, *rad5Δ* strains were grown on 0.001% MMS, *rev1Δ*, *rev3Δ* and *rev7Δ* strains were grown in 0.03%, 0.015% and 0.02% MMS respectively.

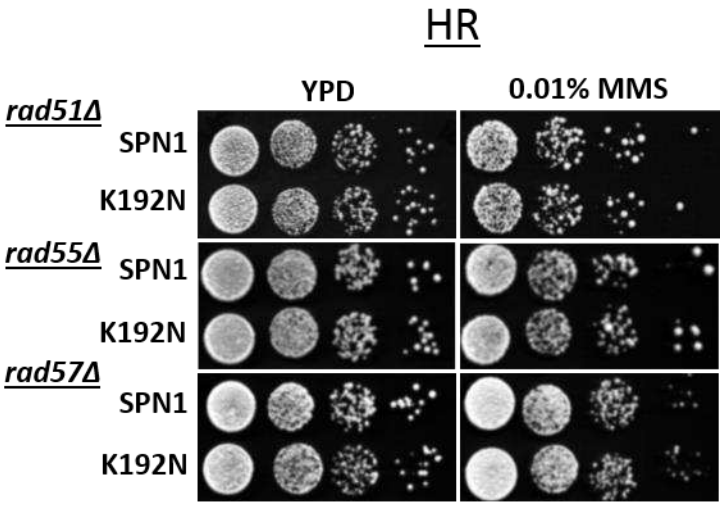


**Figure 4.8. MMS resistance is dependent on HR factors.** Ten-fold serial dilutions of cells expressing Spn1 or spn1$^{K192N}$ in *rad51Δ*, *rad55Δ*, and *rad57Δ.*

observed with the *spn1*$^{141-305}$ strain, although the resistance observed in both strains is dependent on a functional HR pathway.

### *4.2.5 Expression of* spn1$^{k192N}$ *decreases spontaneous and damage induced mutation rates but not loss of heterozygosity*

Expression of spn1$^{141-305}$ lowers spontaneous and damage induced mutation rates (Table 3.1). Transcription, chromatin architecture, replication and DNA damage response have all been shown to influence genome stability in the cell (AGUILERA and GARCIA-MUSE 2013). We were interested if expression of spn1$^{K192N}$ results in changes to the genome integrity. Interestingly, decreases in both spontaneous and damage induced mutation rates were observed (Table 4.2). This is similar to the *spn1*$^{141-305}$ strain. The decrease in genome instability in the *spn1*$^{141-305}$ strain was shown to be dependent on the error free sub-pathway of DDT. The decrease in genome instability in the *spn1*$^{K192N}$ strain is not dependent on the error free sub-pathway (Table 4.2). As deletion of *MMS2* does not result in wild type levels of genome instability. Furthermore how expression of spn1$^{K192N}$ would affect loss of heterozygosity was investigated. No significant decrease in loss of heterozygosity rates in the *spn1*$^{K192N}$ strain was observed (Table 4.2). This suggests the decrease in genome instability detected in the two *spn1* strains is the result of different mechanisms. This is interesting as DDT is known to contribute to a large amount of accumulated point mutations. The differences observed as a result of the two alleles highlights the ability of Spn1 to function with multiple partners, pathways and potentially phases in the cell cycle and yet still have an effect on genome stability.

## 4.3 Discussion

In this chapter, similarities and differences between the two *spn1* alleles and the challenges of interrupting the data to form a comprehensive picture of Spn1 function has been demonstrated. Transcriptional differences observed in these two strains is not surprising. Interestingly, there are more miss regulated genes in the *spn1*$^{141-305}$ strain and the majority of them are down regulated. In comparison, expression of spn1$^{k192N}$ results in bidirectional gene expression changes.

Table 4.2 Spontaneous and damage induced mutation rates of strains expressing Spn1 and spn1$^{K192N}$

| Spontaneous Mutation Rate | | | | | |
|---|---|---|---|---|---|
| **Strain** | **Mutation Rate x10^7** | **Upper Difference** | **Lower Difference** | **Number of Replicates** | **P-Value** |
| *Spn1* | 1.20 | 0.39 | 0.24 | 21 | |
| *spn1$^{K192N}$* | 0.64 | 0.11 | 0.19 | 21 | 0.0001 |
| *mms2Δ* | 25.56 | 6.32 | 2.60 | 14 | |
| *mms2Δspn1$^{K192N}$* | 19.03 | 2.50 | 3.54 | 14 | 0.0054 |
| **Damage Induced Mutation Rate** | | | | | |
| **Strain** | **Mutation Rate x10^7** | **Upper Difference** | **Lower Difference** | **Number of Replicates** | **P-Value** |
| *Spn1* | 22.76 | 3.07 | 3.64 | 21 | |
| *spn1$^{K192N}$* | 13.27 | 3.39 | 2.52 | 21 | < 0.0001 |
| *mms2Δ* | 289.63 | 101.42 | 39.39 | 21 | |
| *mms2Δspn1$^{K192N}$* | 168.59 | 62.59 | 40.97 | 20 | 0.0001 |
| **Loss of Heterozygosity** | | | | | |
| *Spn1* | 85.0928 | 10.1365 | 20.9103 | 27 | |
| *spn1$^{K192N}$* | 65.0022 | 29.0387 | 13.507 | 27 | 0.2666 |

Interestingly, GO-term analysis revealed bidirectional enrichment of processes in cells expressing spn1$^{141-305}$. While, in cells expressing spn1$^{141-305}$ most processes were down regulated. The ability of spn1$^{K192N}$ to still interact with chromatin may allow it to aid in chromatin assembly but localization maybe disrupted. In contrast, spn1$^{141-305}$ maybe localized to the correct location but chromatin processing is affected. Ongoing investigations into whether Spn1 directly interacts with RNAPII will provide insight into how Spn1 is targeted to genes. MNase digestion and nucleosome assembly assays suggests that Spn1 is involved in assembly of nucleosomes or histone exchange (LI *et al.* 2017). The loss of tail function in spn1$^{141-305}$ maybe why there is a greater number of genes affected and why around 70% are down regulated.

Genetic interactions with replication factors such as the CAF1 complex (LI *et al.* 2017) and Asf1 (PAMBLANCO *et al.* 2014; COSTANZO *et al.* 2016; LI *et al.* 2017), along with chromatin binding functions suggested Spn1 may function outside of transcription elongation (MCCULLOUGH *et al.* 2015; LI *et al.* 2017). In order to assess the role of Spn1 in replication and DNA repair the mutant alleles, *spn1$^{141-305}$* and *spn1$^{K192N}$* were introduced into deletion strains involved in DNA repair, DNA replication, chromatin structure, cell cycle regulation and cellular stress response pathways (Table 4.1 and Figure AI.1). Growth media were chosen to create cell stress, replication stress and DNA damage in order to study how Spn1 functions in the related pathways. The introduction of *spn1$^{141-305}$* results in more genetic interactions than *spn1$^{K192N}$* in the tested deletion strains. To evaluate cellular effects due to expression of either protein, cellular growth in all strains were compared on all media. Allele specific difference were observed. The overall analysis supports a role for Spn1 functioning during replication. Growth defects were observed with factors involved in DNA repair, HR, and DDT. These interactions are revealed on media containing MMS, HU and caffeine, which provide stress for those particular pathways. The observed replication defects are primarily due to expression of spn1$^{141-305}$. This implies that the functions lost by spn1$^{141-305}$ are important for

overcoming replication stress and are partially compensated by the ability of spn1$^{k192N}$ to bind to another factor or perform the function itself.

Cells expressing spn1$^{K192N}$ are temperature sensitive and suppression was not observed. Expression of spn1$^{K192N}$ allows for the cells to overcome many of the cellular stresses that cells expressing spn1$^{141-305}$ cannot overcome. Interestingly, both proteins result in MMS resistance in BY4741 and many of the deletion strains (Table 4.1 and Figure AI.1). Further analysis of this allele is necessary to fully comprehend the changes occurring in the cell. Although the interaction between Spn1 and Spt6 is important, disruption of the Spn1-Spt6 interface results in loss of repressive chromatin (McDonald *et al.* 2010). Experimental data has revealed that these two proteins can function independent of each other (ZHANG *et al.* 2008; ENGEL *et al.* 2015). From these analyses how disruption of the Spt6 binding is affecting Spn1 function cannot be concluded. Perhaps disruption of Spn1-Spt6 binding through mutation of Spt6 may shed more light on the importance of this interaction for functioning outside of transcription elongation.

Examining interactions with specific genes may provide more insight into how spn1$^{K192N}$ functions in the cell. One interesting interaction is between *spn1$^{K192N}$* and *RAD14*. Growth of the *rad14Δ* strain on HU is lethal, yet expression of spn1$^{K192N}$ rescues this sensitivity (Figure AI.1). In contrast, expression of spn1$^{141-305}$ cannot. The lack of UV mutant phenotypes suggests that Spn1 does not participate in the NER pathway. In fact, it appears cells can function without it if spn1$^{K192N}$ or spn1$^{141-305}$ are expressed after exposure to MMS. This genetic interaction could be revealing a gained function in cells expressing spn1$^{K192N}$ in overcoming replication stress due to NER defects. Further investigation into this interaction is warranted.

In chapter 3, the *spn1* allele, *spn1$^{141-305}$* was analyzed in specific pathways (BER, NER, DDT and HR) on MMS in a step wise fashion. This type of inquiry allowed for identification of miss regulation of the DDT pathway with the introduction of *spn1$^{141-305}$* (Figure 3.13). Interestingly, the *spn1$^{K192N}$* strain displays the same MMS resistant phenotype. Through genetic analysis the MMS

resistance observed was determined independent of the DNA damage tolerance pathway in cells expressing spn1$^{K192N.}$ The loss of resistance observed in cells expressing spn1$^{K192N}$ in HR defective cells, again highlights similarities and differences between these two alleles. Interestingly, decreases in spontaneous and damage induced mutation rates in the *spn1$^{K192N}$* strain were measured. However, LOH rates remained the same. These data highlights the importance of the chromatin functions of Spn1 during replication. How the expression of spn1$^{K192N}$ also results in decreased mutation rates needs further investigation.

These analyses supports a role for Spn1 outside of transcription and provide evidence for how loss of function and loss of interactions of Spn1 can affect cell growth. The loss of chromatin functions or the association with chromatin appears more detrimental than loss of known interactions with the core domain of Spn1. We predict Spn1 is either targeted or is involved in creating specific chromatin environments. Like transcription regulation, genome stability can also be regulated through the chromatin structure (CONDE and SAN-SEGUNDO 2008; GONZALEZ-HUICI *et al.* 2014; HUNG *et al.* 2017). Chromatin can impede the accessibility, dictate pathway selection and recruit specific factors. Further investigations should focus on where Spn1 is localized to and which factors it associates with.

# CHAPTER 5: POTENTIAL MODIFICATION OF SPN1 IN RESPONSE TO DNA DAMAGE AND REPLICATION STRESS

## 5.1 Introduction

Mec1 and Tel1 are evolutionarily conserved phosphatidylinositol-3 kinase related protein kinases (PIKKs). Mec1 and Tel1 transduce a kinase cascade after sensor proteins detect DNA damage or replication stress. PIKKs activate transducer kinases, such as Rad53 and Dun1, which activate effectors proteins. Effector proteins carry out DNA damage repair, cell cycle arrest, transcription programs, dNTP synthesis, and replication fork stabilization as a response to the cellular stress (CRAVEN *et al.* 2002; TOH and LOWNDES 2003; ENSERINK 2011). A number of studies have used mass spectrometry to identify targets of the Mec1/Tel1 cascade in order to understand cellular response programs. Using such approaches, Serine 23 phosphorylation of Spn1 was identified as a target of the kinase cascade after hydroxyurea (HU) and methyl methanesulfonate (MMS) exposure (SMOLKA *et al.* 2007; CHEN *et al.* 2010; BASTOS DE OLIVEIRA *et al.* 2015; HUSTEDT *et al.* 2015). Spn1 contains the Mec1/Tel1 consensus sequence (S/TQ). Phosphorylation was determined to be dependent on Mec1/Tel1 and not the downstream kinase Rad53 (SMOLKA *et al.* 2007). Rad53 is an essential conserved kinase necessary for proper cell cycle checkpoint functions (BRANZEI and FOIANI 2006). A number of histone chaperones have been identified as phosphorylation targets of the Mec1/Tel1 kinase cascade after exposure to HU or MMS (Figure 5.1, Table 5.1) (BASTOS DE OLIVEIRA *et al.* 2015; HUSTEDT *et al.* 2015). Of these, only Spn1 and Spt16, a subunit of the FACT complex, were identified as Mec1/Tel1 dependent targets (SMOLKA *et al.* 2007; BASTOS DE OLIVEIRA *et al.* 2015). Rlf2 (Cac1), a component of the CAF complex and Hpc2 were identified as Mec1/Tel1/Rad53 dependent targets (BASTOS DE OLIVEIRA *et al.* 2015). In the previous chapters, it was determined that Spn1 plays a role in replication and genome instability. These findings prompted the hypothesis that phosphorylation on S23 is required for the regulation of Spn1 function.

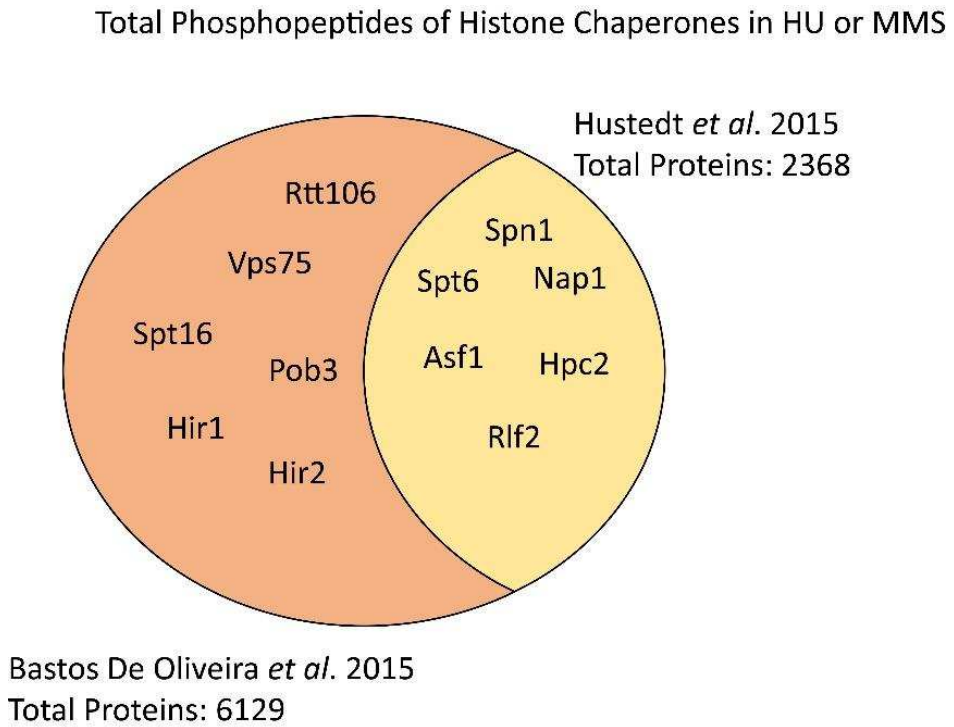


**Figure 5.1. Phosphorylated histone chaperones after HU or MMS exposure.**

Table 5.1 Phosphorylation site on histone chaperone

| Histone Chaperone | Site of Phosphorylation* |
|---|---|
| Spn1 | 15,20,22-23, 40, 89 |
| Spt6 | 94, 134, 136, 146-148, 155, 295, 206 |
| Nap1 | 20, 24, 76, 82, 140, 177 |
| Asf1 | 264-265, 269-270 |
| Vps75 | 3 |
| Rtt106 | 411, 408 |
| Spt16 | 526, 598, 765 |
| Pob3 | 194-195, 428-432 |
| Rlf2 | 77-78, 503 |
| Hir1 | 581, 610 |
| Hir2 | 460 |
| Hpc2 | 45, 81, 83, 221-222, 261-263, 303, 305-306, 310, 328-330, 386-387, 431, 433 |

*Site of phosphorylation detected in Husted *et al* 2015 and Bastos De Oliveira *et al* 2015

## 5.2 Results

### *5.2.1 Single mutants are not sufficient to affect growth*

Spn1 was identified as a target of phosphorylation after MMS and HU exposure (SMOLKA *et al.* 2007; BASTOS DE OLIVEIRA *et al.* 2015; HUSTEDT *et al.* 2015) thus, it was important to investigate if this modification was essential for the function of Spn1 in response to MMS exposure. The hypothesis that loss of phosphorylation at S23 could recapitulate MMS resistance was tested. Phospho-mimetic (*spn1*$^{S23D}$) and phospho-deficient (*spn1*$^{S23A}$) strains were created. Western analysis revealed there was no significant difference in spn1 protein expression levels between the *SPN1*, *spn1*$^{S23A}$ *and spn1*$^{S23D}$ strains (Figure 5.2A). The phosphorylation mutants reveal no cell cycle defects in logarithmic growth in YPD (Figure 5.2B). Phenotypic analysis was performed on a variety of media (Figure 5.2C). No mutant phenotypes were observed with the single point mutants.

### *5.2.2 Double mutants are not sufficient to affect growth*

Directly next to S23 in the amino acid sequence of Spn1 is S22, it seemed possible that S22 could be compensating for mutation to S23 and masking mutant phenotypes. The double amino acid substitution strains *spn1*$^{S22AS23A}$, *spn1*$^{S22AS23D}$*and spn1*$^{S22DS23D}$ were created. Western analysis revealed there was no significant difference in protein expression levels between the *SPN1*, *spn1*$^{S22AS23A}$,*spn1*$^{S22AS23D}$ *and spn1*$^{S22DS23D}$ strains (Figure 5.3A). Phenotypic analysis was performed on a variety of media (Figure 5.3B). We did not observe any mutant growth phenotypes as a result of expressing the double serine point mutants.

### *5.2.3 Serine double mutants do not affect genome stability*

A decrease in spontaneous and damage induced mutation rates were observed in both the *spn1*$^{141-305}$ and *spn1*$^{K192N}$ strains. Although there were no differences in growth between the phosphorylation mutants, it was possible that there were differences in mutation rates.

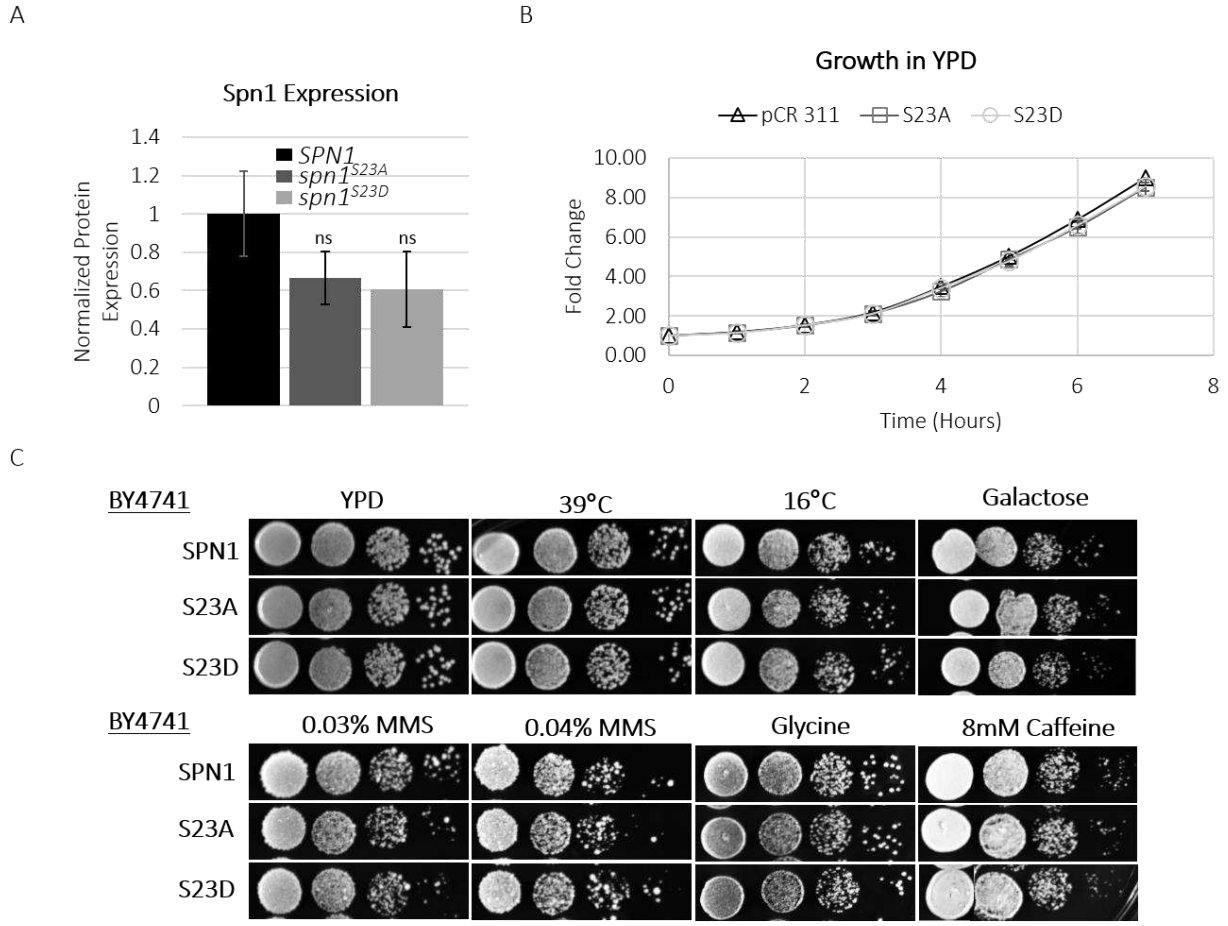


**Figure 5.2. Assessment of *spn1$^{S23D}$* and s*pn1$^{S23A}$*.** (A) Western analysis quantifying Spn1 levels in wildtype and phospho-mutant strains. To quantify the Spn1 levels, Spn1 signal was normalized to TBP signal within a sample. All samples are compare to wildtype expression level. Error bars were determined from the standard deviation of three biological replicates. Standard t-test was used to determine significance. (ns) no significance. (B) Growth curve performed in YPD. Growth curves were performed in duplicate. Fold change is the OD measurement of Tn over T0. T0 is set to 1. (C) Ten-fold serial dilutions of *SPN1*, and *spn1$^{S23A}$* and *spn1$^{S23D}$* were grown on indicated media for phenotypic analysis.

Seven biological replicates of the *SPN1*, and *spn1*$^{S22AS23A}$ *and spn1*$^{S22DS23D}$ strains were exposed to low dose MMS for a total of 72 hours. Damage induced mutation rates of the S22S23 mutants were not significantly different from wildtype levels (Figure 5.4). Spontaneous mutation rates were not examined, since any differences between the strains would have been exacerbated by exposure to a DNA damaging agent.

### *5.2.4 Construction of S22S23 mutants in repair and replication defective strains.*

To test the S22S23 mutants in deletion backgrounds in which mutant phenotypes with *spn1*$^{141\text{-}305}$ were observed. *SPN1* alleles, *spn1*$^{S22AS23A}$, *spn1*$^{S22AS23D}$, and *spn1*$^{S22DS23D}$ were tested in the *rev3Δ*, *mms2Δ* and *sgs1Δ* strains (studies are underway).

## 5.3 Discussion

Mutation of S23 alone or mutation of S23 and S22 did not result in mutant cellular growth. It is possible that single or double amino acid substitutions in the tail domains are not sufficient disruption for function studies. In fact, removal of the entire N and C terminal only results in moderate phenotypes unless in the combination with deletion of other genes (LI *et al.* 2017). Introduction of the double serine mutant alleles into DDT deletion background strains could result in observable mutant growth phenotypes. Although the amino acid substitutions, have not been successful in providing mutant alleles for study, this does not negate the importance of these modifications on Spn1 function. There are eighteen reported phosphorylation sites in Spn1 (CHERRY *et al.* 2012) (Figure 5.5). The majority of these are located within the disordered N-terminal tail. These phosphorylation events are regulated by a variety of kinases and phosphates, many of which are involved in response to replication stress (Table 5.2). In addition to the phosphorylated amino acids; sites of sumoylation, ubiquitination, and acetylation have also been identified on Spn1 (CHERRY *et al.* 2012; HENRIKSEN *et al.* 2012) (Figure 5.5).

A

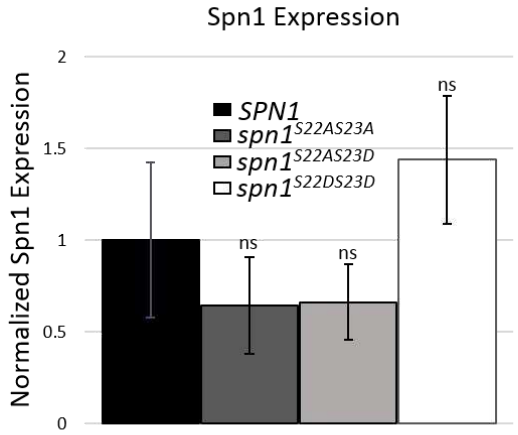


B

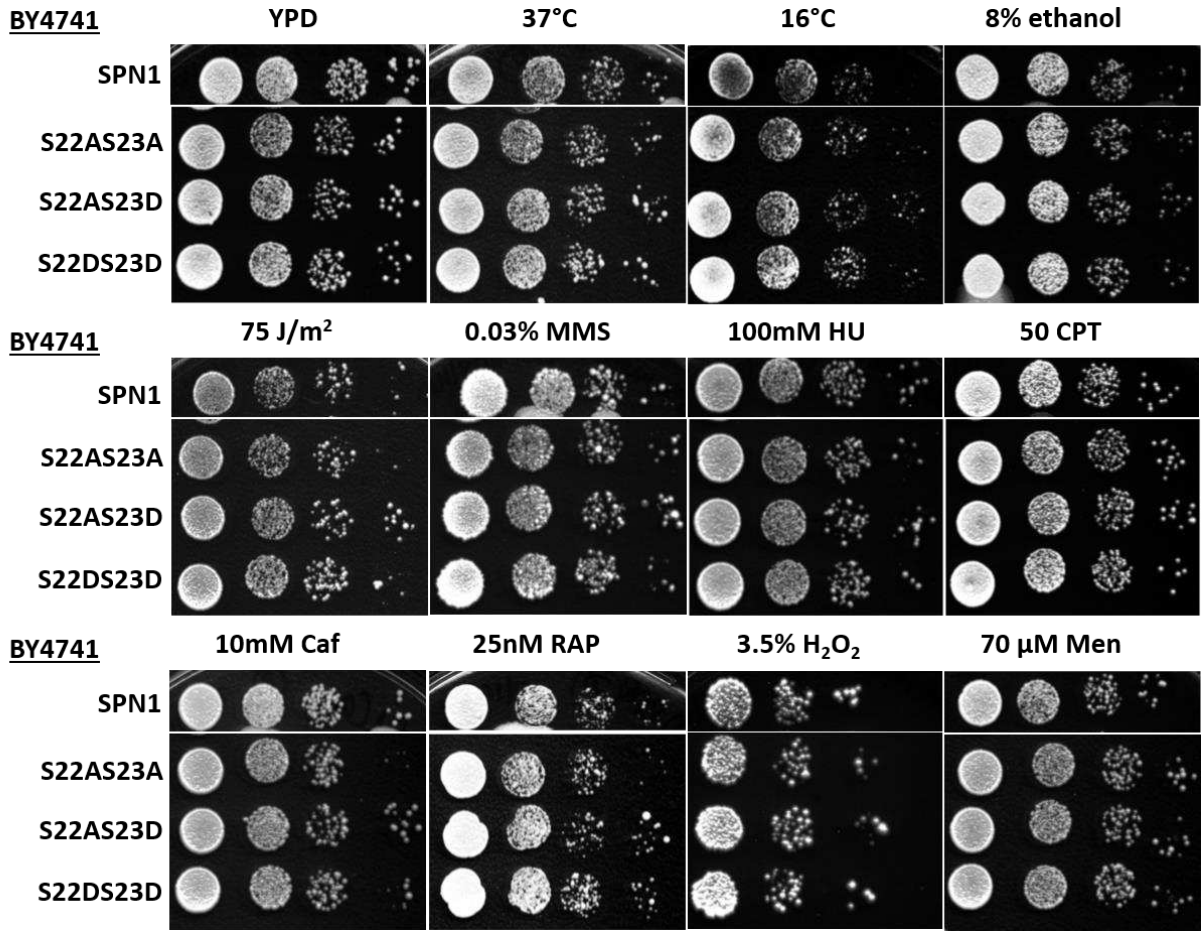


**Figure 5.3. Assessment of s*pn1*$^{S22AS23A}$, *spn1*$^{S22AS23D}$, and *spn1*$^{S22DS23D}$.** (A) Western analysis quantifying Spn1 levels in wildtype and phospho-mutant strains. To quantify the Spn1 levels, Spn1 signal was normalized to TBP signal within a sample. All samples are compare to wildtype expression level. Error bars were determined from the standard deviation of two biological replicates. Standard t-test was used to determine significance. (ns) no significance. (B) Ten-fold serial dilutions of the *SPN1*, *spn1*$^{S22AS23A}$, *spn1*$^{S22AS23D}$ *and spn1*$^{S22DS23D}$ strains were grown on indicated media for phenotypic analysis.

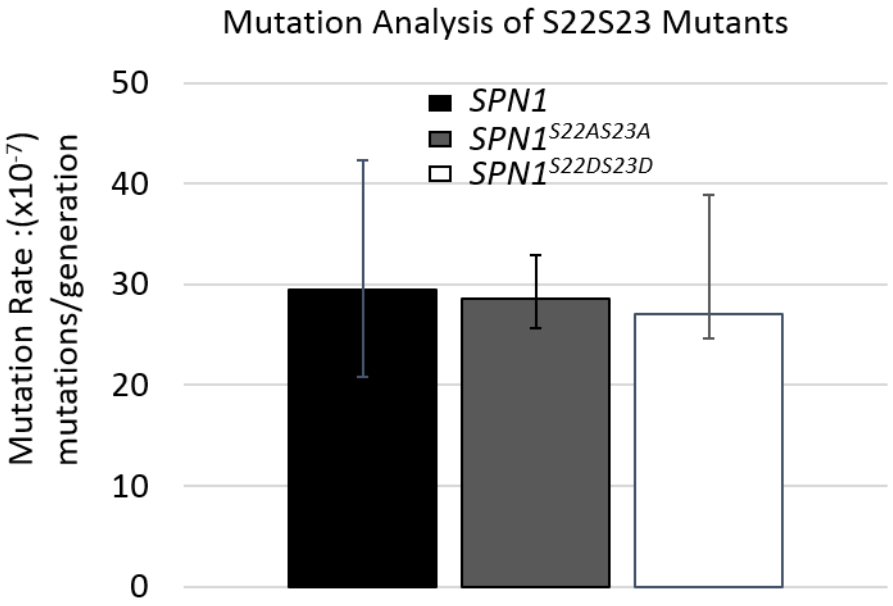


**Figure 5.4. Damage induced mutation rate of *SPN1*, *spn1*$^{S22AS23A}$, and *spn1*$^{S22DS23D}$ strains**. Mutation rates were calculated by the Lea-Coulson method of the median using the FALCOR program. Significance was determined using the Mann-Whitney nonparametric t-test on GraphPad. Fluctuation assay was performed twice with 7 replicates.

Many of these modifications occur together (SWANEY *et al.* 2013). Thus further directed genetic studies could enlighten how these modification most likely regulate binding partners, structure and function of Spn1. PTMs has been shown to regulate human Spn1 function and binding partners. The phosphorylation of S720/T721 of human Spn1 is correlated to the invasiveness, migration and proliferation of lung cancer cells (SANIDAS *et al.* 2014). Similar to its yeast counterpart human Spn1 can be heavily modified by PTMs (HORNBECK *et al.* 2015). Additionally, the N-terminal tail is predicted to be highly disordered, although it is much longer than yeast Spn1, containing up to 500 amino acids (PUJARI *et al.* 2010). Interestingly, the length of the N-terminal tail is what varies between the three detected isoforms of human Spn1 (OTA *et al.* 2004) (Figure 5.6B). The extent of PTM modification greatly varies between the three isoforms (Figure 5.6B). Using RADAR software, a repeat sequence was detected within the N-terminal tail of Isoform1 (HEGER and HOLM 2000) (Figure 5.6A). The sequence which is removed in Isoform 2 and Isoform 3 contains a 24 amino acid repetitive sequence, containing between four and six residues per repeat available for PTM (Figure 5.6A), indicating a possibly important regulatory domain in human Spn1 that has yet to be investigated.

MSTADQEQPK VVEATPEDGT ASSQKSTINA ENENTKQNQS MEPQETSKGT SNDTKDPDNG EKNEEAAIDEN SNVEAAERK RKHISTDFSD DDLEKEEHND QSLQPTVENR ASKDRDSSAT PSSRQELEEK LDRILKKPKV RRTRRDEDDL EQYLDEKILR LKDEMNIAAQ LDIDTLNKRI ETGDTSLIAM QKVKLLPKVV SVLSKANLAD TILDNNLLQS VRIWLEPLPD GSLPSFEIQK SLFAALNDLP VKTEHLKESG LGRVVIFYTK SKRVEAQLAR LAEKLIAEWT RPIIGASDNY RDKRIMQLEF DSEKLRKKSV MDSAKNRKKK SKSGEDPTSR GSSVQTLYEQ AAARRNRAAA PAQTTTDYKY APVSNLSAVP TNARAVGVGS TLNNSEMYKR LTSRLNKKHK

**Figure 5.5. Amino acid sequence of Spn1.** Highlighted amino acids are reported as sites for PTM in vivo and in vitro. Red: Phosphorylation Blue: Ubiquitination Green: Acetylation Purple: Ubiquitination and Acetylation. Phosphorylation and Ubiquitination (CHERRY *et al.* 2012) Acetylation (HENRIKSEN *et al.* 2012) and unpublished work performed by Lillian Huang.

Table 5.2 Reported modifiers of Spn1

| **Kinase*** | |
|---|---|
| *CHK1* | Serine/threonine kinase and DNA damage checkpoint effector; mediates cell cycle arrest, mammalian Chk1 checkpoint kinase |
| *BUB1* | Protein kinase involved in the cell cycle checkpoint into anaphase |
| *RIM11* | Protein kinase; required for signal transduction during entry into meiosis |
| *SKY1* | SR protein kinase (SRPK); involved in regulating proteins involved in mRNA metabolism and cation homeostasis |
| *TDA1* | Protein kinase of unknown cellular role, relocalizes from nucleus to cytoplasm upon DNA replication stress |
| *SSK2* | MAP kinase kinase kinase of HOG1 mitogen-activated signaling pathway |
| *PSK2* | serine/threonine protein kinase; regulates sugar flux and translation |
| *KNS1* | Protein kinase involved in negative regulation of PolIII transcription; effector kinase of the TOR signaling pathway and phosphorylates Rpc53p to regulate ribosome and tRNA biosynthesis |
| *YPS34* | Phosphatidylinositol (PI) 3-kinase that synthesizes PI-3-phosphate,may facilitate transcription elongation for genes positioned at the nuclear periphery |
| *MEC1* | Genome integrity checkpoint protein and PI kinase superfamily member; regulate dNTP pools and telomere length; signal transducer required for cell cycle arrest and transcriptional responses to damaged or unreplicated DNA; facilitates replication fork progression and regulates P-body formation under replication stress |
| *TEL1* | Protein kinase primarily involved in telomere length regulation; contributes to cell cycle checkpoint control in response to DNA damage |
| **Phosphatase*** | |
| *PSR2* | Plasma membrane phosphatase involved in the general stress response |
| *OCA1* | Putative protein tyrosine phosphatase; required for cell cycle arrest in response to oxidative damage of DNA |

Gene descriptions were adapted from the *Saccharomyces* Genome Database (CHERRY *et al.* 2012)

A

```
--------------------------------------------------------------------------------
No. of Repeats|Total Score|Length  |Diagonal| BW-From|   BW-To|   Level
             9|     346.26|      24|      24|     229|     252|       1
--------------------------------------------------------------------------------
   60-   86 (29.13/ 8.52)       LPKgHHVTDSENdePLNLNASDSESEE
   87-  112 (33.11/10.72)       LHR.QKDSDSESeeRAEPPASDSENED
  113-  137 (32.01/10.12)       VNQ..HGSDSESeeTRKLPGSDSENEE
  138-  163 (32.09/10.16)       LLN.GHASDSENedVGKHPASDSEIEE
  177-  202 (42.44/15.88)       ALK.PQISDSESeePPRHQASDSENEE
  216-  241 (45.75/17.71)       LPK.PQVSDSESeePPRHQASDSENEE
  242-  267 (46.36/18.05)       LPK.PRISDSESedPPRHQASDSENEE
  268-  293 (44.86/17.23)       LPK.PRISDSESedPPRNQASDSENEE
  294-  319 (40.50/14.81)       LPK.PRVSDSESegPQKGPASDSETED
--------------------------------------------------------------------------------
```

B

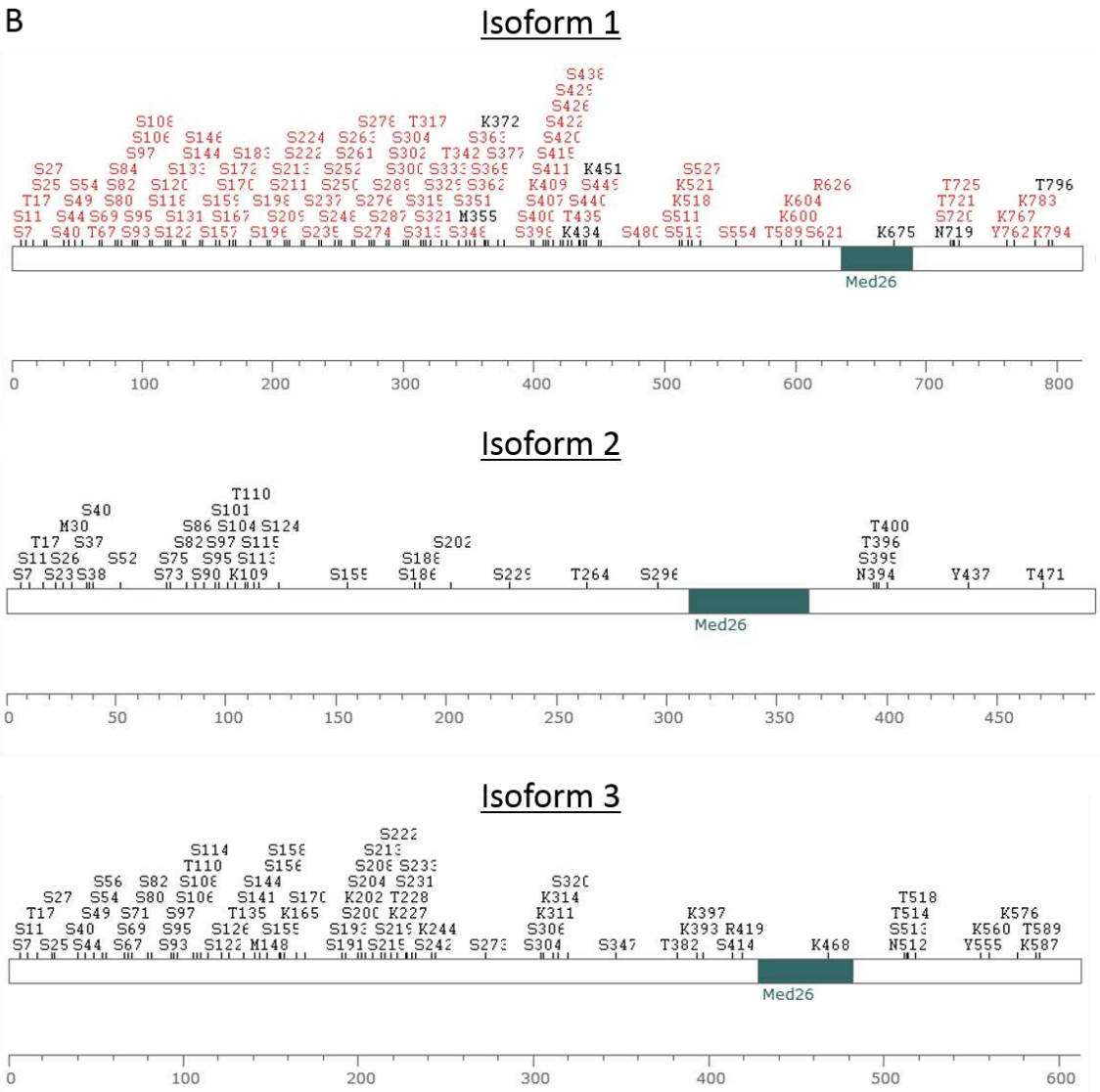


**Figure 5.6. Human Spn1 Isoforms.** (A) Repetitive sequences identified in human Spn1 isoform 1 using RADAR. (B) PTMs identified in the three isoforms of human Spn1.

# CHAPTER 6: SUMMARY AND FUTURE DIRECTIONS

In this thesis, the role of the essential transcription elongation and chromatin binding factor Spn1 was investigated in DNA damage response, cell cycle progression and genome instability. Other essential chromatin binding factors, such as the FACT complex have been shown to regulate chromatin structure in transcription, replication, and DNA repair (MACALPINE and ALMOUZNI 2013; BONDARENKO *et al.* 2015). The regulation of chromatin structure in multiple cellular process could be why the FACT complex is essential. Genetic interactions with histone chaperones involved in replication and DNA repair (LI *et al.* 2017), genetic interactions with the DNA replicative polymerases Polα and Polε (DUBARRY *et al.* 2015) and elongated telomeres as a result of decreased levels of Spn1 (UNGAR *et al.* 2009), led to inquiry if Spn1 could have functions in DNA replication and DNA repair (Figure 6.1). Upon depletion of Spn1, an increase in the number of cells in G2/M phase were observed by flow cytometry and budding index (Appendix V). This supported a role for Spn1 in replication and cell cycle progression.

The genetic interactions between *SPN1* and genes involved in DNA damage repair, replication, cell cycle progression, chromatin and DNA processing were assessed. In deletion strain backgrounds, the two mutant alleles of *SPN1* displayed similarities and differences in mutant phenotypic growth. The number of genetic interactions observed in cells expressing $spn1^{141\text{-}305}$ on HU and caffeine, suggest the chromatin functions of Spn1 are important for overcoming replication stress. In contrast, very few genetic interactions resulted from cells expressing $spn1^{K192N}$ on HU. The $spt6^{F249K}$ mutant results in disruption of the Spt6-Spn1 interface (MCDONALD *et al.* 2010). Interestingly, expression of the protein results in sensitivity to HU, in contrast expression of $spn1^{K129N}$ does not result in HU sensitivity in the wildtype background (MCCULLOUGH *et al.* 2015). This suggests that the interaction with Spt6 is not necessary for overcoming replication stress.

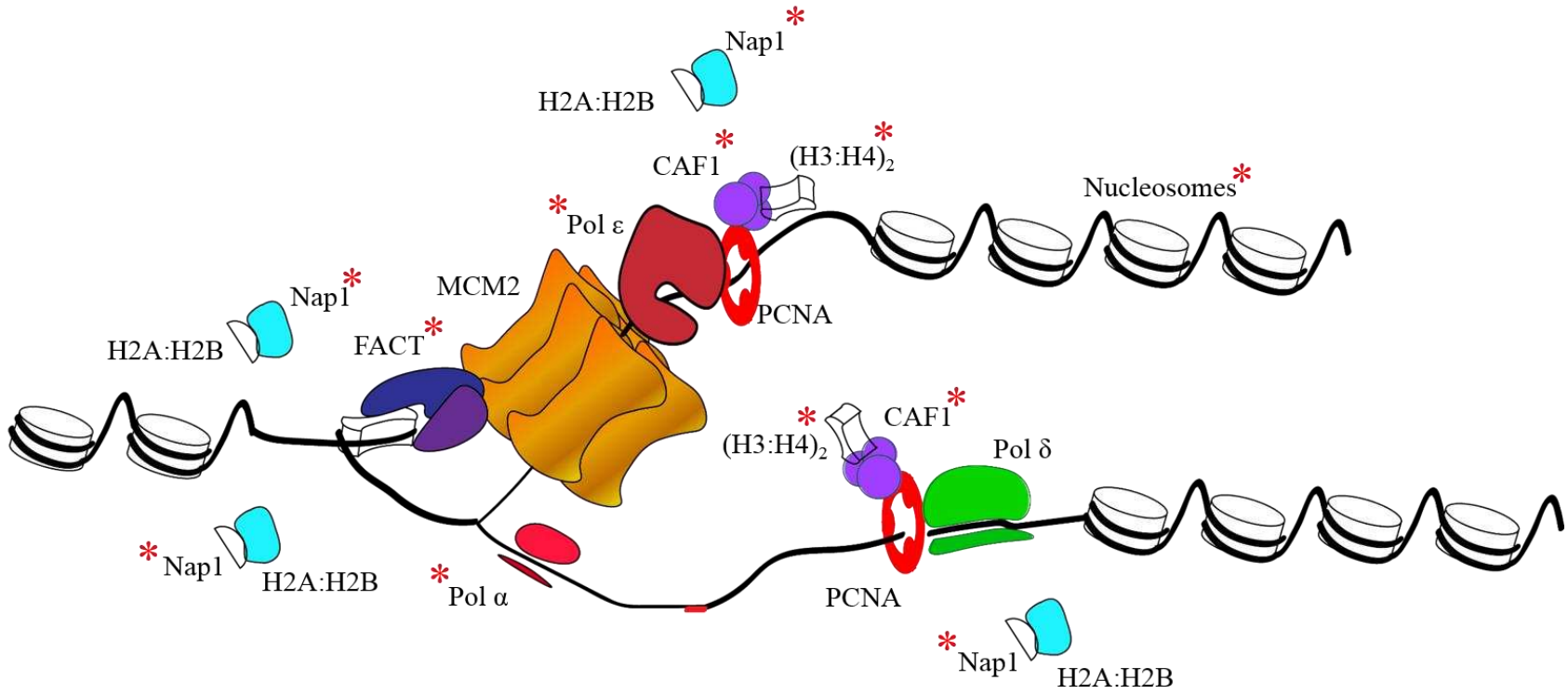


**Figure 6.1. Factors associated with replication that interact with Spn1.** Model depicting replication fork, red asterisk signifies genetic or physical interaction with Spn1. Nucleosomes, DNA, histones, CAF1 complex, Nap1 (LI *et al.* 2017) Polα and Polε (DUBARRY *et al.* 2015), FACT complex (unpublished by Cathy Radebaugh). Image adapted from (BELLUSH and WHITEHOUSE 2017).

During replication, chromatin structure is disrupted to allow for semi-conservative DNA synthesis. The DNA double helix must re-associate with histone octamers to form the chromatin structure of the newly synthesized sister chromatids. Maturation of chromatin after histone deposition involves establishing the proper histone code, association of linker histones, and establishment of higher order chromatin structure (MACALPINE and ALMOUZNI 2013; ALABERT *et al.* 2014; BELLUSH and WHITEHOUSE 2017). Genetic interactions have been shown between the mutant alleles of *SPN1* and the replicative histone chaperone complexes, CAF1 and FACT (LI *et al.* 2017) (Radebaugh, unpublished). The histone chaperone CAF-1 has been shown to localize to the replication fork through interactions with PCNA (SHIBAHARA and STILLMAN 1999). CAF-1 along with histone chaperone Asf1 aids in the proper assemble of newly formed chromatin after DNA synthesis (MACALPINE and ALMOUZNI 2013). Human Spn1 and yeast Spn1 have both been shown to associate with chromatin throughout the cell cycle (KUBOTA *et al.* 2012; ALABERT *et al.* 2014; DUNGRAWALA *et al.* 2015). In addition, human Spn1 was determined to be an early arriving chromatin component factor during replication (ALABERT *et al.* 2014). The role of Spn1 during replication could be associating with newly replicated DNA to aid in the maturation of chromatin.

An unusual mutant growth phenotype was observed in cells expressing either spn1$^{K192N}$ or spn1$^{141-305}$ in the BY4741 background. An increase in resistant growth on plates containing the DNA damaging agent, MMS was observed. To evaluate the source of this resistance, genetic interactions between *SPN1* and genes involved in base excision repair (BER), nucleotide excision repair (NER), homologous recombination (HR), and the DNA damage tolerance (DDT) pathway were examined. Through these genetic interactions, the resistance to MMS observed in the *spn1$^{141-305}$* strain was determined to be dependent on both HR and the DDT pathways. Interestingly, the MMS resistance phenotype observed in the *spn1$^{K192N}$* strain was also dependent on the HR pathway but independent of the DDT pathway. Human Spn1 recruits the HYPB/Setd2 methyltransferase required for H3K36 trimethylation (H3K36me3) (YOH *et al.* 2008). H3K36me3

through Setd2 activity has been shown to recruit HR factors to DSBs (PFISTER *et al.* 2014). Investigations into Spn1 localization at DSBs should be pursued. Spn1 could function in the recognition, recruitment of HR factors or reestablishment of the chromatin structure.

Deletion of the H3K79 methyltransferase, Dot1 also results in resistance to MMS (CONDE and SAN-SEGUNDO 2008). The loss of TLS inhibition resulting in MMS resistance in the *dot1Δ* strain was determined to be due to the loss of the methylase activity (CONDE *et al.* 2010). Interestingly, extreme growth is observed in the *spn1*$^{141\text{-}305}$*dot1*Δ strain suggesting deregulation of both sub-pathways of DDT. This may be due to aberrant chromatin structure. Investigations into Spn1-Dot1 interaction, and Spn1-Dot1 and Spn1-H3K79me3 genome localization should be investigated. The chromatin environment related to DNA damage tolerance is not well understood. The ubiquitination of H2B (H2Bub) at L123 through the actions of Bre1, an ubiquitin ligase, and Rad6 have been shown to influence both template switching and TLS during S and G2/M respectively (HUNG *et al.* 2017). In addition to a role in DDT, H2Bub is involved in transcription and mRNA processing (HUNG *et al.* 2017). Genetic interactions between *BRE1* and *SPN1* should be examined. These investigations could lead to substantial increases in understanding both Spn1 function on chromatin and chromatin structure regulation of the DDT pathway.

Both *spn1*$^{k192N}$ and *spn1*$^{141\text{-}305}$ strains had significant decreases in spontaneous and damage induced mutation rates. Furthermore, the *spn1*$^{141\text{-}305}$ strain had decreased levels of LOH. This indicates that Spn1 promotes multiple types of genome instability in the cell. There are a few known cellular processes that promote genome instability: genetic recombination during meiosis, non-homologous end joining (NHEJ), and the TLS polymerase activities. Beyond these pathways, very few studies have identified or discussed genes whose wildtype protein products increase genome instability. A genome wide study identified a small percentage of genes whose deletion decreased formation of Rad52 foci in response to DNA damage (ALVARO *et al.* 2007).

While this subgroup was not investigated, it was suggested that this subset of genes could contribute to spontaneous damage within the genome (ALVARO *et al.* 2007). The decrease in mutation rate in cells expressing spn1$^{141-305}$ is dependent on DDT, while cells expressing spn1$^{K192N}$ were not. We hypothesize that expression of Spn1 promotes progression through the TLS sub-pathway during G2, while expression of spn1$^{141-305}$ promotes progression through the error free sub-pathway during S phase (Figure 3.13). How the decrease in spontaneous and damage induced mutation rates arise in cells expressing spn1$^{K192N}$ needs further investigation. Highly transcribed genes accumulate more spontaneous damage, and strong genetic interactions with *RAD14* could imply an unknown role contributing to NER.

Through molecular and biochemical approaches, evidence for Spn1 function during S phase and cell cycle progression as well as contributing to increased genome instability has been provided. The ability for Spn1 to associate with chromatin appears important for overcoming replication stress. We predict that upon further investigations, Spn1 will be revealed as an important factor in regulating the chromatin environment throughout the cell cycle.

# REFERENCES


ACUNA, G., F. E. WURGLER and C. SENGSTAG, 1994 Reciprocal mitotic recombination is the predominant mechanism for the loss of a heterozygous gene in Saccharomyces cerevisiae. Environ Mol Mutagen **24:** 307-316.

AGUILERA, A., and T. GARCIA-MUSE, 2013 Causes of genome instability. Annu Rev Genet **47:** 1-32.

ALABERT, C., J. C. BUKOWSKI-WILLS, S. B. LEE, G. KUSTATSCHER, K. NAKAMURA *et al.*, 2014 Nascent chromatin capture proteomics determines chromatin dynamics during DNA replication and identifies unknown fork components. Nat Cell Biol **16:** 281-293.

ALLEN, C., S. BUTTNER, A. D. ARAGON, J. A. THOMAS, O. MEIRELLES *et al.*, 2006 Isolation of quiescent and nonquiescent cells from yeast stationary-phase cultures. J Cell Biol **174:** 89-100.

ALVARO, D., M. LISBY and R. ROTHSTEIN, 2007 Genome-wide analysis of Rad52 foci reveals diverse mechanisms impacting recombination. PLoS Genet **3:** e228.

ANDERSEN, M. P., Z. W. NELSON, E. D. HETRICK and D. E. GOTTSCHLING, 2008 A genetic screen for increased loss of heterozygosity in Saccharomyces cerevisiae. Genetics **179:** 1179-1195.

BASTOS DE OLIVEIRA, F. M., D. KIM, J. R. CUSSIOL, J. DAS, M. C. JEONG *et al.*, 2015 Phosphoproteomics reveals distinct modes of Mec1/ATR signaling during DNA replication. Mol Cell **57:** 1124-1132.

BAUER, N. C., A. H. CORBETT and P. W. DOETSCH, 2015 The current state of eukaryotic DNA base damage and repair. Nucleic Acids Res **43:** 10083-10101.

BELLUSH, J. M., and I. WHITEHOUSE, 2017 DNA replication through a chromatin environment. Philos Trans R Soc Lond B Biol Sci **372**.

BENTON, M. G., S. SOMASUNDARAM, J. D. GLASNER and S. P. PALECEK, 2006 Analyzing the dose-dependence of the Saccharomyces cerevisiae global transcriptional response to methyl methanesulfonate and ionizing radiation. BMC Genomics **7:** 305.

BERNSTEIN, K. A., E. SHOR, I. SUNJEVARIC, M. FUMASONI, R. C. BURGESS *et al.*, 2009 Sgs1 function in the repair of DNA replication intermediates is separable from its role in homologous recombinational repair. EMBO J **28:** 915-925.

BONDARENKO, M. T., N. V. MALUCHENKO, M. E. VALIEVA, N. S. GERASIMOVA, O. I. KULAEVA *et al.*, 2015 [Structure and function of histone chaperone FACT]. Mol Biol (Mosk) **49:** 891-904.

BRAMBATI, A., A. COLOSIO, L. ZARDONI, L. GALANTI and G. LIBERI, 2015 Replication and transcription on a collision course: eukaryotic regulation mechanisms and implications for DNA stability. Frontiers in Genetics **6**.

BRANZEI, D., and M. FOIANI, 2006 The Rad53 signal transduction pathway: Replication fork stabilization, DNA repair, and adaptation. Exp Cell Res **312:** 2654-2659.

BRANZEI, D., and M. FOIANI, 2008 Regulation of DNA repair throughout the cell cycle. Nat Rev Mol Cell Biol **9:** 297-308.

BRANZEI, D., and I. PSAKHYE, 2016 DNA damage tolerance. Curr Opin Cell Biol **40:** 137-144.

BRANZEI, D., and B. SZAKAL, 2016 DNA damage tolerance by recombination: Molecular pathways and DNA structures. DNA Repair (Amst) **44:** 68-75.

BRESLOW, D. K., D. M. CAMERON, S. R. COLLINS, M. SCHULDINER, J. STEWART-ORNSTEIN *et al.*, 2008 A comprehensive strategy enabling high-resolution functional analysis of the yeast genome. Nat Methods **5:** 711-718.

CAMPOS-DOERFLER, L., S. SYED and K. H. SCHMIDT, 2018 Sgs1 Binding to Rad51 Stimulates Homology-Directed DNA Repair in Saccharomyces cerevisiae. Genetics **208:** 125-138.

CAVALLI, G., and F. THOMA, 1993 Chromatin transitions during activation and repression of galactose-regulated genes in yeast. Embo J **12:** 4603-4613.

CHANG, M., M. BELLAOUI, C. BOONE and G. W. BROWN, 2002 A genome-wide screen for methyl methanesulfonate-sensitive mutants reveals genes required for S phase progression in the presence of DNA damage. Proc Natl Acad Sci U S A **99:** 16934-16939.

CHATTERJEE, N., and G. C. WALKER, 2017 Mechanisms of DNA damage, repair, and mutagenesis. Environ Mol Mutagen **58:** 235-263.

CHEN, C., and R. D. KOLODNER, 1999 Gross chromosomal rearrangements in Saccharomyces cerevisiae replication and recombination defective mutants. Nat Genet **23:** 81-85.

CHEN, J., B. DERFLER, A. MASKATI and L. SAMSON, 1989 Cloning a eukaryotic DNA glycosylase repair gene by the suppression of a DNA repair defect in Escherichia coli. Proc Natl Acad Sci U S A **86:** 7961-7965.

CHEN, S. H., C. P. ALBUQUERQUE, J. LIANG, R. T. SUHANDYNATA and H. ZHOU, 2010 A proteome-wide analysis of kinase-substrate network in the DNA damage response. J Biol Chem **285:** 12803-12812.

CHERRY, J. M., E. L. HONG, C. AMUNDSEN, R. BALAKRISHNAN, G. BINKLEY *et al.*, 2012 Saccharomyces Genome Database: the genomics resource of budding yeast. Nucleic Acids Res **40:** D700-705.

COLLINS, S. R., K. M. MILLER, N. L. MAAS, A. ROGUEV, J. FILLINGHAM *et al.*, 2007 Functional dissection of protein complexes involved in yeast chromosome biology using a genetic interaction map. Nature **446:** 806-810.

CONDE, F., D. ONTOSO, I. ACOSTA, A. GALLEGO-SANCHEZ, A. BUENO *et al.*, 2010 Regulation of tolerance to DNA alkylating damage by Dot1 and Rad53 in Saccharomyces cerevisiae. DNA Repair (Amst) **9:** 1038-1049.

CONDE, F., and P. A. SAN-SEGUNDO, 2008 Role of Dot1 in the response to alkylating DNA damage in Saccharomyces cerevisiae: regulation of DNA damage tolerance by the error-prone polymerases Polzeta/Rev1. Genetics **179:** 1197-1210.

COSTANZO, M., B. VANDERSLUIS, E. N. KOCH, A. BARYSHNIKOVA, C. PONS *et al.*, 2016 A global genetic interaction network maps a wiring diagram of cellular function. Science **353**.

CRAVEN, R. J., P. W. GREENWELL, M. DOMINSKA and T. D. PETES, 2002 Regulation of genome stability by TEL1 and MEC1, yeast homologs of the mammalian ATM and ATR genes. Genetics **161:** 493-507.

DAIGAKU, Y., A. A. DAVIES and H. D. ULRICH, 2010 Ubiquitin-dependent DNA damage bypass is separable from genome replication. Nature **465:** 951-955.

DIEBOLD, M. L., M. KOCH, E. LOELIGER, V. CURA, F. WINSTON *et al.*, 2010 The structure of an Iws1/Spt6 complex reveals an interaction domain conserved in TFIIS, Elongin A and Med26. EMBO J **29:** 3979-3991.

DINANT, C., G. AMPATZIADIS-MICHAILIDIS, H. LANS, M. TRESINI, A. LAGAROU *et al.*, 2013 Enhanced chromatin dynamics by FACT promotes transcriptional restart after UV-induced DNA damage. Mol Cell **51:** 469-479.

DOWNS, J. A., N. F. LOWNDES and S. P. JACKSON, 2000 A role for Saccharomyces cerevisiae histone H2A in DNA repair. Nature **408:** 1001-1004.

DUBARRY, M., C. LAWLESS, A. P. BANKS, S. COCKELL and D. LYDALL, 2015 Genetic Networks Required to Coordinate Chromosome Replication by DNA Polymerases alpha, delta, and epsilon in Saccharomyces cerevisiae. G3 (Bethesda) **5:** 2187-2197.

DUINA, A. A., M. E. MILLER and J. B. KEENEY, 2014 Budding yeast for budding geneticists: a primer on the Saccharomyces cerevisiae model system. Genetics **197:** 33-48.

DUNGRAWALA, H., K. L. ROSE, K. P. BHAT, K. N. MOHNI, G. G. GLICK *et al.*, 2015 The Replication Checkpoint Prevents Two Types of Fork Collapse without Regulating Replisome Stability. Mol Cell **59:** 998-1010.

ENSERINK, J. M., 2011 Cell Cycle Regulation of DNA Replication in S. cerevisiae. DNA Replication - Current Advances**:** 391-408.

FARRUGIA, G., and R. BALZAN, 2012 Oxidative stress and programmed cell death in yeast. Front Oncol **2:** 64.

FISCHBECK, J. A., S. M. KRAEMER and L. A. STARGELL, 2002 SPN1, a conserved gene identified by suppression of a postrecruitment-defective yeast TATA-binding protein mutant. Genetics **162:** 1605-1616.

FOSTER, E. R., and J. A. DOWNS, 2005 Histone H2A phosphorylation in DNA double-strand break repair. FEBS J **272:** 3231-3240.

FOSTER, P. L., 2006 Methods for determining spontaneous mutation rates. Methods Enzymol **409:** 195-213.

GASCH, A. P., M. HUANG, S. METZNER, D. BOTSTEIN, S. J. ELLEDGE *et al.*, 2001 Genomic expression responses to DNA-damaging agents and the regulatory role of the yeast ATR homolog Mec1p. Mol Biol Cell **12:** 2987-3003.

GERARD, A., E. SEGERAL, M. NAUGHTIN, A. ABDOUNI, B. CHARMETEAU *et al.*, 2015 The integrase cofactor LEDGF/p75 associates with Iws1 and Spt6 for postintegration silencing of HIV-1 gene expression in latently infected cells. Cell Host Microbe **17:** 107-117.

GHAEMMAGHAMI, S., W. K. HUH, K. BOWER, R. W. HOWSON, A. BELLE *et al.*, 2003 Global analysis of protein expression in yeast. Nature **425:** 737-741.

GONZALEZ-HUICI, V., B. SZAKAL, M. URULANGODI, I. PSAKHYE, F. CASTELLUCCI *et al.*, 2014 DNA bending facilitates the error-free DNA damage tolerance pathway and upholds genome integrity. Embo Journal **33:** 327-340.

GOSPODINOV, A., and Z. HERCEG, 2013 Chromatin structure in double strand break repair. DNA Repair (Amst) **12:** 800-810.

GUZDER, S. N., Y. HABRAKEN, P. SUNG, L. PRAKASH and S. PRAKASH, 1996a RAD26, the yeast homolog of human Cockayne's syndrome group B gene, encodes a DNA-dependent ATPase. J Biol Chem **271:** 18314-18317.

GUZDER, S. N., P. SUNG, L. PRAKASH and S. PRAKASH, 1996b Nucleotide excision repair in yeast is mediated by sequential assembly of repair factors and not by a pre-assembled repairosome. J Biol Chem **271:** 8903-8910.

HALL, B. M., C. X. MA, P. LIANG and K. K. SINGH, 2009 Fluctuation analysis CalculatOR: a web tool for the determination of mutation rate using Luria-Delbruck fluctuation analysis. Bioinformatics **25:** 1564-1565.

HANAMSHET, K., O. M. MAZINA and A. V. MAZIN, 2016 Reappearance from Obscurity: Mammalian Rad52 in Homologous Recombination. Genes (Basel) **7**.

HARUKI, H., J. NISHIKAWA and U. K. LAEMMLI, 2008 The anchor-away technique: rapid, conditional establishment of yeast mutant phenotypes. Mol Cell **31:** 925-932.

HASSAN, H. M., and I. FRIDOVICH, 1979 Intracellular production of superoxide radical and of hydrogen peroxide by redox active compounds. Arch Biochem Biophys **196:** 385-395.

HEGER, A., and L. HOLM, 2000 Rapid automatic detection and alignment of repeats in protein sequences. Proteins **41:** 224-237.

HENRIKSEN, P., S. A. WAGNER, B. T. WEINERT, S. SHARMA, G. BACINSKAJA *et al.*, 2012 Proteome-wide analysis of lysine acetylation suggests its broad regulatory scope in Saccharomyces cerevisiae. Mol Cell Proteomics **11:** 1510-1522.

HORNBECK, P. V., B. ZHANG, B. MURRAY, J. M. KORNHAUSER, V. LATHAM *et al.*, 2015 PhosphoSitePlus, 2014: mutations, PTMs and recalibrations. Nucleic Acids Res **43:** D512-520.

HUANG, D., B. D. PIENING and A. G. PAULOVICH, 2013 The preference for error-free or error-prone postreplication repair in Saccharomyces cerevisiae exposed to low-dose methyl methanesulfonate is cell cycle dependent. Mol Cell Biol **33:** 1515-1527.

HUANG, M. E., A. G. RIO, A. NICOLAS and R. D. KOLODNER, 2003 A genomewide screen in Saccharomyces cerevisiae for genes that suppress the accumulation of mutations. Proc Natl Acad Sci U S A **100:** 11529-11534.

HUMPAL, S. E., D. A. ROBINSON and J. E. KREBS, 2009 Marks to stop the clock: histone modifications and checkpoint regulation in the DNA damage response. Biochem Cell Biol **87:** 243-253.

HUNG, S. H., R. P. WONG, H. D. ULRICH and C. F. KAO, 2017 Monoubiquitylation of histone H2B contributes to the bypass of DNA damage during and after DNA replication. Proc Natl Acad Sci U S A **114:** E2205-E2214.

HUSTEDT, N., S. M. GASSER and K. SHIMADA, 2013 Replication Checkpoint: Tuning and Coordination of Replication Forks in S Phase. Genes **4:** 388-434.

HUSTEDT, N., A. SEEBER, R. SACK, M. TSAI-PFLUGFELDER, B. BHULLAR *et al.*, 2015 Yeast PP4 interacts with ATR homolog Ddc2-Mec1 and regulates checkpoint signaling. Mol Cell **57:** 273-289.

JELINSKY, S. A., and L. D. SAMSON, 1999 Global response of Saccharomyces cerevisiae to an alkylating agent. Proc. Natl. Acad. Sci. USA **96:** 1486-1491.

JENSEN, R., G. F. SPRAGUE, JR. and I. HERSKOWITZ, 1983 Regulation of yeast mating-type interconversion: feedback control of HO gene expression by the mating-type locus. Proc Natl Acad Sci U S A **80:** 3035-3039.

KAWASAKI, Y., and A. SUGINO, 2001 Yeast replicative DNA polymerases and their role at the replication fork. Molecules and Cells **12:** 277-285.

KIM, J. A., and J. E. HABER, 2009 Chromatin assembly factors Asf1 and CAF-1 have overlapping roles in deactivating the DNA damage checkpoint when DNA repair is complete. Proc Natl Acad Sci U S A **106:** 1151-1156.

KOLODNER, R. D., C. D. PUTNAM and K. MYUNG, 2002 Maintenance of genome stability in Saccharomyces cerevisiae. Science **297:** 552-557.

KROGAN, N. J. M., M. KIM, S. H. AHN, G. ZHONG, M. S. KOBOR *et al.*, 2002 RNA polymerase II elongation factors of Saccharomyces cerevisiae: a targeted proteomics approach. Mol Cell Biol **22:** 6979-6992.

KUBOTA, T., D. A. STEAD, S. HIRAGA, S. TEN HAVE and A. D. DONALDSON, 2012 Quantitative proteomic analysis of yeast DNA replication proteins. Methods **57:** 196-202.

KULAK, N. A., G. PICHLER, I. PARON, N. NAGARAJ and M. MANN, 2014 Minimal, encapsulated proteomic-sample processing applied to copy-number estimation in eukaryotic cells. Nat Meth **11:** 319-324.

KUMARAN, R., S. Y. YANG and J. Y. LEU, 2013 Characterization of chromosome stability in diploid, polyploid and hybrid yeast cells. PLoS One **8:** e68094.

LAURENT, J. M., J. H. YOUNG, A. H. KACHROO and E. M. MARCOTTE, 2016 Efforts to make and apply humanized yeast. Brief Funct Genomics **15:** 155-163.

LEA, D. E., and C. A. COULSON, 1949 The Distribution of the Numbers of Mutants in Bacterial Populations. Journal of Genetics **49:** 264-285.

LEE, K. Y., and K. MYUNG, 2008 PCNA modifications for regulation of post-replication repair pathways. Mol Cells **26:** 5-11.

LI, S., A. R. ALMEIDA, C. A. RADEBAUGH, L. ZHANG, X. CHEN *et al.*, 2017 The elongation factor Spn1 is a multi-functional chromatin binding protein. Nucleic Acids Res.

LI, S. R., C. A.; STARGELL, L. A.; LUGER, K. , 2018 Coordinated regulation of chromatin dynamics by Spn1-Spt6 complex. Manuscript in preparation.

LIU, Z., Z. ZHOU, G. CHEN and S. BAO, 2007 A putative transcriptional elongation factor hIws1 is essential for mammalian cell proliferation. Biochem Biophys Res Commun **353:** 47-53.

LONGO, V. D., and P. FABRIZIO, 2012 Chronological Aging in Saccharomyces cerevisiae. Aging Research in Yeast **57:** 101-121.

LUGER, K., A. W. MADER, R. K. RICHMOND, D. F. SARGENT and T. J. RICHMOND, 1997 Crystal structure of the nucleosome core particle at 2.8 A resolution. Nature **389:** 251-260.

LURIA, S. E., and M. DELBRUCK, 1943 Mutations of Bacteria from Virus Sensitivity to Virus Resistance. Genetics **28:** 491-511.

MACALPINE, D. M., and G. ALMOUZNI, 2013 Chromatin and DNA replication. Cold Spring Harb Perspect Biol **5:** a010207.

MADIA, F., C. GATTAZZO, P. FABRIZIO and V. D. LONGO, 2007 A simple model system for age-dependent DNA damage and cancer. Mech Ageing Dev **128:** 45-49.

MADIA, F., M. WEI, V. YUAN, J. HU, C. GATTAZZO *et al.*, 2009 Oncogene homologue Sch9 promotes age-dependent mutations by a superoxide and Rev1/Polzeta-dependent mechanism. J Cell Biol **186:** 509-523.

MAYER, A., M. LIDSCHREIBER, M. SIEBERT, K. LEIKE, J. SODING *et al.*, 2010 Uniform transitions of the general RNA polymerase II transcription complex. Nat Struct Mol Biol **17:** 1272-1278.

MCCULLOUGH, L., Z. CONNELL, C. PETERSEN and T. FORMOSA, 2015 The Abundant Histone Chaperones Spt6 and FACT Collaborate to Assemble, Inspect, and Maintain Chromatin Structure in Saccharomyces cerevisiae. Genetics **201:** 1031-1045.

MCDONALD, S. M., D. CLOSE, H. XIN, T. FORMOSA and C. P. HILL, 2010 Structure and biological importance of the Spn1-Spt6 interaction, and its regulatory role in nucleosome binding. Mol Cell **40:** 725-735.

MEAS, R., M. J. SMERDON and J. J. WYRICK, 2015 The amino-terminal tails of histones H2A and H3 coordinate efficient base excision repair, DNA damage signaling and postreplication repair in Saccharomyces cerevisiae. Nucleic Acids Res **43:** 4990-5001.

MEMISOGLU, A., and L. SAMSON, 2000 Base excision repair in yeast and mammals. Mutat Res **451:** 39-51.

MIMITOU, E. P., and L. S. SYMINGTON, 2008 Sae2, Exo1 and Sgs1 collaborate in DNA double-strand break processing. Nature **455:** 770-774.

MITCHEL, K., K. LEHNER and S. JINKS-ROBERTSON, 2013 Heteroduplex DNA position defines the roles of the Sgs1, Srs2, and Mph1 helicases in promoting distinct recombination outcomes. PLoS Genet **9:** e1003340.

MULLEN, J. R., F. S. NALLASETH, Y. Q. LAN, C. E. SLAGLE and S. J. BRILL, 2005 Yeast Rmi1/Nce4 controls genome stability as a subunit of the Sgs1-Top3 complex. Mol Cell Biol **25:** 4476-4487.

NAIR, N., M. SHOAIB and C. S. SORENSEN, 2017 Chromatin Dynamics in Genome Stability: Roles in Suppressing Endogenous DNA Damage and Facilitating DNA Repair. Int J Mol Sci **18**.

NOVOA, C. A., J. S. ANG and P. C. STIRLING, 2018 The A-Like Faker Assay for Measuring Yeast Chromosome III Stability. Methods Mol Biol **1672:** 1-9.

O'BRIEN, K. P., M. REMM and E. L. SONNHAMMER, 2005 Inparanoid: a comprehensive database of eukaryotic orthologs. Nucleic Acids Res **33:** D476-480.

ODELL, I. D., S. S. WALLACE and D. S. PEDERSON, 2013a Rules of engagement for base excision repair in chromatin. Journal of Cellular Physiology **228:** 258-266.

ODELL, I. D., S. S. WALLACE and D. S. PEDERSON, 2013b Rules of engagement for base excision repair in chromatin. J Cell Physiol **228:** 258-266.

OTA, T., Y. SUZUKI, T. NISHIKAWA, T. OTSUKI, T. SUGIYAMA *et al.*, 2004 Complete sequencing and characterization of 21,243 full-length human cDNAs. Nat Genet **36:** 40-45.

PAMBLANCO, M., P. OLIETE-CALVO, E. GARCIA-OLIVER, M. LUZ VALERO, M. M. SANCHEZ DEL PINO *et al.*, 2014 Unveiling novel interactions of histone chaperone Asf1 linked to TREX-2 factors Sus1 and Thp1. Nucleus **5:** 247-259.

PFISTER, S. X., S. AHRABI, L. P. ZALMAS, S. SARKAR, F. AYMARD *et al.*, 2014 SETD2-dependent histone H3K36 trimethylation is required for homologous recombination repair and genome stability. Cell Rep **7:** 2006-2018.

POLO, S. E., and G. ALMOUZNI, 2015 Chromatin dynamics after DNA damage: The legacy of the access-repair-restore model. DNA Repair (Amst) **36:** 114-121.

PRADO, F., and M. CLEMENTE-RUIZ, 2012 Nucleosome assembly and genome integrity: The fork is the link. Bioarchitecture **2:** 6-10.

PRAKASH, L., and S. PRAKASH, 1977 Isolation and characterization of MMS-sensitive mutants of Saccharomyces cerevisiae. Genetics **86:** 33-55.

PRAKASH, S., and L. PRAKASH, 2000 Nucleotide excision repair in yeast. Mutat Res **451:** 13-24.

PUJARI, V., C. A. RADEBAUGH, J. V. CHODAPARAMBIL, U. M. MUTHURAJAN, A. R. ALMEIDA *et al.*, 2010 The transcription factor Spn1 regulates gene expression via a highly conserved novel structural motif. J Mol Biol **404:** 1-15.

SANIDAS, I., C. POLYTARCHOU, M. HATZIAPOSTOLOU, S. A. EZELL, F. KOTTAKIS *et al.*, 2014 Phosphoproteomics screen reveals akt isoform-specific signals linking RNA processing to lung cancer. Mol Cell **53:** 577-590.

SCHULDINER, M., S. R. COLLINS, N. J. THOMPSON, V. DENIC, A. BHAMIDIPATI *et al.*, 2005 Exploration of the function and organization of the yeast early secretory pathway through an epistatic miniarray profile. Cell **123:** 507-519.

SHIBAHARA, K., and B. STILLMAN, 1999 Replication-dependent marking of DNA by PCNA facilitates CAF-1-coupled inheritance of chromatin. Cell **96:** 575-585.

SHIMADA, K., Y. OMA, T. SCHLEKER, K. KUGOU, K. OHTA *et al.*, 2008 Ino80 chromatin remodeling complex promotes recovery of stalled replication forks. Curr Biol **18:** 566-575.

SKONECZNA, A., A. KANIAK and M. SKONECZNY, 2015 Genetic instability in budding and fission yeast-sources and mechanisms. Fems Microbiology Reviews **39:** 917-967.

SMOLKA, M. B., C. P. ALBUQUERQUE, S. H. CHEN and H. ZHOU, 2007 Proteome-wide identification of in vivo targets of DNA damage checkpoint kinases. Proc Natl Acad Sci U S A **104:** 10364-10369.

SPENCER, F., S. L. GERRING, C. CONNELLY and P. HIETER, 1990 Mitotic Chromosome Transmission Fidelity Mutants in Saccharomyces-Cerevisiae. Genetics **124:** 237-249.

STIRLING, P. C., M. S. BLOOM, T. SOLANKI-PATIL, S. SMITH, P. SIPAHIMALANI *et al.*, 2011 The complete spectrum of yeast chromosome instability genes identifies candidate CIN cancer genes and functional roles for ASTRA complex components. PLoS Genet **7:** e1002057.

STONE, J. E., S. A. LUJAN, T. A. KUNKEL and T. A. KUNKEL, 2012 DNA polymerase zeta generates clustered mutations during bypass of endogenous DNA lesions in Saccharomyces cerevisiae. Environ Mol Mutagen **53:** 777-786.

SUGAWARA, N., and J. E. HABER, 2012 Monitoring DNA recombination initiated by HO endonuclease. Methods Mol Biol **920:** 349-370.

SUPEK, F., M. BOSNJAK, N. SKUNCA and T. SMUC, 2011 REVIGO summarizes and visualizes long lists of gene ontology terms. PLoS One **6:** e21800.

SWANEY, D. L., P. BELTRAO, L. STARITA, A. GUO, J. RUSH *et al.*, 2013 Global analysis of phosphorylation and ubiquitylation cross-talk in protein degradation. Nat Methods **10:** 676-682.

SYMINGTON, L. S., R. ROTHSTEIN and M. LISBY, 2014 Mechanisms and regulation of mitotic recombination in Saccharomyces cerevisiae. Genetics **198:** 795-835.

TOH, G. W., and N. F. LOWNDES, 2003 Role of the Saccharomyces cerevisiae Rad9 protein in sensing and responding to DNA damage. Biochem Soc Trans **31:** 242-246.

TSUKUDA, T., A. B. FLEMING, J. A. NICKOLOFF and M. A. OSLEY, 2005 Chromatin remodelling at a DNA double-strand break site in Saccharomyces cerevisiae. Nature **438:** 379-383.

UNGAR, L., N. YOSEF, Y. SELA, R. SHARAN, E. RUPPIN *et al.*, 2009 A genome-wide screen for essential yeast genes that affect telomere length maintenance. Nucleic Acids Res **37:** 3840-3849.

VAN ATTIKUM, H., O. FRITSCH and S. M. GASSER, 2007 Distinct roles for SWR1 and INO80 chromatin remodeling complexes at chromosomal double-strand breaks. EMBO J **26:** 4113-4125.

VAN, C., J. S. WILLIAMS, T. A. KUNKEL and C. L. PETERSON, 2015 Deposition of histone H2A.Z by the SWR-C remodeling enzyme prevents genome instability. DNA Repair (Amst) **25:** 9-14.

VIJG, J., and Y. SUH, 2013 Genome instability and aging. Annu Rev Physiol **75:** 645-668.

WALLACE, S. S., 2014 Base excision repair: a critical player in many games. DNA Repair (Amst) **19:** 14-26.

WELLINGER, R. J., and V. A. ZAKIAN, 2012 Everything you ever wanted to know about Saccharomyces cerevisiae telomeres: beginning to end. Genetics **191:** 1073-1105.

WYATT, M. D., and D. L. PITTMAN, 2006 Methylating agents and DNA repair responses: Methylated bases and sources of strand breaks. Chem Res Toxicol **19:** 1580-1594.

XU, X., S. BLACKWELL, A. LIN, F. LI, Z. QIN *et al.*, 2015 Error-free DNA-damage tolerance in Saccharomyces cerevisiae. Mutat Res Rev Mutat Res **764:** 43-50.

YANG, Y., D. A. GORDENIN and M. A. RESNICK, 2010 A single-strand specific lesion drives MMS-induced hyper-mutability at a double-strand break in yeast. DNA Repair (Amst) **9:** 914-921.

YEARLING, M. N., C. A. RADEBAUGH and L. A. STARGELL, 2011 The Transition of Poised RNA Polymerase II to an Actively Elongating State Is a "Complex" Affair. Genet Res Int **2011:** 206290.

YOH, S. M., H. CHO, L. PICKLE, R. M. EVANS and K. A. JONES, 2007 The Spt6 SH2 domain binds Ser2-P RNAPII to direct Iws1-dependent mRNA splicing and export. Genes Dev **21:** 160-174.

YOH, S. M., J. S. LUCAS and K. A. JONES, 2008 The Iws1:Spt6:CTD complex controls cotranscriptional mRNA biosynthesis and HYPB/Setd2-mediated histone H3K36 methylation. Genes Dev **22:** 3422-3434.

YUEN, K. W., C. D. WARREN, O. CHEN, T. KWOK, P. HIETER *et al.*, 2007 Systematic genome instability screens in yeast and their potential relevance to cancer. Proc Natl Acad Sci U S A **104:** 3925-3930.

ZHANG, H., A. F. ZEIDLER, W. SONG, C. M. PUCCIA, E. MALC *et al.*, 2013 Gene copy-number variation in haploid and diploid strains of the yeast Saccharomyces cerevisiae. Genetics **193:** 785-801.

ZHANG, L., A. G. FLETCHER, V. CHEUNG, F. WINSTON and L. A. STARGELL, 2008 Spn1 regulates the recruitment of Spt6 and the Swi/Snf complex during transcriptional activation by RNA polymerase II. Mol Cell Biol **28:** 1393-1403.

ZHANG, Z., and Q. REN, 2015 Why are essential genes essential? - The essentiality of Saccharomyces genes. Microb Cell **2:** 280-287.

ZHU, Y. O., M. L. SIEGAL, D. W. HALL and D. A. PETROV, 2014 Precise estimates of mutation rate and spectrum in yeast. Proc Natl Acad Sci U S A **111:** E2310-2318.

# APPENDIX I. COMPILATION OF PHENOTYPIC GROWTH ANALYSIS STUDIES

In this appendix the images used for the phenotypic growth analysis have been compiled. This set consists of media selected to test strains for defects in DNA damage repair and replication. Each image captures the best representation of the growth phenotype under the tested condition, although many strains were tested under multiple concentrations for a single agent. Each strain was tested under standard conditions: YPD growth at 30°C, 39°C, 75 J/m$^2$ ultraviolet radiation (UV), 50 µg/mL camptothecin (CPT), 3.5% hydrogen peroxide ($H_2O_2$), 0.03% methyl methanesulfonate (MMS), 10 mM caffeine (CAF), 150 mM hydroxyurea (HU), 25 nM rapamycin (RAP). Many strains required lower concentrations of damaging agents, these changes are noted below the accompanying the figure.

### *AI.1 Phenotypic analysis of spn1$^{K192N}$ and spn1$^{141-305}$*

The *spn1* alleles, *spn1$^{K192N}$* and *spn1$^{141-305}$* were introduced into deletion strains to test a possible role for Spn1 in DNA damage repair and replication. Introduction of these alleles is described in the materials and methods section. This set consists of strains created and tested by Alison Thurston and Cathy Radebaugh, with the help of Tyler Glover, Colin Sempack, Sarah Stonedahl, Racheal Carstens, Raira Ank, and Dustin Steele. Genetic effects were tested with genes involved in chromatin structure, DNA processing, base excision repair, nucleotide excision repair, DNA damage tolerance, homologous recombination, cell cycle signaling, DNA damage response, stress induced transcription response, and cell cycle progression. Deletion strains were selected through literature investigations. Table AI.1 is a summary of all the phenotypes. Figure AI.1 presents images of every strain. Some strains were not tested under every condition.

Table AI.1 Comparison of genetic interactions of *spn1*$^{K192N}$ and *spn1*$^{141-305}$ in deletion strains

| | ***spn1*$^{K192N}$** | | | ***spn1*$^{141-305}$** | | |
|---|---|---|---|---|---|---|
| | **Sensitive** | **Deletion Background** | **Resistant** | **Sensitive** | **Deletion Background** | **Resistant** |
| **YPD** | *rad6* | *BY4741, apn1, apn2, clb1, cln3, dot1, exo1, hfm1, isw1, mag1, mms2, msn2, msn4, mre11, ntg1, pol4, rad5, rad9, rad14, rad17, rad18, rad23, rad24, rad26, rad30, rad51, rad55, rad57, rev1, rev3, rev7, rmi1, rtt109, sae2, sgs1, siz1, srs2, tel1, top3, ubc13, xrs2* | | | *BY4741, apn1, apn2, clb1, cln3, exo1, hfm1, isw1, mag1, mms2, msn2, msn4, mre11, ntg1, pol4, rad5, rad6, rad9, rad14, rad17, rad18, rad23, rad24, rad26, rad30, rad51, rad55, rad57, rev1, rev3, rev7, rmi1, rtt109, sae2, sgs1, siz1, srs2, tel1, top3, ubc13, xrs2* | *dot1* |
| **39°C** | No growth in all backgrounds | | | *apn1, clb1, cln3, exo1, rad6, rad9 isw1, msn2, msn4, rad18, rad23, rad55, rad57, rev1,rev3, rmi1, siz1, tel1, ubc13* | *BY4741, hfm1, mms2, mre11, ntg1, pol4, rad5, rad14 (dead), rad17, rad24, rad26, rad30, rad51, rev7, rtt109, sae2, sgs1, srs2, top3, xrs2* | *dot1* |
| **UV** | | *BY4741, apn1, apn2, clb1, cln3, dot1, exo1, hfm1, isw1, mag1, mms2, msn2, msn4, mre11, ntg1, pol4, rad5, rad6, rad9, rad14 (dead), rad17, rad18 (dead), rad23, rad26, rad30, rad51, rad55, rad57, rev1, rev3, rev7, rmi1, rtt109, sae2, sgs1, srs2, tel1, top3, ubc13, xrs2* | | | *BY4741, apn1, apn2, clb1, cln3, exo1, hfm1, isw1, mag1, mms2, msn2, msn4, mre11, ntg1, pol4, rad5 (dead), rad6, rad9, rad14 (dead), rad17, rad18 (dead), rad23, rad26, rad30, rad51, rad55, rad57, rev1, rev3, rev7, rmi1, rtt109, sae2, sgs1, srs2, tel1, top3, ubc13, xrs2* | *dot1* |
| **CPT** | *rad6,rad55, rad57, sae2* | *BY4741, apn1, apn2, clb1, cln3, dot1, exo1, mms2, msn4, mre11, ntg1, pol4, rad5, rad9, rad14, rad18, rad23, rad26, rad51 (dead), rev7, rmi1, rtt109 (dead), srs2, tel1, top3 (dead)* | | *rmi1* | *BY4741, apn1, apn2, clb1, cln3, exo1, mms2, msn4, mre11, ntg1, pol1, rad5, rad6, rad9, rad14, rad18, rad23, rad26, rad51 (dead), rad55, rad57, rev7, rtt109 (dead), srs2, tel1, top3 (dead)* | *dot1, sae2* |

| | ***spn1*$^{K192N}$** | | | ***spn1*$^{141\text{-}305}$** | | |
|---|---|---|---|---|---|---|
| | **Sensitive** | **Deletion Background** | **Resistant** | **Sensitive** | **Deletion Background** | **Resistant** |
| **MMS** | | *dot1, rad5, rad6, rad23, rad18, rad17, rad51, rad55, rad57, rtt109, sae2, sgs1, siz1, top3, xrs2, tel1* | *BY4741, apn1, apn2, clb1, cln3, exo1, hfm1, isw1, mag1, mms2, msn2, msn4, mre11, ntg1, pol4, rad9, rad14, rad24, rad26, rad30, rev1, rev3, rev7, rmi1, srs2, ubc13* | *mag1, mms2, rad5, rad51, rmi1, rtt109, sgs1, siz1* | *mre11, rad6, rad9, rad17, rad23, rad55, rad57, sae2, tel1, top3, ubc13, xrs2* | *BY4741, apn1, apn2, clb1, cln3, dot1, exo1, hfm1, isw1, msn2, msn4, ntg1, pol4, rad14, rad18, rad24, rad26, rad30, rev1, rev3, rev7, srs2* |
| **CAF** | | *BY4741, apn1, apn2, clb1, cln3, dot1, exo1, hfm1, isw1, mms2, msn2, msn4, mre11, ntg1, pol4, rad5, rad6, rad9, rad17, rad18, rad23, rad24, rad26, rad30, rad51, rad55, rad57, rev1, rev3, rev7, rmi1, sae2, sgs1, siz1, srs2, tel1, top3, ubc13, xrs2* | *rad14* | *BY4741, clb1, cln3, dot1, exo1, hfm1, isw1, mms2, msn2, msn4, ntg1, pol4, rad6, rad9, rad23, rad26, rad30, rad51, rad55, rev1, rev3, rev7, sae2, siz1, srs2, top3, ubc13* | *apn1, apn2, mre11, rad5, rad14, rad17, rad18, rad24, rad57, rmi1, sgs1, tel1, xrs2* | |
| **HU** | *dot1, rad6, rad23, rad57, tel1, xrs2* | *BY4741, apn1, apn2, clb1, cln3, exo1, hfm1, isw1, mms2, msn2, msn4, mre11, ntg1, pol4, rad5, rad9, rad17, rad18, rad24, rad26, rad30, rad51, rad55(dead), rev1, rev3, rev7, rmi1, sae2, sgs1, siz1, srs2, top3 (dead), ubc13* | *rad14* | *BY4741, apn1, clb1, cln3, isw1, mms2, msn2, msn4,ntg1, pol4, rad6, rad9, rad17, rad23, rad24, rad26, rad30, rev1, rev3, rev7, rmi1, sae2, sgs1, siz1, srs2, tel1, ubc13, rs2* | *apn2, dot1, exo1, hfm1, mre11, rad5, rad51, rad55, rad57, top3 (dead)* | *rad14, rad18* |
| **RAP** | *rad6, rev7* | *BY4741, apn1, apn2, clb1, cln3, dot1, exo1, mms2, msn2, msn4, mre11, pol4, rad5, rad9, rad14, rad17, rad18, rad23, rad24, rad26, rad51, rad55, rad57, rmi1, sae2, sgs1, siz1, srs2, tel1, top3, xrs2* | | *rad14* | *BY4741, apn1, apn2, clb1, cln3, exo1, mms2, msn2, msn4, mre11, pol4, rad5, rad6, rad9, rad17, rad18, rad23, rad24, rad26, rad51, rad55, rad57, rev7, rmi1, sae2, sgs1, siz1, srs2, tel1, top3, xrs2* | *dot1* |

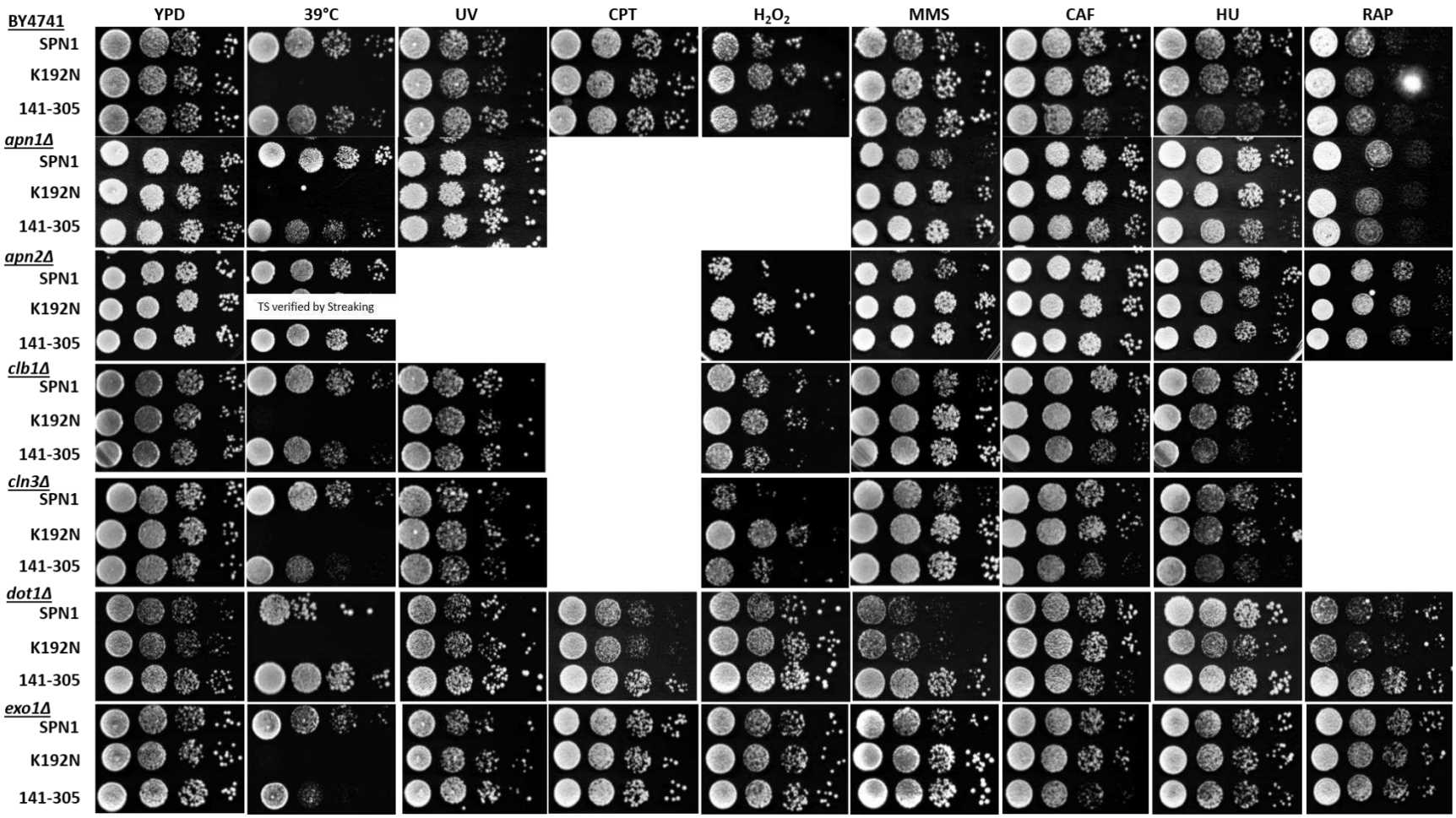


***apn1Δ***: 0.01% MMS, 8mM caffeine
***dot1Δ***: originally phenotyped by Cathy Radebaugh, re-tested by Alison Thurston

**Figure AI.1. Phenotypic growth analysis of deletion strains containing *SPN1, spn1$^{K192N}$ or spn1$^{141-305}$* allele.** Ten-fold dilutions of logarithmically growing cells. Cells are grown on YPD at 30°C, 39°C, 75 J/m2 UV, 50 ug/mL CPT, 3.5% $H_2O_2$, 0.03% MMS, 10 mM Caf, 150 mM HU, 25 nM RAP unless indicated below figure. Growth phenotypes in the BY4741 background are provided on the top of each image for reference.

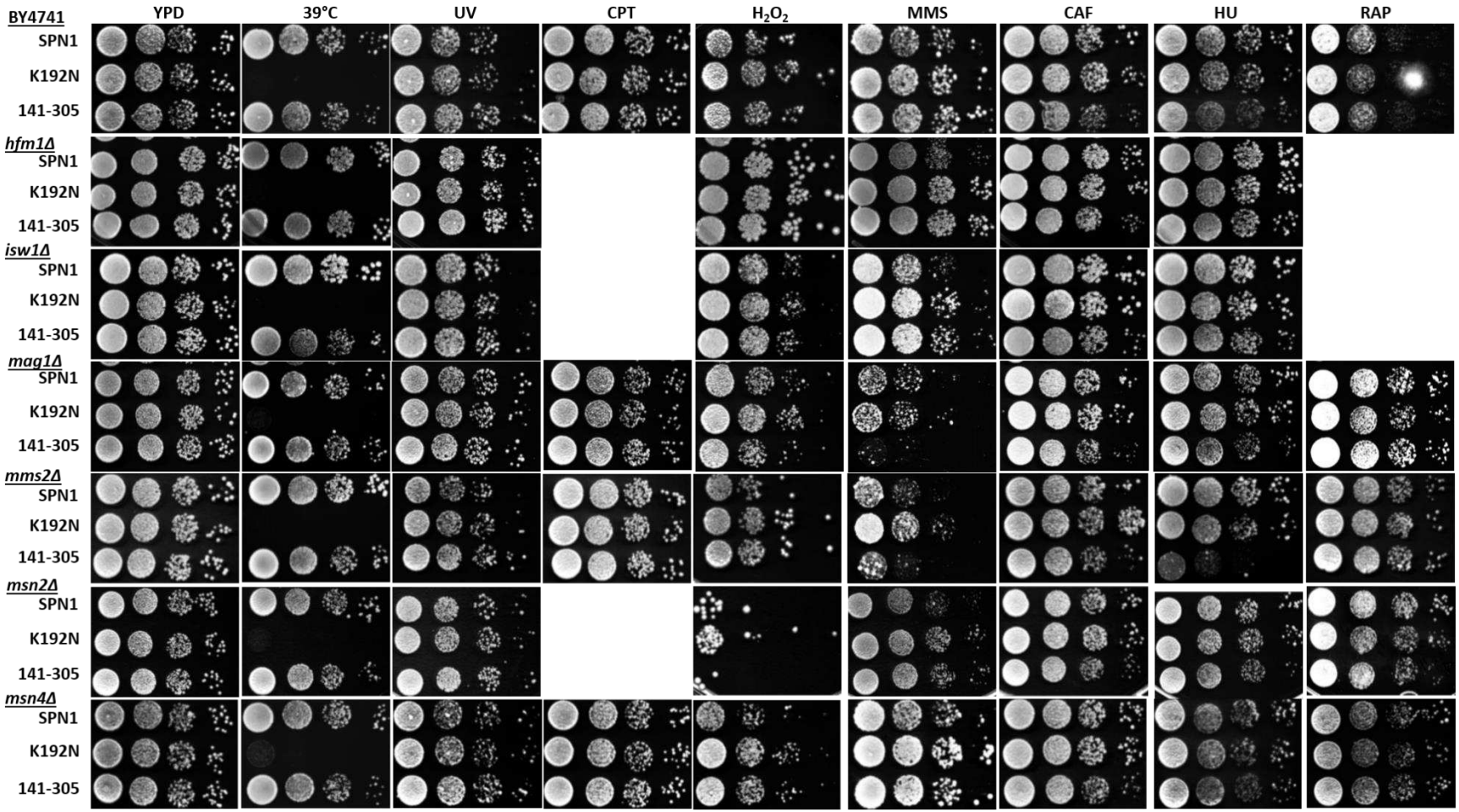


***mms2Δ*** : 25 J/m$^2$, 3.0% $H_2O_2$, 0.01% MMS ***msn2Δ***: 100mM HU

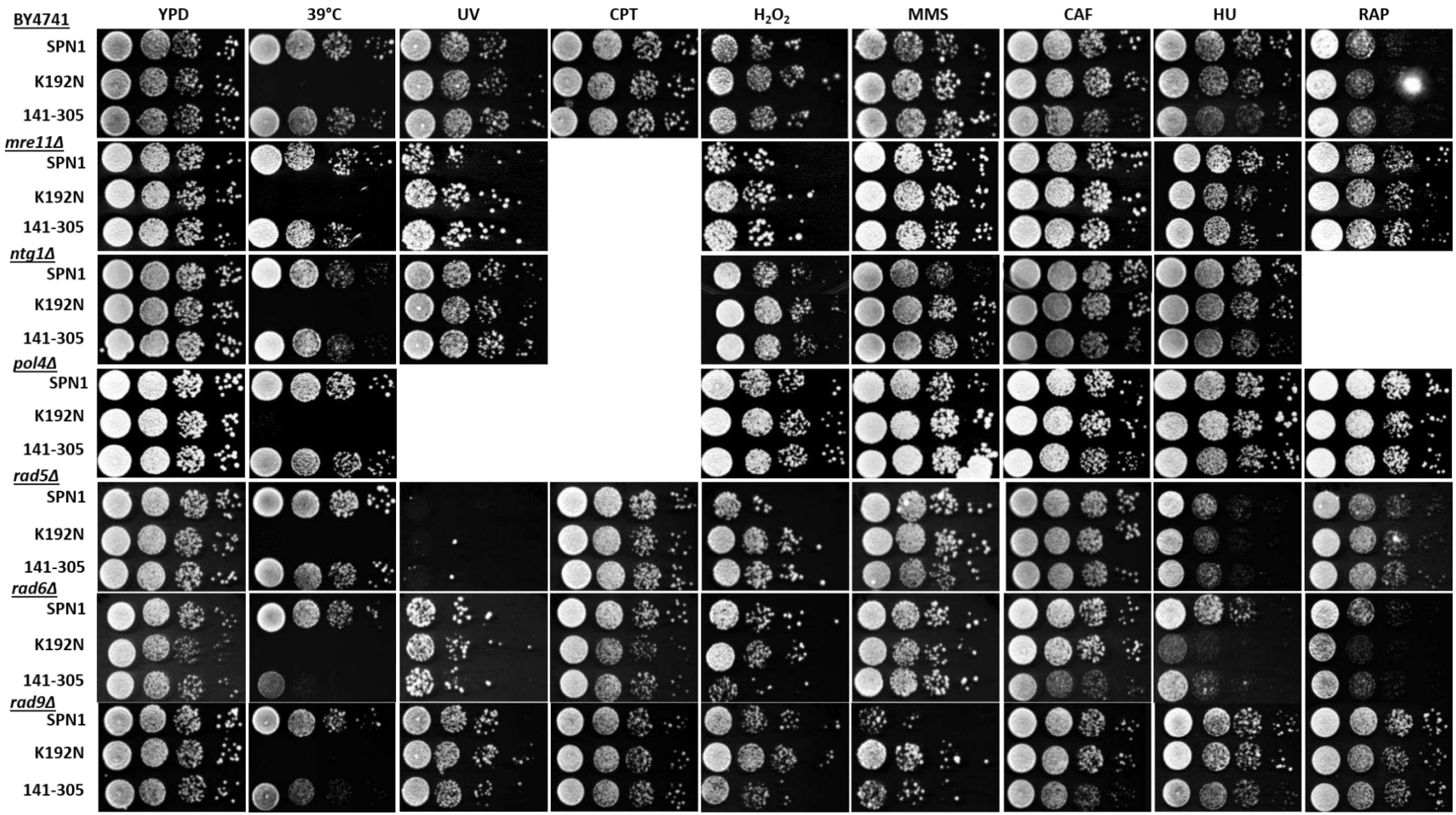


***mre11Δ:*** 0.001% MMS, 10mM HU ***rad5Δ***: 25 J/m$^2$, 0.001% MMS ***rad6Δ:*** 50 J/m$^2$ , 3.0% $H_2O_2$, 0.01% MMS, 50mM HU ***rad9Δ:*** 25 J/m$^2$
***mre11Δ, pol4 Δ:*** strain created and tested by Cathy Radebaugh
***rad6Δ, rad9Δ:*** strain created and tested by Cathy Radebaugh, re-tested by Alison Thurston

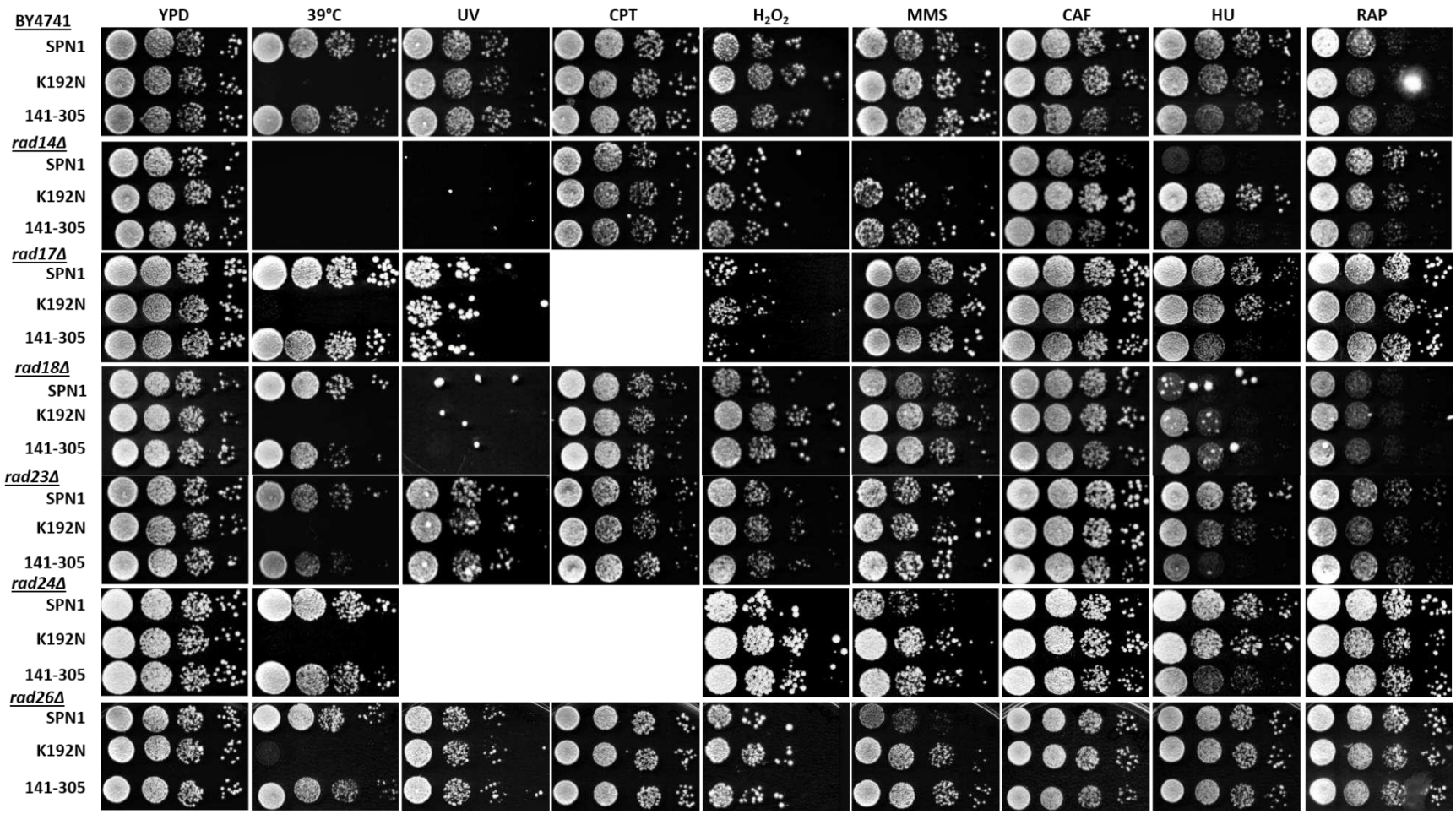


***rad14Δ:*** <12.5 J/m$^2$, 3.0% $H_2O_2$, 100mM HU ***rad17Δ:*** 0.01% MMS ***rad18Δ:*** 50 J/m$^2$ , 0.00025% MMS, 50 mM HU ***rad23Δ:*** 25 J/m$^2$ ***rad24Δ:***0.02% MMS ***rad26Δ:*** 100 mM HU

***rad17Δ, rad24Δ:*** strain created and tested by Cathy Radebaugh

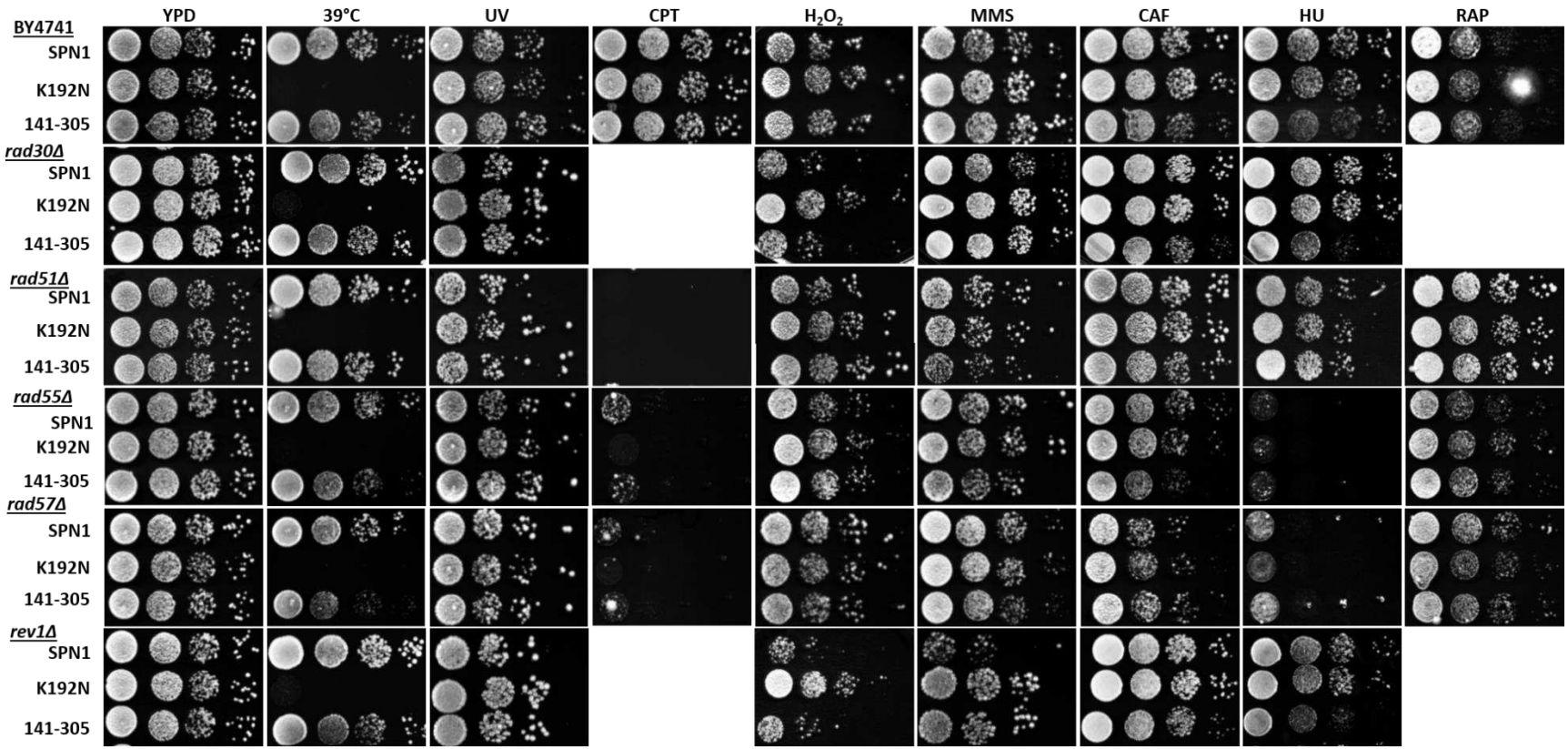


***rad51Δ:*** 0.01% MMS, 25 mM HU ***rad52Δ:*** ***rad55Δ:*** 0.01% MMS, 100 mM HU ***rad57Δ:*** 0.01% MMS, 100 mM HU

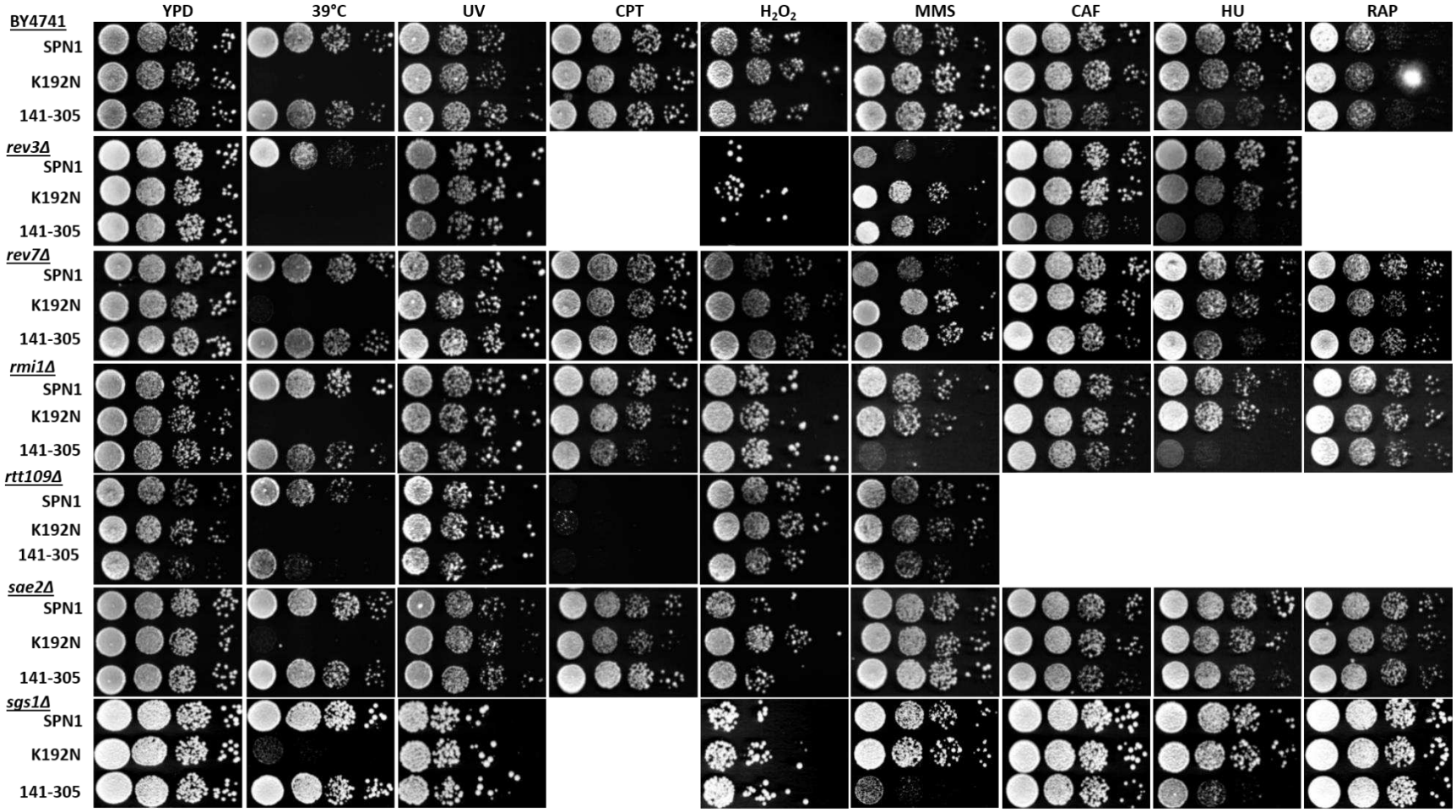


***rev3Δ:*** 0.015% MMS ***rev7Δ:*** 0.02% MMS ***rmi1Δ:*** 0.01% MMS, 50 mM HU ***sgs1Δ:*** 0.005% MMS, 25 mM HU ***rtt109Δ:*** 0.005% MMS
***sgs1Δ:*** strain created and tested by Cathy Radebaugh
***rtt109Δ:*** strain created and tested by Cathy Radebaugh, retested by Alison Thurston

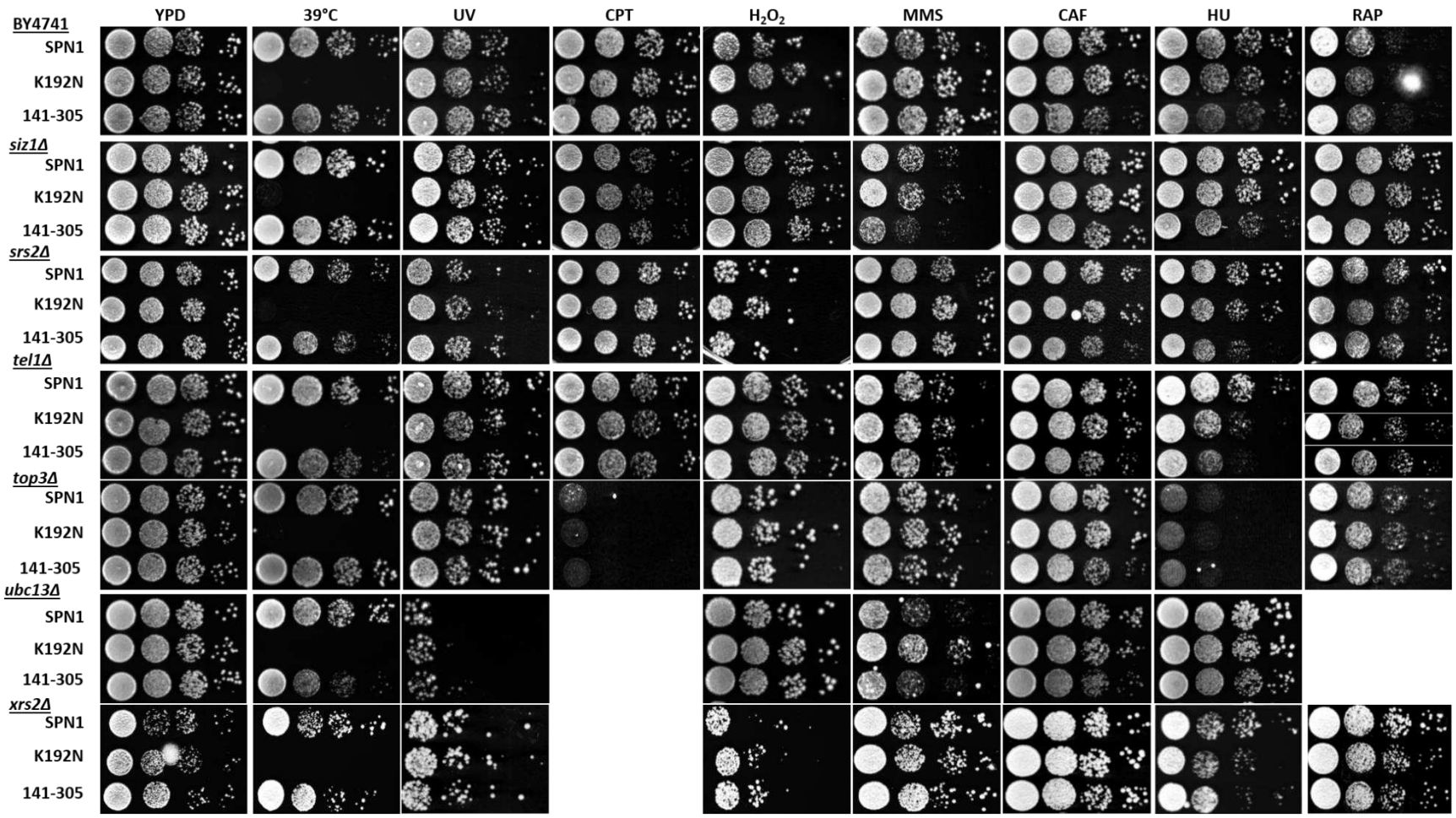


***siz1Δ:*** 50 mM HU ***srs2Δ:*** 0.01% MMS 100 mM HU ***top3Δ:*** 0.01% MMS 50 mM HU ***ubc13Δ:*** 0.01% MMS, ***xrs2Δ:*** 3.0% $H_2O_2$ 0.001% MMS, 10 mM HU
***xrs2Δ:*** strain created and tested by Cathy Radebaug

### *AI.2 Phenotypic analysis on Hydrogen Peroxide*

Hydrogen Peroxide ($H_2O_2$) is a commonly used DNA damaging agent. Hydrogen peroxide results in DNA lesions such as 8-oxo-guanine, 8-oxo adenine, ssDNA breaks, dsDNA breaks and in high concentrations cell death (FARRUGIA and BALZAN 2012). Growth on plates containing $H_2O_2$ are inconsistent (Figure AI.2A). At times, expression of spn1$^{K192N}$ and spn1$^{141-305}$ appear to give cellular resistance to $H_2O_2$ compared to the wildtype strain. However, the observed resistance does not occur every time the strains were tested. In contrast, every time the *spn1* strains are grown on MMS, they exhibit resistance compared to wildtype.

Hydrogen peroxide decomposes at higher temperatures, thus it is possible that variation in the temperature of media at the time of $H_2O_2$ addition could account for plate to plate variation. The *spn1* strains were tested on plates containing menadione. Exposure to menadione causes intracellular superoxide radicals and hydrogen peroxide, which results in cellular oxidative stress (HASSAN and FRIDOVICH 1979). No mutant phenotypes were observed when strains were grown on menadione (Figure AI.2B) and thus further investigation was not pursued. Genetic interactions on $H_2O_2$ plates were assessed and images were provided (Table AI.2 and Figure AI.1).

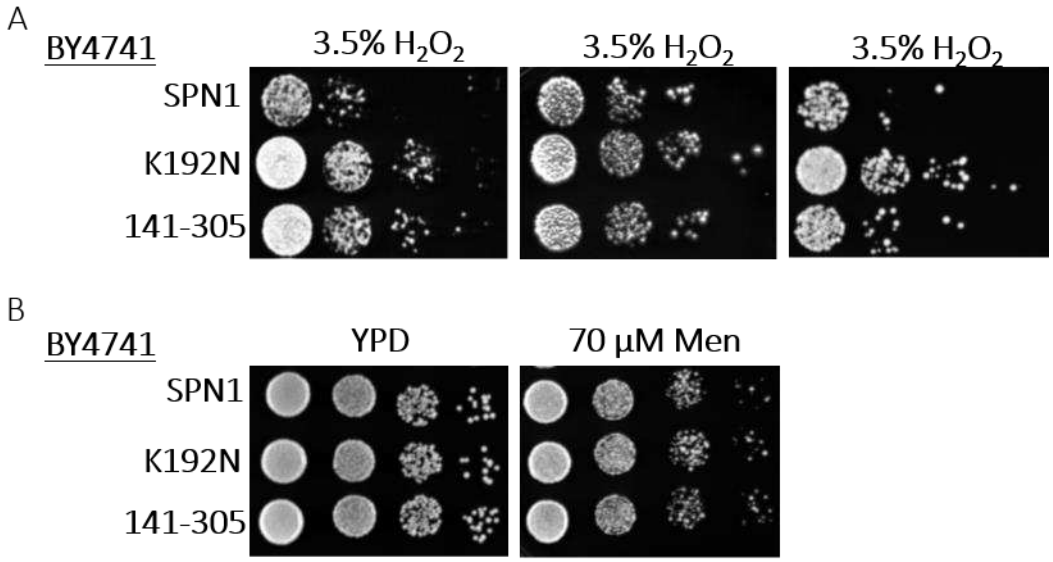


**Figure AI.2. Phenotypic analysis of *spn1*$^{K192N}$ and *spn1*$^{141-305}$ strains grown on $H_2O_2$ and menadione.** Ten-fold serial dilutions of *SPN1*, *spn1*$^{K192N}$ and *spn1*$^{141-305}$ strains were grown on plates containing A) $H_2O_2$ and B) menadione.

Table AI.2 Comparison of genetic interactions between *SPN1* and *spn1*$^{K192N}$ or *spn1*$^{141-305}$ in deletion strains grown on plates containing $H_2O_2$

| | ***spn1*$^{K192N}$** | | | ***spn1*$^{141-305}$** | | |
|---|---|---|---|---|---|---|
| | **Sensitive** | **Deletion Background** | **Resistance** | **Sensitive** | **Deletion Background** | **Resistance** |
| **$H_2O_2$** | | *clb1, dot1, exo1, mms2, msn4, mre11, pol4, rad6, rad14, rad17, rad23, rad55, rad57, rev3 (dead), rmi1 rtt109, sgs1, srs2, ttel1, top3, xrs2* | *apn2, cln3, ntg1, rad5, rad9, rad18, rad24, rad26, rad30, rad51, rev1, rev7, sae2, ubc13* | *clb1, rad6* | *BY4741,cln3, exo1, mms2, msn4, mre11, pol4, rad9, rad14, rad17, rad23, rad26, rad30, rad555, rad57, rev1, rev3(dead) rmi1 rtt109, sae2, sgs1, srs2, tel1, top3, xrs2* | *apn2 dot1, ntg1, rad5, rad18, rad24, rad51, rev7, ubc13* |

# APPENDIX II. ANALYSIS OF THE SPN1 TAILS

In chapter 3, a role for Spn1 in promoting genome instability and progression through replication was outlined using a truncated mutant allele of *SPN1*, *spn1*$^{141\text{-}305}$. spn1$^{141\text{-}305}$ is defective for nucleic acid binding, histone binding, nucleosome binding and nucleosome assembly (LI *et al.* 2017). This indicates these functions are important for genome instability and the progression through replication during times of stress. Biochemical analysis has revealed domain specific chromatin interactions (LI 2018). Addition of the N-terminal region (1-140) to the core domain (141-305) partially restores DNA binding and restores histone binding in vitro (LI 2018). The C-terminal domain of Spn1 (306-410) is basic and can bind both DNA and nucleosomes in vitro *(LI 2018)*. Addition of the C terminal domain (306-410) to the core domain (141-305) partially restores DNA binding and restores nucleosome binding in vitro (LI 2018). As the binding regions of Spn1 appear modular, we wanted to investigate if one specific region or interaction was responsible for the observed mutant phenotypes.

The *SPN1* tail deletion alleles, *spn1*$^{1\text{-}305}$ and *spn1*$^{141\text{-}410}$, were utilized to further investigate chromatin binding and Spn1 function. In the wildtype background, no mutant growth phenotypes were observed in strains expressing spn1$^{1\text{-}305}$ or spn1$^{141\text{-}410}$ (Figure AII.1A)[2]. The observed resistance to MMS in cells expressing spn1$^{141\text{-}305}$ is lost with the addition of the either the N or the C terminal tail. Additionally, we did not observed a difference in the damage induced mutation rates between *SPN1*, *spn1*$^{1\text{-}305}$ or *spn1*$^{141\text{-}410}$ strains (Figure AII.1B). Indicating loss of both tails are necessary for MMS resistance and decreased genome instability in the BY4741 background.

[2]The *spn1*$^{1\text{-}305}$ and *spn1*$^{141\text{-}410}$ strains were created and originally tested by Adam Almeida.

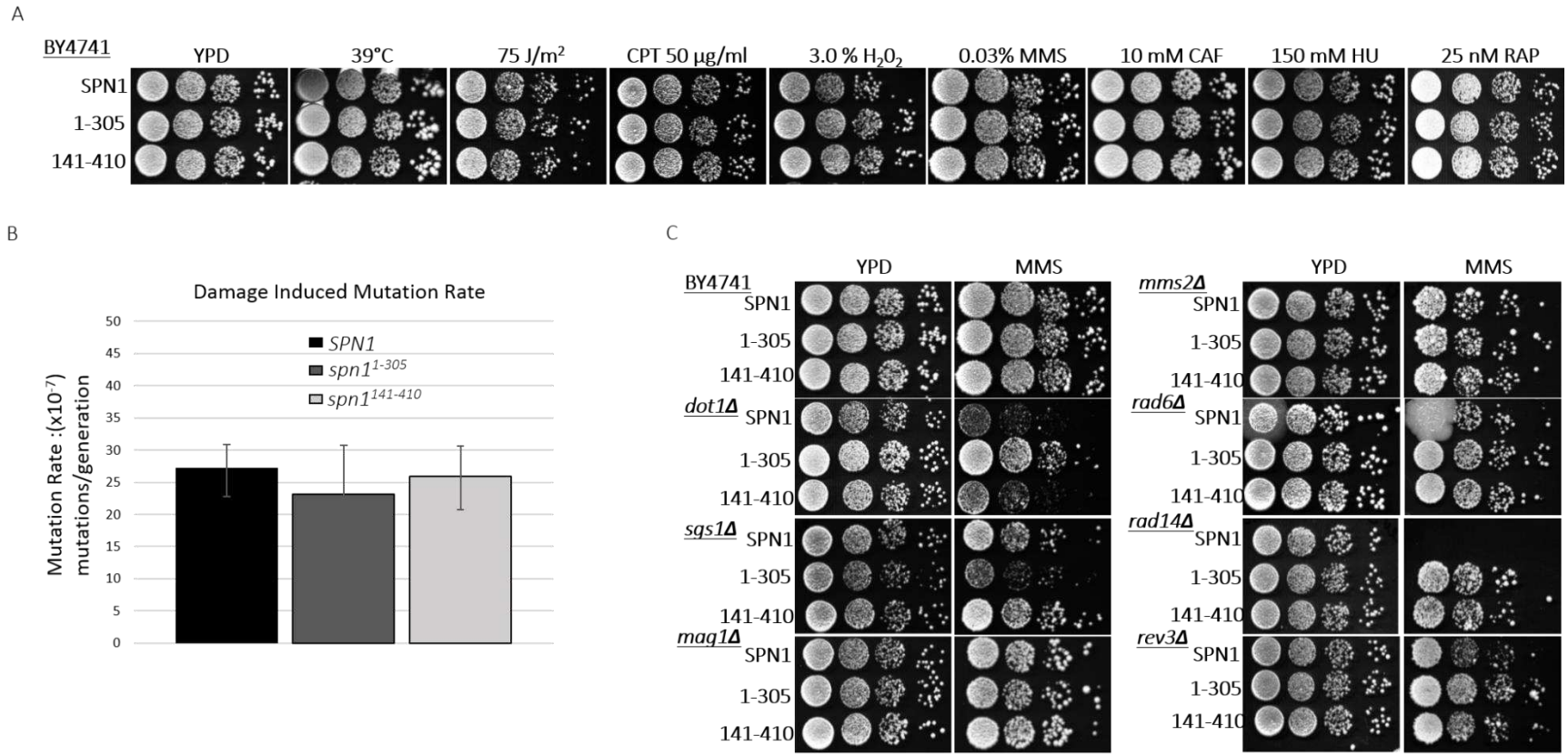


**Figure AII.1. Analysis of *spn1* tail mutants**. A) Ten-fold serial dilutions of *SPN1*, *spn1*$^{1-305}$ and *spn1*$^{141-410}$ strains on various media. B) Damage induce mutation rate of *SPN1*, *spn1*$^{1-305}$ and *spn1*$^{141-410}$ strains. Mutation rates were calculated by the Lea-Coulson method of the median using the FALCOR program. Significance was determined using the Mann-Whitney nonparametric t-test on GraphPad. Fluctuation assay was performed twice with 7 replicates. C) Ten-fold serial dilutions of *SPN1*, *spn1*$^{1-305}$ and *spn1*$^{141-410}$ strains in selected deletion backgrounds. *SPN1*, *dot1Δ,* and *rad14 Δ* strains were grown on 0.03% MMS, *sgs1Δ*, *mag1Δ*, *mms2Δ*, *rad6Δ, and rev3Δ* strains were grown on 0.01% MMS.

We further examined the genetic interactions between the mutant alleles, *spn1*$^{1-305}$ (deletion of C terminus) and *spn1*$^{141-410}$ (deletion of N terminus) and *DOT1, MAG1, MMS2, RAD6, RAD14,* and *SGS1.* These strains were selected to due to their genetic interactions with *spn1*$^{141-305}$. Figure AII.2 and Table AII.1 summarize cellular growth on all tested media in all strains. Provided below is an explanation of the mutant phenotypes observed on MMS plates.

Cells expressing spn1$^{1-305}$ in the *dot1Δ* strain exhibit increased growth on YPD (Figure AII.1C). This was also observed in the *dot1Δspn1*$^{141-305}$ strain. The increased growth is further exacerbated on MMS (Figure AII.1C). Cells expressing spn1$^{141-305}$ in the *sgs1Δ* background are extremely sensitive to MMS (Figure 3.11). Cells expressing spn1$^{1-305}$ remain sensitive, while cells expressing spn1$^{141-410}$ grow similar to *sgs1Δ* cells (Figure AII.1C). In both *dot1Δ* and *sgs1Δ* strains, loss of the C terminal domain of Spn1 causes mutant phenotype growth.

Cells expressing spn1$^{141-305}$ were resistant to MMS in *rad14Δ* and *rev3Δ* strains. Resistance to MMS is observed when *spn1*$^{1-305}$ or *spn1*$^{141-410}$ is introduced into the *rad14Δ* and *rev3Δ* strains (Figure AII.1C). Although the amount of resistance has decreased in the *rev3Δ* strain. This indicates that loss of either tail or both tails can result in resistance to MMS.

Expression of spn$^{141-305}$ in *mag1Δ*, *mms2Δ*, and *rad6Δ* strains resulted in loss of resistance observed in the wildtype cells. No mutant phenotype growth was observed when the *spn1*$^{1-305}$ or the *spn1*$^{141-410}$ allele was introduced into the *mag1Δ*, *mms2Δ*, and *rad6Δ* strains and grown on MMS (Figure AII.1C). Combined with the mutation rate analysis this would suggest that the DDT pathway regulation is not significantly altered in the s*pn1* tail deletion strains.

From these genetic analyses, rescuing the histone, DNA, or nucleosome binding does not universally suppress the s*pn1* growth phenotypes. The observed resistance to MMS in cells expressing *spn1*$^{141-305}$ in the wildtype background is lost with the addition of the either the N or the C terminal tail. In vitro, spn1$^{1-305}$ and spn1$^{141-410}$ can both bind DNA while spn1$^{141-305}$ cannot (Li

2018). A possible interpretation is the loss of DNA binding of Spn1 results in resistance to MMS. However, when combined with deletion strains it appears that the C terminal domain maybe more responsible for the observed mutant phenotypes. In the *dot1Δ* and *sgs1Δ* backgrounds, loss of the C tail results in mutant phenotypes suggesting nucleosome binding is important for wildtype function in these deletion backgrounds. Although not statistically different, the calculated mutation rate in the *spn1*$^{1\text{-}305}$ strain is lower. When comparing the appearance of mutant growth phenotypes, more are observed in strains expressing spn1$^{1\text{-}305}$ than spn1$^{141\text{-}410}$ (Table AII.1). From this genetic analysis one specific Spn1 chromatin function, which is imperative for wildtype growth, could not be selected. However, the functions within the C terminal domain maybe more critical than those in the N terminal domain, further investigation is needed.

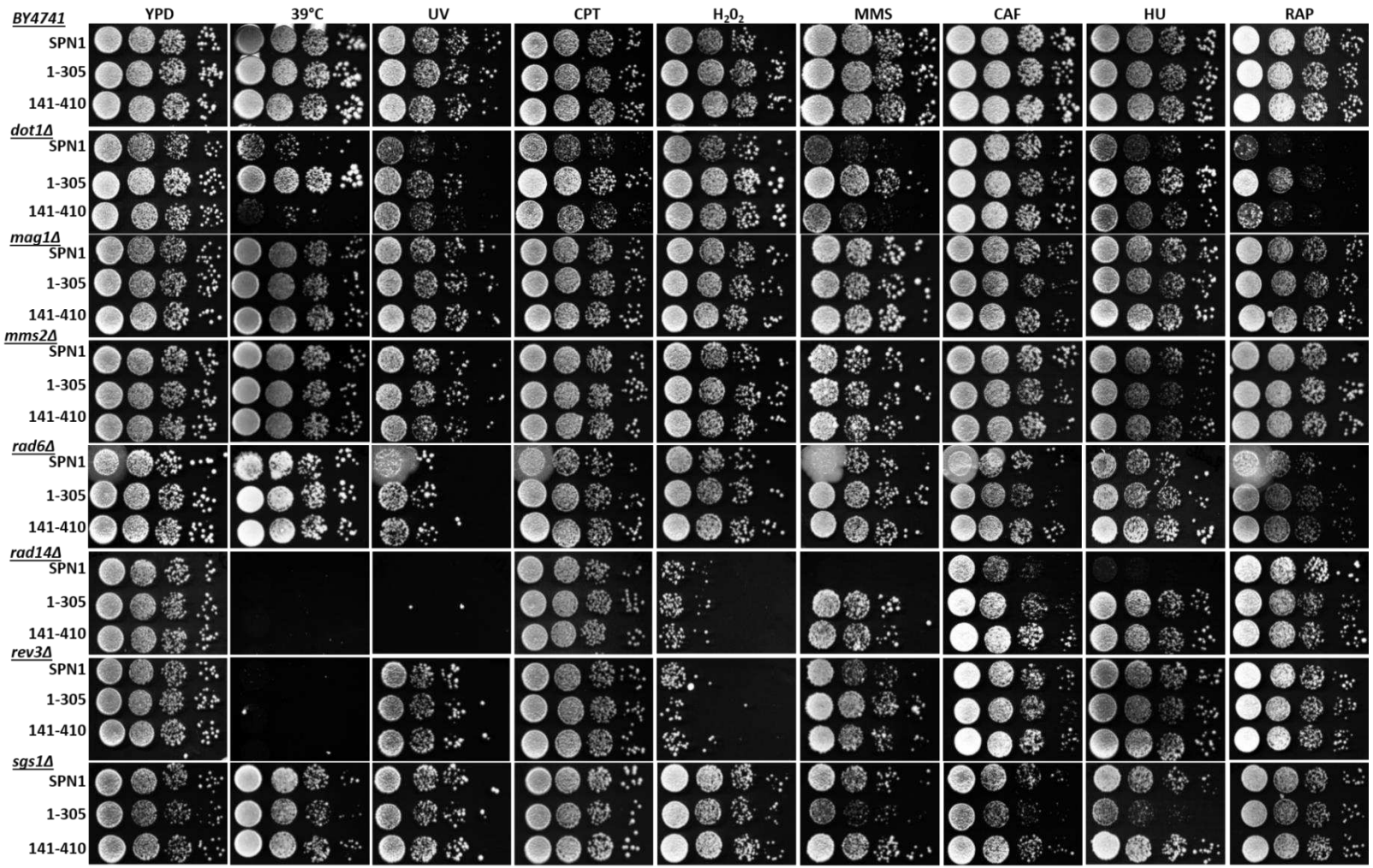


**Figure AII.2. Phenotypic growth analysis of deletion strains with *SPN1*, *spn1*$^{1-305}$ or *spn1*$^{141-410}$.** Ten-fold dilutions of logarithmically growing cells. Cells are grown on YPD at 30°C, 39°C, 75 J/m2 UV, 50 µg/mL CPT, 3.0% $H_2O_2$, 0.03% MMS, 10 mM Caf, 150 mM HU, 25 nM RAP with the exception of ***mag1Δ:*** 0.01% MMS ***mms2Δ:*** 50 J/m$^2$ 0.01% MMS ***rad6Δ:*** 50 J/m$^2$ 0.01% MMS 50 mM HU ***rad14Δ:*** <12.5 J/m$^2$ 100 mM HU, ***rev3Δ:*** 0.01% MMS, ***sgs1Δ:*** 0.01% MMS 50 mM HU.
*spn1*$^{1-305}$ and *spn1*$^{141-410}$ strains were created and originally tested by Adam Almeida.

Table AII.1 Comparison of genetic interactions of *spn1*$^{1-305}$and *spn1*$^{141-410}$ in deletion strains

| | ***spn1*$^{1-305}$** | | | ***spn1*$^{141-410}$** | | |
|---|---|---|---|---|---|---|
| | **Sensitive** | **Deletion Background** | **Resistance** | **Sensitive** | **Deletion Background** | **Resistance** |
| **YPD** | | *BY4741, mag1, mms2, rad6, rad14, rev3, sgs1* | *dot1* | | *BY4741, dot1, mag1, mms2, rad6, rad14, rev3, sgs1* | |
| **39°C** | *sgs1* | *BY4741, mag1, mms2, rad6, rad14 (dead), rev3 (dead)* | *dot1* | *dot1* | *BY4741, mag1, mms2, rad6, rad14 (dead), rev3 (dead), sgs1* | |
| **UV** | | *BY4741, mag1, mms2, rad6, rad14 (dead), rev3, sgs1* | *dot1* | | *BY4741, dot1, mag1, mms2, rad6, rad14, rev3, sgs1* | |
| **CPT** | | *BY4741, mag1, mms2, rad6, rad14, rev3, sgs1* | *dot1* | | *BY4741, mag1, mms2, rad6, rad14, rev3, sgs1* | *dot1* |
| **$H_2O_2$** | | *BY4741, mag1, mms2, rad6, rad14, rev3, sgs1* | *dot1* | | *BY4741, mag1, mms2, rad6, rad14, rev3, sgs1* | *dot1* |
| **MMS** | | *BY4741, mag1, mms2, rad6, sgs1* | *dot1, rad14, rev3* | | *BY4741, dot1, mag1, mms2, rad6, sgs1* | *rad14, rev3* |
| **CAF** | *dot1, mag1, rad6, rev3, sgs1* | *BY47471, mms2* | *rad14* | | *BY4741, dot1, mag1, mms2, rad6, sgs1, dot1* | *rad14,* |
| **HU** | *mms2, sgs1* | *BY4741, mag1, rad6, rev3* | *dot1, rad14* | | *BY4741, dot1, mag1, mms2, rev3* | *rad6, rad14, sgs1* |
| **RAP** | *rad14* | *BY4741, mag1, mms2, rad6, rev3, sgs1* | *dot1* | | *BY4741, dot1, mag1, mms2, rad6, rad14, rev3, sgs1* | |

# APPENDIX III. THE USE OF THE DECREASED ABUNDANCE BY mRNA PERTURBATION STRAINS

To further investigate the function of Spn1 in the cell, a commercially available Decreased Abundance mRNA Perturbation (DAmP) system was utilized (BRESLOW *et al.* 2008). The DAmP construct provides consistently decreased expression of essential proteins without the addition of external stimuli. The insertion of a kanamycin resistant cassette in between the stop codon and 3'UTR at a specific gene causes the destabilization of the transcribed mRNA resulting in decreased levels of the protein within the cell (BRESLOW *et al.* 2008).

To investigate how decreased Spn1 expression could affect nucleosome occupancy, micrococcal nuclease digestion (MNase) was performed followed by indirect end labeling at the *GAL1* gene. Interestingly, less defined bands were observed in Spn1_DAmP_GE DNA compared to BY4741 or Spt6_DAmP DNA extracted from cells exposed to the lowest MNase concentration (compare red arrows). Furthermore, a persistence of higher molecular weight bands were observed in lanes containing DNA extracted from cells exposed to higher MNase concentrations in Spn1_DAmP_GE compare to BY4741 and Spt6_DAmP (compare green arrows) (Figure AIII.1A). This occurs in both the global chromatin DNA and at the *GAL1* locus (Figure AIII.1A and AIII.1B). These digestion patterns illustrate resistance to MNase digestion in Spn1_DAmP_GE strain compared to BY4741 and Spt6_DAmP strains, suggesting a difference in the nucleosome occupancy. A difference in the nucleosome digestion patterns between Spn1_DAmP_GE and Spt6_DAmP was not expected. The two proteins are known to function together in vivo (KROGAN *et al.* 2002; YOH *et al.* 2007; ZHANG *et al.* 2008; MCDONALD *et al.* 2010).

Investigations into genome stability were pursued in the Spn1_DAmP_GE strain but were unable to be completed. Interestingly, the strain was unable to grow on plates containing canavanine.

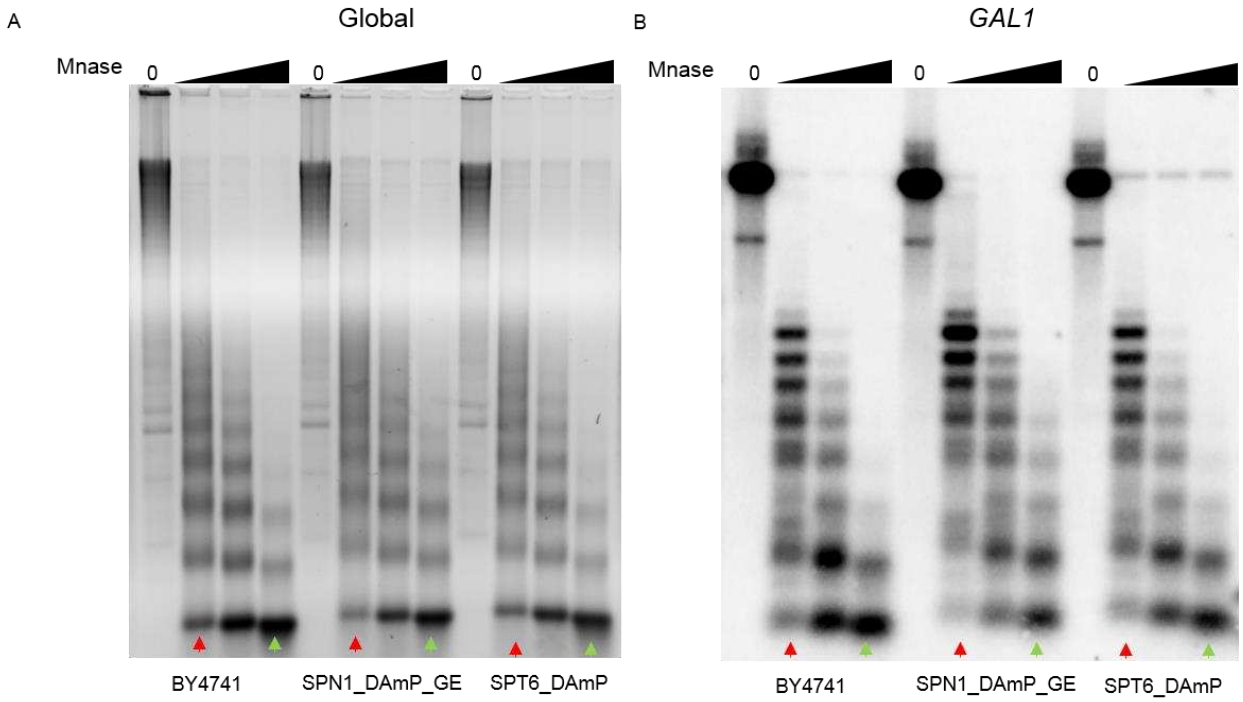


**Figure AIII.1. The Spn1_DAmP_GE strain exhibits increased resistance to MNase digestion.** MNase digested chromatin DNA from BY4741, Spn1_DAmP_GE and Spt6_DAmP was digested with EcoRV, followed by indirect end labeling analysis at the *GAL1* locus. (A) Agarose gel stained with ethidium bromide showing MNase digestion of chromatin. (B) Phospho-image of MNase digested chromatin DNA at *GAL1* locus. Colored arrow pairs indicate lanes which should be compared.

(SC-Arg + Can). The inability to grow on canavanine would indicate disruption in arginine synthesis or an unknown background mutation. Spn1_DAmP_GE was viable on SC-Arg plates. This indicates that endogenous production of arginine is functioning and is not responsible for the lack of growth observed in plates containing canavanine.

These perplexing mutant phenotypes, prompted the re-creation of the DAmP strain in the Stargell stock of BY4741 (Spn1_DAmP_LAS). Both strains decreased Spn1 levels by 50% (Figure AIII.2A). To compare the strains, phenotypic growth assays were performed. Spn1_DAmP_GE strain displayed sensitivity when grown on rapamycin, MMS, and caffeine (Figure AIII.2B). Notably, the Spn1_DAmP_LAS strain does not exhibit mutant growth phenotypes (Figure AIII.2B). As the Spn1 protein levels are the same in the two strains we predict that the Spn1_DAmP_GE strain contains secondary mutation(s). Use of the Spn1_DAmP_GE strain ceased and results are not used as evidence for Spn1 function.

***AIII.2 Decreased Spn1 levels do not affect cellular function (analysis of Spn1_DAmP_LAS)***

Decreased levels of Spn1 did not result in mutant growth phenotypes (Figure AIII.2B). To determine if decreased levels of Spn1 affect the stability of the genome, fluctuation analysis to determine the spontaneous and damage induced mutation rates of the *CAN1* gene were performed. Mutation rates between BY4741 and Spn1_DAmP_LAS strains were the same (Table AIII.1).

The lack of mutant phenotypes in the Spn1_DAmP_LAS strain prompted investigation into Spn1 levels in the cell. The number of Spn1 molecules per cell is reported to be around 3000 as determined by western blot analysis and mass spectrometry analysis (GHAEMMAGHAMI *et al.* 2003; KULAK *et al.* 2014). The levels of other chromatin associated factors range from hundreds to tens of thousands (Table AIII.2). Spn1 protein levels in BY4741 logarithmic growing cells were

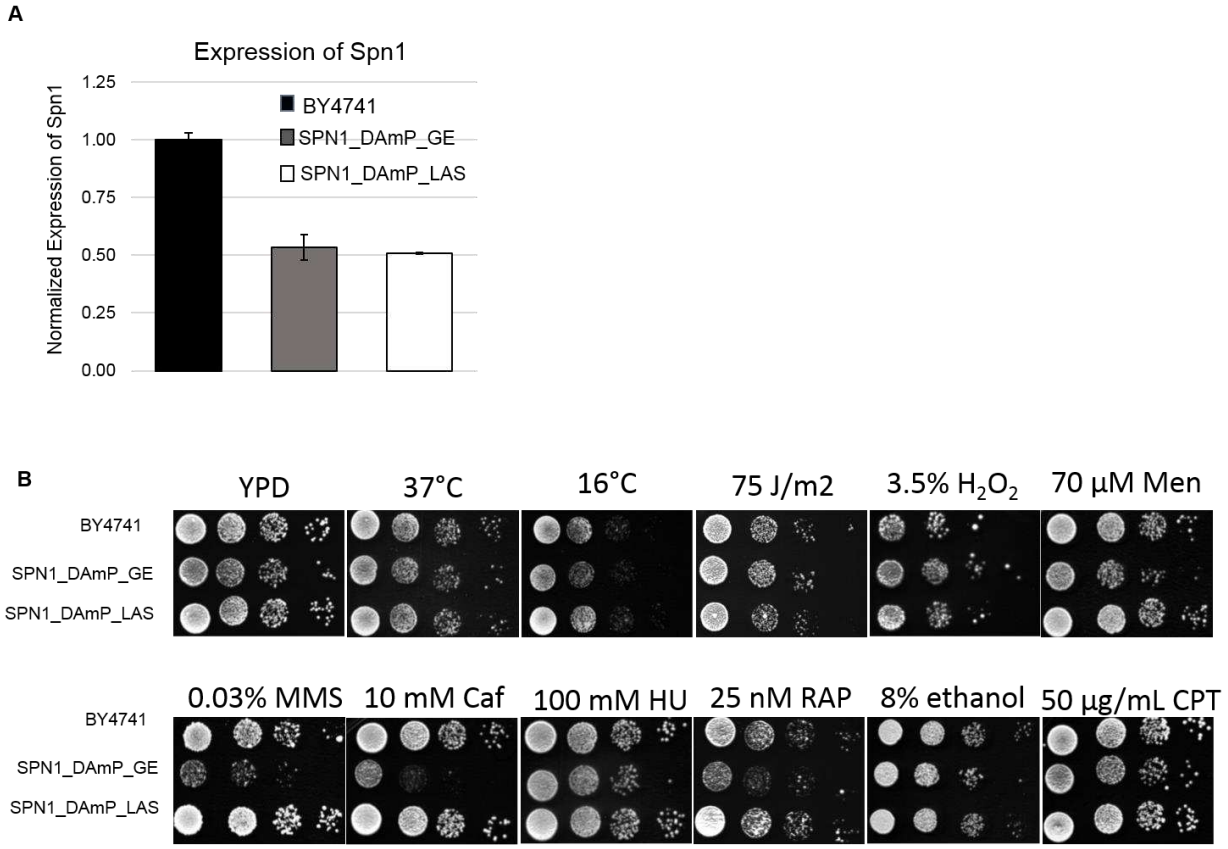


**Figure AIII.2. Analysis of Spn1_DAmP strains.** A) Western analysis to examine Spn1 expression levels in BY4741, Spn1_DAmP_GE and Spn1_DAmP_LAS strains B) Ten-fold serial dilutions of BY4741, Spn1_DAmP_GE, Spn1_DAmP_LAS were grown on indicated media for phenotypic analysis.

Table AIII.1 Spontaneous and damage induced mutation rates of the BY4741 and Spn1_DAmP_LAS strains

| **Spontaneous Mutation Rate** | | | |
|---|---|---|---|
| | *Mutation Rate* | *Upper Difference* | *Lower Difference* |
| | | | |
| **BY4741** | 0.9254 | 0.6659 | 0.4598 |
| **Spn1_DAmP_LAS** | 0.9974 | 0.5397 | 0.6784 |
| **Damage Induced Mutation Rate** | | | |
| | *Mutation Rate* | *Upper Difference* | *Lower Difference* |
| **BY4741** | 18.6788 | 1.6247 | 1.0559 |
| **Spn1_DAmP_LAS** | 19.9832 | 2.5375 | 3.3852 |

assessed by quantitative western blot analysis (Figure AIII.3A). Briefly, the signal from recombinant Spn1 was used to generate a standard curve (Figure AIII.3B). To determine the number of Spn1 molecules per cell, the Spn1 signal from whole cell lysates were compared to the signal from the standard curve (McCullough *et al.* 2015). This analysis measured 1848 Spn1 molecules per cell. The experimental value is similar to literature values (Table AIII.2). Although the levels of Spn1 appear low, they are on par with other histone chaperones, like Cac1 (CAF complex) and Vps75 (Ghaemmaghami *et al.* 2003; Kulak *et al.* 2014).

Combining the experimental analyses of the SPN1_DAmP_LAS, *spn1*$^{141\text{-}305}$ and *spn1*$^{K192N}$ strains suggests loss or alteration of Spn1 function affects cellular growth more substantially than decreased levels of Spn1. The cells can tolerate loss of Spn1 up to a point, as complete loss of Spn1 is lethal (Fischbeck *et al.* 2002).

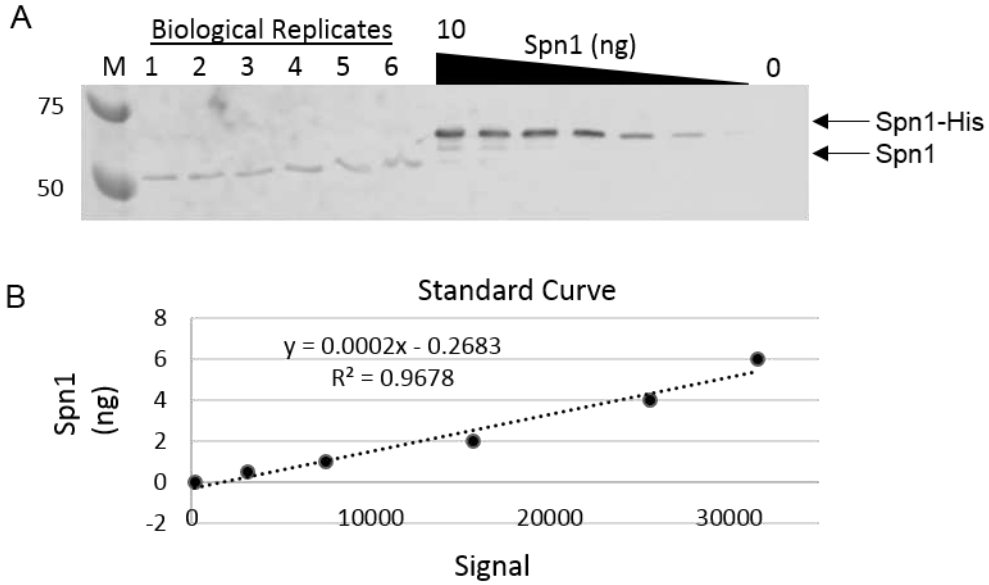


**Figure AIII.3. Determination of the number of Spn1 molecules per cell.** Spn1 abundance was determined by western blot analysis. (A) An example of a western blot used to determine Spn1 abundance. Recombinant Spn1 was used to create a standard curve (protein provided by Sha Li). Recombinant Spn1 runs higher than endogenous due to the presence of a His-tag. Anti-Spn1 sera followed by anti-rabbit secondary antibody was used to detect the Spn1 protein. (B) The reported signal in (A) was plotted against nanograms of Spn1 protein (adjusted for presence of his tag) to create a standard curve. Biological sample signals fell within the standard curve values.

Table AIII.2 Reported protein abundance of chromatin associated factors

| Protein | Molecules/Cell | Reference |
|---|---|---|
| Spn1 | 1848 | This Study |
| | 2830 | 2 |
| | 3086 | 3 |
| Spt6 | 24000 | 1 |
| | 8890 | 2 |
| | 3944 | 3 |
| Pob3 | 41000 | 1 |
| | 22400 | 2 |
| | 5615 | 3 |
| Spt16 | 44000 | 1 |
| | 18500 | 2 |
| | 5920 | 3 |
| Asf1 | 6230 | 2 |
| | 2697 | 3 |
| Cac1 | 1590 | 2 |
| | 524 | 3 |
| Vps75 | 3120 | 2 |
| | 344 | 3 |
| Nap1 | 8070 | 2 |
| | 18619 | 3 |
| Dot1 | 2160 | 2 |
| | 144 | 3 |
| H3 (*HHT2*) | 248000 | 2 |

1. (McCullough *et al.* 2015)
2. (Ghaemmaghami *et al.* 2003)
3. (Kulak *et al.* 2014)

# APPENDIX IV. COMPARISON OF TRANSCRIPTIONAL PROFILES[3]

Expression of spn1$^{141-305}$ or spn1$^{k192N}$ results in cellular resistance to MMS. The resistance observed in the *spn1*$^{141-305}$ strain is dependent on the error free sub-pathway of the DNA damage tolerance (DDT) pathway, while the MMS resistance in observed in the *spn1*$^{K192N}$ strain is not. In response to methyl methanesulfonate (MMS), activation and repression of genes span a multitude of processes ranging from DNA repair, DNA replication, RNA regulation and transcription, protein regulation and translation, stress response, cellular transport, and metabolic processes (JELINSKY and SAMSON 1999; GASCH *et al.* 2001; BENTON *et al.* 2006). To investigate if a subset of genes could potentially result in resistance to MMS, we collaborated with Wei-Sheng Wu from the National Cheng Kung University. Differentially expressed genes in the *spn1*$^{K192N}$ or the *spn1*$^{141-305}$ strains grown in YPD were compared to differential gene lists created when cells were exposed to various concentrations of MMS (0.001%, 0.01%, 0.1%) (BENTON *et al.* 2006). The dosage of MMS evokes variation in the transcriptional profile changes (BENTON *et al.* 2006). The computational analysis revealed no significant overlap between genes down regulated as a result of MMS exposure and differentially expressed genes in either the *spn1*$^{K192N}$ or *spn1*$^{141-305}$ strains (Table AIV.1 and Table AIV.2). There was no significant overlap determined between genes differential expressed after exposure to 0.001% MMS and genes that are differentially expressed in either the *spn1*$^{K192N}$ *or spn1*$^{141-305}$ strains (Table AIV.1 and Table AIV.2). The analysis determined significant overlap between genes down regulated in *spn1*$^{K192N}$ cells and up regulated after exposure to 0.01% MMS and 0.1% MMS. Additionally, there was significant overlap determined between genes up regulated in *spn1*$^{K192N}$ cells and up regulated after exposure to 0.01% MMS (Table AIV.1). Significant overlap was determined between genes down regulated

[3] Tables AIV.1 and AIV.2 were generated by Wei-Sheng Wu from the National Cheng Kung University

in *spn1*$^{141\text{-}305}$ cells and up regulated after exposure to 0.01% MMS and 0.1% MMS (Table AIV.2). Lists of the overlapping genes were compiled and were submitted for gene ontology (GO) term enrichment analysis followed by REVIGO (SUPEK *et al.* 2011) to eliminate statistically similar terms. The GO-term enrichment analysis did not reveal processes which would account for the MMS resistance in either *spn1* mutant strains. Processes that appear in multiple lists are highlighted (Table AIV.3).

Table AIV.1 Comparison between transcripts altered by exposure to increasing MMS concentrations and transcripts whose expression is altered in the *spn1*$^{k192N}$ strain

| ***spn1*$^{K192N}$_Up MMS _Up** | | | | | | |
|---|---|---|---|---|---|---|
| **MMS Concentration** | **Yeast Genome** | **MMS genes** | **SPN1 genes** | **overlap** | **over-represented p-value** | **under-represented p-value** |
| 0.001% | 6572 | 44 | 173 | 2 | 0.323148991 | 0.891422654 |
| 0.01% | 6572 | 63 | 173 | 7 | **0.001239096** | 0.999779144 |
| 0.1% | 6572 | 601 | 173 | 21 | 0.108312085 | 0.93074308 |
| ***spn1*$^{K192N}$_Down MMS _Up** | | | | | | |
| 0.001% | 6572 | 44 | 200 | 5 | 0.010284373 | 0.998018195 |
| 0.01% | 6572 | 63 | 200 | 7 | **0.002841249** | 0.999411664 |
| 0.1% | 6572 | 601 | 200 | 46 | **2.11E-09** | 0.999999999 |
| ***spn1*$^{K192N}$_Up MMS _Down** | | | | | | |
| 0.001% | 6572 | 64 | 173 | 2 | 0.505871577 | 0.762831308 |
| 0.01% | 6572 | 55 | 173 | 1 | 0.770843317 | 0.572801416 |
| 0.1% | 6572 | 64 | 173 | 1 | 0.820151787 | 0.494128423 |
| ***spn1*$^{K192N}$_Down MMS _Down** | | | | | | |
| 0.001% | 6572 | 64 | 200 | 5 | 0.044506132 | 0.987247127 |
| 0.01% | 6572 | 55 | 200 | 1 | 0.818572066 | 0.497304363 |
| 0.1% | 6572 | 64 | 200 | 2 | 0.584975276 | 0.691197109 |

Table AIV.2 Comparison between transcripts altered by exposure to increasing MMS concentrations and transcripts whose expression is altered in the *spn1*$^{141-305}$ strain

| ***spn1*$^{141-305}$_Up MMS _Up** | | | | | | |
|---|---|---|---|---|---|---|
| **MMS Concentration** | **Yeast Genome** | **MMS genes** | **SPN1 genes** | **Overlap** | **over-represented p-value** | **under-represented p-value** |
| 0.001% | 6572 | 44 | 184 | 0 | 1 | 0.285466245 |
| 0.01% | 6572 | 63 | 184 | 5 | 0.030949598 | 0.991966722 |
| 0.1% | 6572 | 601 | 184 | 17 | 0.520415256 | 0.58200168 |
| ***spn1*$^{141-305}$_Down MMS _Up** | | | | | | |
| 0.001% | 6572 | 44 | 483 | 7 | 0.039638746 | 0.986462308 |
| 0.01% | 6572 | 63 | 483 | 12 | **0.001823609** | 0.99946161 |
| 0.1% | 6572 | 601 | 483 | 106 | **5.12E-19** | 1 |
| ***spn1*$^{141-305}$_Up MMS _Down** | | | | | | |
| 0.001% | 6572 | 64 | 184 | 2 | 0.539223828 | 0.733936545 |
| 0.01% | 6572 | 55 | 184 | 2 | 0.45867851 | 0.800997914 |
| 0.1% | 6572 | 64 | 184 | 2 | 0.539223828 | 0.733936545 |
| ***spn1*$^{141-305}$_Down MMS _Down** | | | | | | |
| 0.001% | 6572 | 64 | 483 | 8 | 0.09516892 | 0.957035417 |
| 0.01% | 6572 | 55 | 483 | 4 | 0.583251859 | 0.620404481 |
| 0.1% | 6572 | 64 | 483 | 3 | 0.859520827 | 0.297608236 |

Table AIV.3 GO-term enrichment due to transcript changes in cells expressing spn1$^{K192N}$ or spn1$^{141-305}$ and MMS exposed cells

| **0.01% MMS_UP *spn1$^{K192N}$*_UP** | |
|---|---|
| GO:0006525 | arginine metabolic process |
| GO:0009064 | glutamine family amino acid metabolic process |
| **0.01% MMS_UP *spn1$^{K192N}$*_DOWN** | |
| No significant GO-terms | |
| **0.1% MMS_UP *spn1$^{K192N}$*_DOWN** | |
| GO:0005991 | trehalose metabolic process |
| GO:0006457 | protein folding |
| **0.01% MMS_UP *spn1$^{141-305}$*_DOWN*** | |
| GO:0023052 | signaling |
| GO:0046578 | regulation of Ras protein signal transduction |
| GO:0050896 | response to stimulus |
| GO:0035556 | intracellular signal transduction |
| **0.1% MMS_UP *spn1$^{141-305}$*_DOWN** | |
| GO:0006457 | protein folding |
| GO:0009408 | response to heat |
| GO:0044723 | single-organism carbohydrate metabolic process |
| GO:0050896 | response to stimulus |
| GO:0005975 | carbohydrate metabolic process |
| GO:1901575 | organic substance catabolic process |
| GO:0009056 | catabolic process |
| GO:0006950 | response to stress |
| GO:0033554 | cellular response to stress |
| GO:0005991 | trehalose metabolic process |
| GO:0051716 | cellular response to stimulus |
| * p value set at 0.1 for GO-term generation | |

# APPENDIX V. REMOVAL OF SPN1 RESULTS IN G2/M DELAY[4]

SPN1 is an essential gene (FISCHBECK *et al.* 2002). Approximately 20% of yeast genes in *S. cerevisiae* are essential (ZHANG and REN 2015). Using GO-term enrichment analysis one study found, around 74% of essential genes were identified as being involved in metabolism and close to14% were involved in cell cycle progression regulation (ZHANG and REN 2015). This is logical, since survival of an organism requires energy production and the ability to reproduce. The impact of Spn1 on genome instability through manipulation of the DNA damage tolerance pathway, led to the question if Spn1 could be involved in cell cycle progression. To examine this, the anchor away system was utilized (HARUKI *et al.* 2008). The ribosomal protein RPL13A is FKB12 tagged, the tagged protein cycles in and out of the nucleus. Addition of rapamycin binds the ribosomal protein to FRB tagged Spn1 and Spn1 is shuttled out of the nucleus to the cytoplasm (Figure AV.1A). Using flow cytometry we assessed the cell cycle distribution before and after the removal of Spn1. An increase in the number of cells in G2/M upon the removal of Spn1 was observed (Figure AV.1B). The addition of rapamycin does not affect cell cycle progression in the background strain (Figure AV.1B). This phenomenon was also observed by budding index, indicating Spn1 is important for the progression through G2 of the cell cycle (Figure AV.1C).

[4] I would like to thank Chris Allen and the CSU flow cytometry and cell sorting facility for help in developing a protocol for cell collection and staining as well as instruction on running the instrumentation and analyzing the data. I would like to thank Sha Li for the anchor away strains.

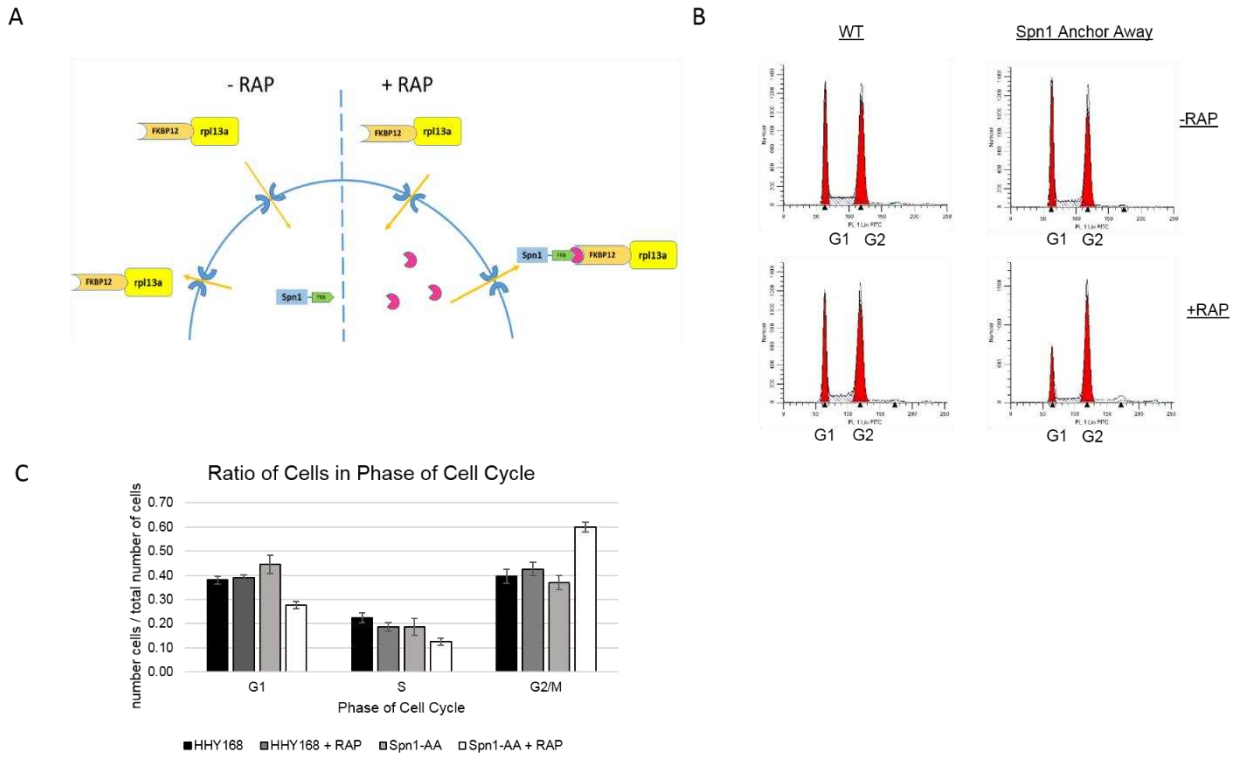


**Figure AV.1. Removal of Spn1 results in a G2/M delay.** A) Pictorial representation of anchor away system. B) Cell cycle distribution determined by flow cytometry. Data was analyzed and modeled using MODFIT. C) Cell cycle distribution determined by budding index.